# APPENDIX E
# GEOHYDROLOGICAL ANALYSIS

# APPENDIX E
# GEOHYDROLOGICAL ANALYSIS

## E.1 Introduction

A three-dimensional far-field site groundwater flow model has been implemented for the *Revised Draft Environmental Impact Statement for Decommissioning and/or Long-Term Stewardship at the West Valley Demonstration Project and Western New York Nuclear Service Center (Decommissioning and/or Long-Term Stewardship EIS)*. This model extends the model domain beyond that of models previously employed at the site. Both model conceptual development and model parameterization incorporated recent data along with those used in prior modeling efforts. The updated model confirms historical understanding of upper layer hydrology with an improved understanding of flows through the slack-water sequence and the Kent recessional sequence (see Chapter 3.6). In addition, three-dimensional near-field models for the North and South Plateau were developed for the evaluation of the environmental impact statement (EIS) alternatives. These models facilitate understanding of near-field flow and the impacts of design decisions for the facilities involved.

This appendix provides descriptions of the groundwater models used in the assessment of the impacts for the West Valley decommissioning alternatives under consideration. The objectives of the EIS groundwater modeling activities were:

- To develop an updated 3D groundwater model that utilizes the additional characterization data collected since the last local model was developed in the mid 1990s.
- To extend the model domain beyond that used in previous modeling at the site to investigate the potential flow in the Kent recessional sequence (in particular) and deeper units.
- To establish a methodology for estimating how local hydrology will change as a result of the engineering features being planned for the various decommissioning alternatives.
- To provide a basis for estimating contaminant transport needed in the assessments of the West Valley decommissioning alternative impacts.

The approach taken to meeting these objectives was 1) to develop the site groundwater flow model for determining flow patterns and exploring conceptual issues at the site scale, 2) to develop the near-field 3D numerical models, consistent with the site model, for the evaluation of changes in local hydrology as a result of proposed alternative actions, and 3) to extract from the near-field models key transport parameters needed for the performance assessments of the alternatives. The two near-field models' domains were the North Plateau and South Plateau.

The site model (covering much of the site area and extending into the bedrock) was implemented using the U.S. Department of Energy (DOE) Finite Element Heat and Mass Transfer Code developed at Los Alamos National Laboratory (LANL 2003) and the near field models that were developed using the DOE Subsurface Transport Over Multiple Phases (STOMP) code developed at the Pacific Northwest National Laboratory (PNNL 2000). FEHM is a finite element code and STOMP is a finite difference code. Both are capable of modeling partially saturated-saturated systems. The focus of this appendix is on model conceptualization and parameterization along with the presentation of key results as well as data analyses.

A significant amount of the effort expended in the development of the groundwater models was directed toward data reduction and evaluation of the large and varied amount of data available. Several notable findings came out of these analyses. Perhaps of most interest, for some geohydrological units, statistically significant differences exist in same-hole hydraulic conductivities determined before and after 1999. As might be expected, the amount of available data varies widely from unit to unit with those of more historical interest being better represented. A preliminary geostatistical characterization of the thick-bedded unit hydraulic conductivity was performed.

Section E.2 provides a discussion on the site environs, the geology of the site relevant to the groundwater modeling activities, identification of the geohydrological units on site, flow systems found at the site, and a general discussion of groundwater conditions. Section E.3 provides information on the implementation of the sub-regional FEHM model, calibration and sensitivity analyses, and a summary of results from the base case model. Details of the near field STOMP models are presented in Section E.4. The discussion is broken down by North and South Plateau and by alternative. In addition to the geohydrological parameters, the discussion includes the identification and characterization of design elements and parameters used in the models. Transport parameters needed for impact assessment of the alternatives are derived from the corresponding STOMP results.

## E.2 Site Characteristics

This section summarizes available site information used to support the development and testing of the groundwater flow models. General information regarding the site geology and hydrogeology is provided in Chapter 3, of the EIS.

### E.2.1 Overview of Geologic and Hydrogeologic Setting

The hydrostratigraphy underlying the North and South Plateaus is summarized in the following sections including a description of the saturated zone characteristics, delineation of the direction and rate of groundwater flow, and the distribution and nature of groundwater contamination as derived from historical studies and ongoing investigations. Information regarding the hydrostratigraphic units and their properties is provided in Section 3.0 in the support analyses for the development of a three-dimensional groundwater flow model and the associated long-term performance assessment in Appendix H.

#### E.2.1.1 Location and Main Features

**Figure E–1** shows the general location of the Western New York Nuclear Service Center (WNYNSC) and the West Valley Demonstration Project (WVDP). The site is located 50 kilometers (30 miles) south of Buffalo, New York. The entire WNYNSC is located within the Buttermilk Creek drainage basin, which is part of the Cattaraugus Creek watershed. Cattaraugus Creek is located north of the site and flows westward to Lake Erie. Within the WNYNSC, the Project Premises and State-licensed Disposal Area (SDA) occupy about 80 hectares (200 acres), and most of the developed portion of the site.

The developed portion of the site is divided geographically by Erdman Brook into the North Plateau and South Plateau and operationally into waste management areas (WMAs). The North Plateau contains the majority of the processing plant facilities. The area covered by the groundwater monitoring network on the North Plateau includes the Main Plant Process Building and Vitrification Facility Area (WMA 1), Low-Level Waste Treatment Facility Area (WMA 2), Waste Tank Farm Area (WMA 3), Waste Storage Area (WMA 5), Construction and Demolition Debris Landfill (CDDL, WMA 4), Central Project Premises (WMA 6), and Support and Services Area (WMA 10). The monitoring network on the South Plateau includes the Central Project Premises (WMA 6), the inactive U.S. Nuclear Regulatory Commission (NRC)-licensed Disposal Area (NDA) and Associated Facilities (WMA 7), the inactive SDA and Associated Facilities (WMA 8), Radwaste Treatment System Drum Cell (WMA 9), and Support and Services Area (WMA 10). **Figure E–2** shows the layout of major site features and WMAs across the WNYNSC and WVDP.

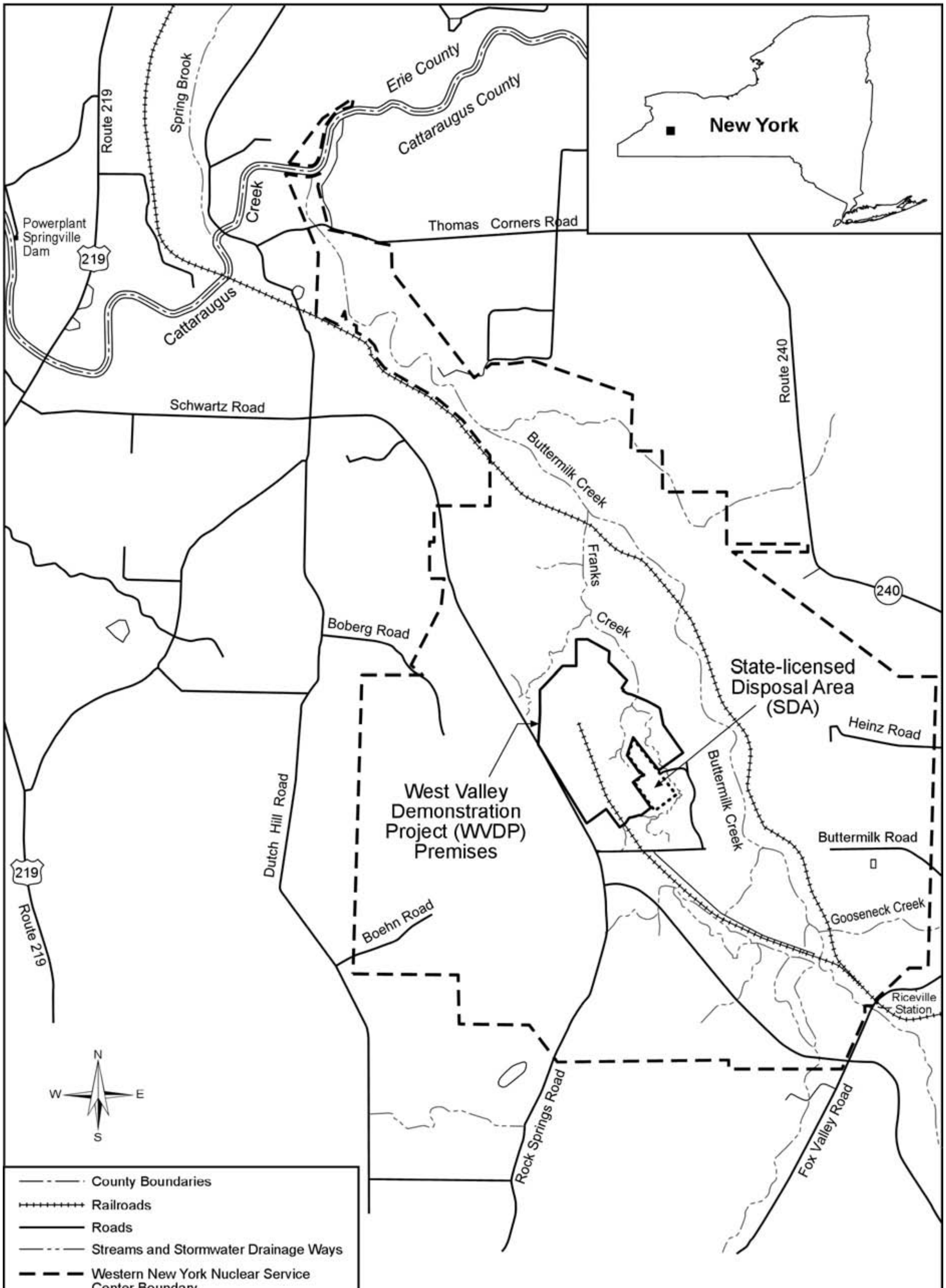


**Figure E–1 General Location Map of the Western New York Nuclear Service Center and the West Valley Demonstration Project**

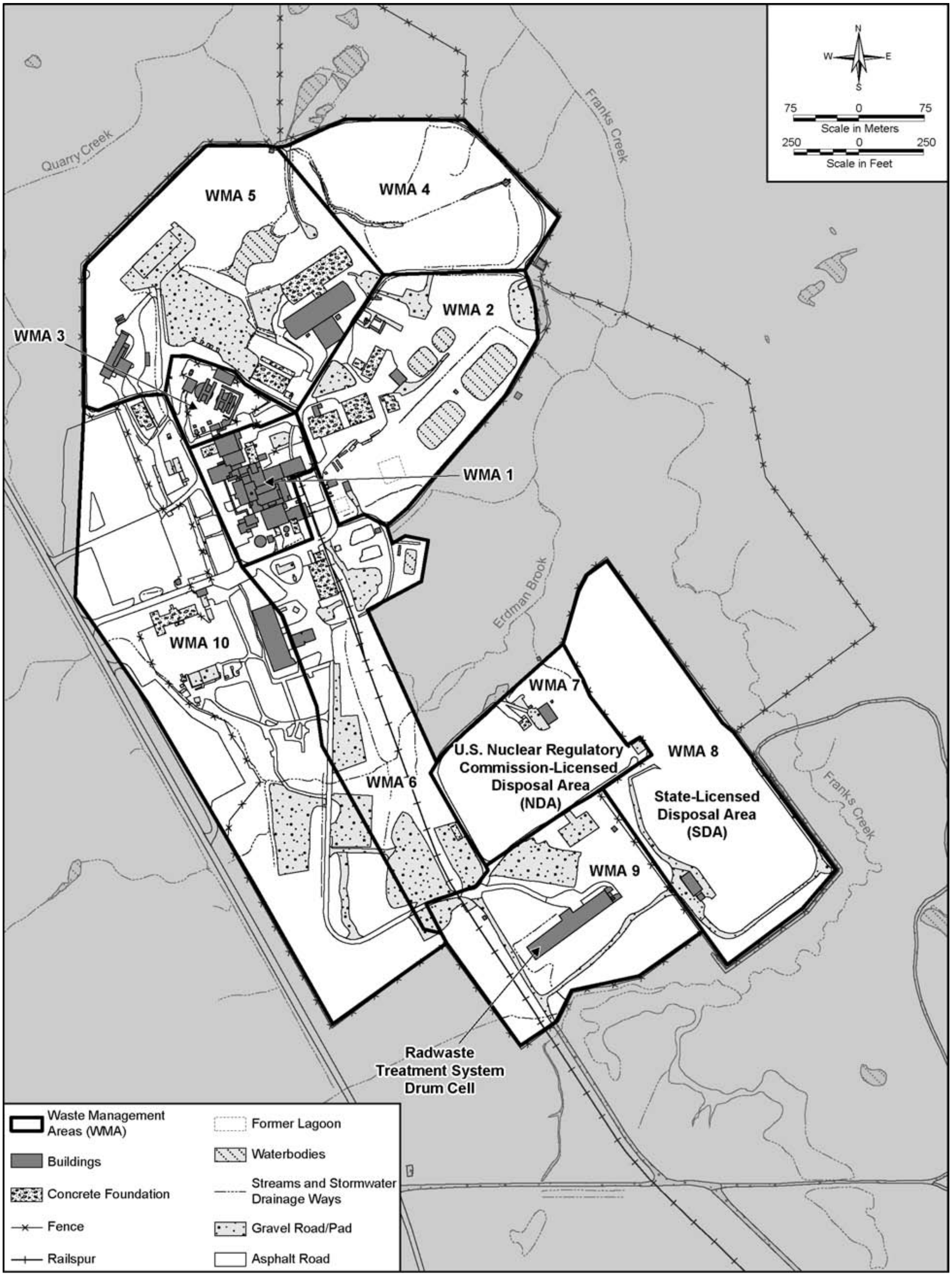


**Figure E–2 West Valley Demonstration Project Site and Waste Management Areas**

The area between Franks Creek and Buttermilk Creek, referred to as the East Plateau in this appendix, comprises a third plateau area located east and northeast of the project premises (Figure E–1). The East plateau area is overlain by sand and gravel deposits in the north and weathered till in the south. While part of the same units that underlie the main WVDP facilities areas, the shallow geologic units on the East plateau are isolated from the WVDP by the Franks Creek stream valley. The deeper till units underlying the East plateau are laterally contiguous with the till to the west.

#### E.2.1.2 Geology

The WNYNSC is located within the glaciated northern portion of the Appalachian Plateau physiographic province at an average elevation of 396 meters (1,300 feet) above mean sea level (WVNS 1993a, WVNS and URS 2005). The site is approximately midway between the boundary delineating the southernmost extent of Wisconsinan glaciation and a stream-dissected escarpment to the north that establishes the boundary between the Appalachian Plateau and the Interior Low Plateau Province.

The WNYNSC is located in the Buttermilk Creek Valley west of the Creek. The valley is a steep-sided, northwest-trending U-shaped valley that has been incised into the underlying Devonian bedrock. A sequence of Pleistocene-aged deposits and overlying Holocene (recent) sediments up to 150 meters (500 feet) thick occupies the valley. Repeated glaciation of the ancestral bedrock valley occurred between 14,500 and 38,000 years ago resulting in the deposition of a sequence of three glacial tills (Lavery, Kent, and Olean tills) that comprise the majority of the valley fill deposits (WVNS 1993a, WVNS and URS 2005). The Holocene deposits are principally deposited as alluvial fans and aprons derived from the glacial sediments that cover the uplands surrounding the WNYNSC and from floodplain deposits derived from Pleistocene valley-fill sequences (WVNS 1993a, 2007).

Glacial tills of Lavery, Kent, and Olean formations separated by stratified, interstadial, fluvio-lacustrine deposits overlie the bedrock beneath the North, South and East Plateaus. Repeated glaciation of the Buttermilk Creek Valley occurred between 24,000 and 15,000 years ago, ending with the deposition of approximately 40 meters (130 feet) of Lavery till. Outwash and alluvial fan deposits were deposited on the Lavery till between 15,000 and 14,200 years ago (URS 2002). **Figure E–3** shows the surface geology of the Buttermilk Creek basin in the vicinity of the WNYNSC.

The uppermost Lavery till and younger surficial deposits form a till plain covering 25 percent of the Buttermilk Creek basin with elevations ranging from 490 meters to 400 meters (1,600 to 1,300 feet) from south to north. The WVDP Premises and the SDA are located on this stream-dissected till plain west of Buttermilk Creek at an elevation of 430 meters (1,400 feet). Erdman Brook divides the WVDP Premises into North and South Plateaus (WVNS 1993a).

#### E.2.1.3 Site Stratigraphy

Sediments overlying the bedrock consist of glacial tills of the Lavery, Kent, and Olean (WVNS and URS 2005) formations that are separated by stratified fluvio-lacustrine deposits (**Figure E–4** and **Table E–1**). The glacial layers dip to the south at approximately 5 meters (16 feet) per kilometer. The stratigraphic units present at the North Plateau and the South Plateau are shown in **Figure E–5** and **Figure E–6**, respectively. The stratigraphy of the North and South plateau areas is differentiated by sand and gravel deposits that overlie the till on the northern plateau areas and the lack of sand and gravel deposits overlying the till on the southern plateau areas. Unit designations in the vicinity of the site are also indicated in Figure E–4, developed from La Fleur (La Fleur 1979) and Prudic (Prudic 1986). The continuity of the shallow deposits is interrupted by the deeply incised stream valleys occurring between the plateaus. Deposition of the sand and gravel has significantly reduced the depth of weathering in the underlying till on the northern plateau areas while weathered till is exposed at the surface on the southern part of the site (WVNS 1993a).

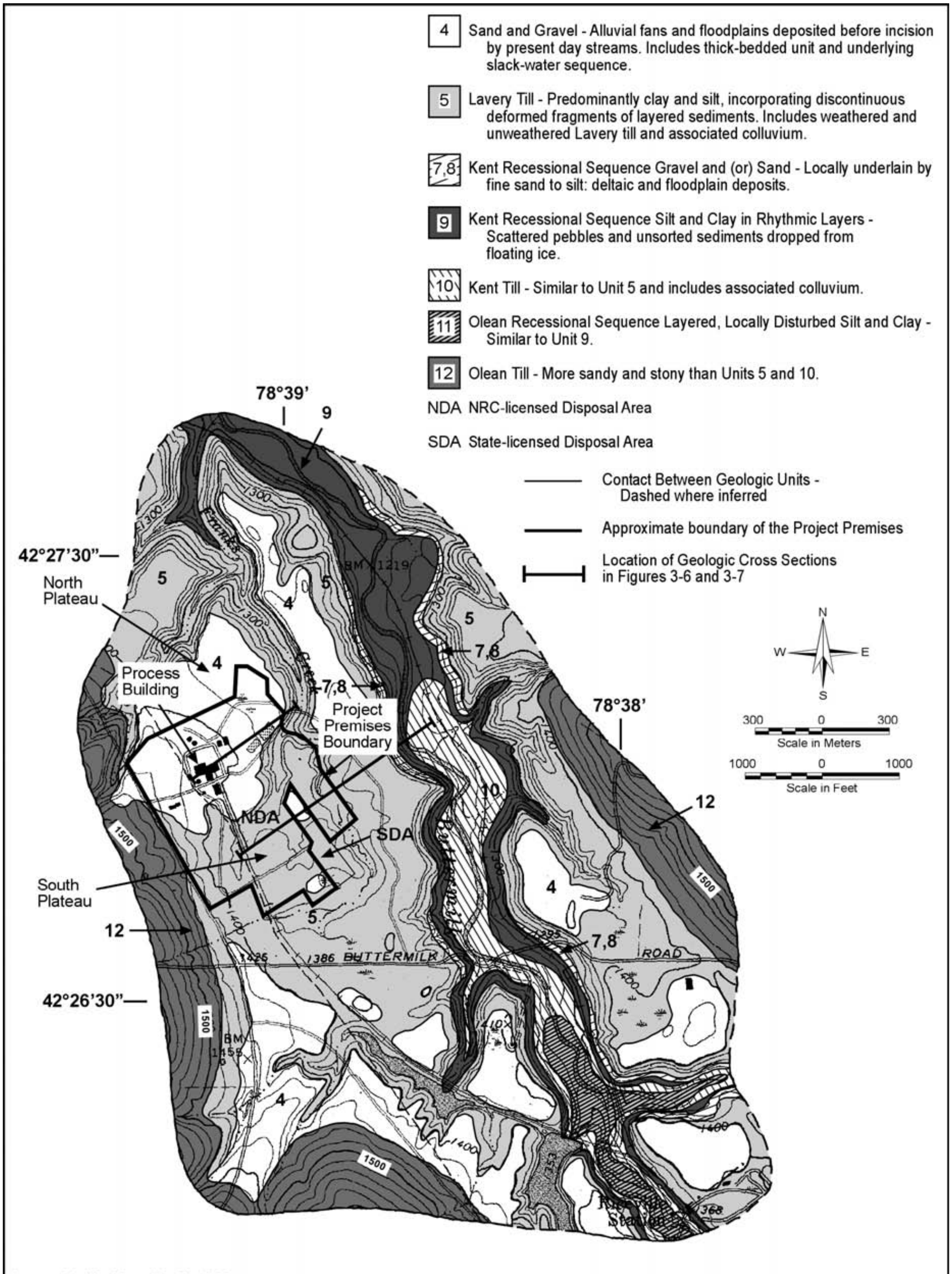


Source: Modified from Prudic 1986.
Note: Topographic contours are in feet. Multiply by 0.3048 to convert to meters.

**Figure E–3 Surface Geology in the Vicinity of the Western New York Nuclear Service Center**

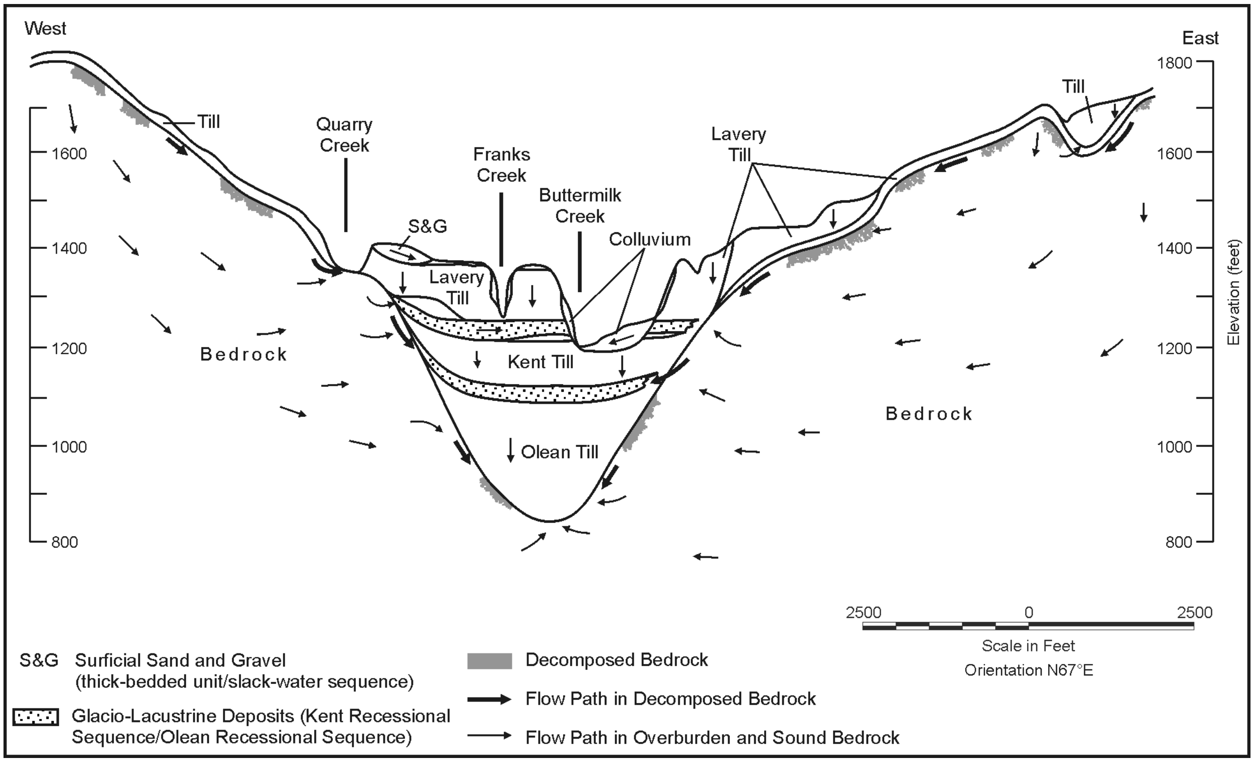


**Figure E–4 Geologic Cross-section through the Buttermilk Creek Valley**

The clay layer that differentiates the sand and gravel (thick-bedded unit and slack-water sequence) units in the subsurface underlying the North Plateau has previously been interpreted as unweathered Lavery till, resulting in portions of the slack-water sequence being interpreted as Lavery till-sand. However, recent reinterpretation of the sandy interval as slack-water sequence, has revised the extent of the Lavery till-sand and the slack-water sequence beneath the North Plateau (WVES 2007). The primary justification for the stratigraphic revision to the model is based on the elevation of the encountered units as delineated from borings. As a result of the reinterpretation, the horizontal extent of the slack-water sequence has been expanded from previous delineations to encompass areas located upgradient of the Main Plant Process Building and has also been extended to conform to the surface of the underlying unweathered Lavery till. Since fewer borings are now considered to have encountered Lavery till-sand, the horizontal extent of the Lavery till-sand has been reduced (WVES 2007). The new interpretation is a recent development and is still evolving. Potential impacts on flow at the site are considered in the discussion of the modeling results in Section E.3.7.

### E.2.2 Definition of Hydrostratigraphic Units

The stratigraphic units underlying the WVDP area are subdivided into hydrostratigraphic units on the basis of lithology and hydrogeologic properties. In this regard, contiguous layers with similar lithologic and hydrogeologic characteristics may be combined into a single hydrostratigraphic unit. The various hydrostratigraphic units are shown by the generalized geologic cross-sections in Figures E–5 and E–6. **Figure E–7** illustrates a conceptual block model of the groundwater flow systems underlying the North and South Plateaus. This model is conceptual and flows between the units are mostly inferred from the known hydrostratigraphy—with the exception of where recharge from or discharge to the surface is clearly observed. Groundwater movement beneath the East plateau combines elements of both conceptual flow systems.

**Table E–1 Stratigraphy of the West Valley Demonstration Project Premises and the State-licensed Disposal Area [a]**

| ***Geologic Unit*** | ***Description*** | ***Origin*** | ***Thickness [b]*** | |
|---|---|---|---|---|
| | | | ***North Plateau (meters)*** | ***South Plateau (meters)*** |
| Colluvium | Soft plastic pebbly silt only on slopes, includes slump blocks several meters thick | Reworked Lavery or Kent till | 0.3 to 0.9 | 0.3 to 0.9 |
| Thick-bedded unit | Sand and gravel, moderately silty | Alluvial fan and terrace deposits | 0 to 12.5 | 0 to 1.5 at Well 905[c]; not found at other locations |
| Slack-water sequence | Thin-bedded sequence of clays; silts, sands, and fine-grained gravel at base of sand and gravel layer | Lake deposits | 0 to 4.6 | Not present |
| Weathered Lavery till | Fractured and moderately porous till, primarily comprised of clay and silt | Weathered glacial ice deposits | 0 to 2.7 (commonly absent) | 0.9 to 4.9, average = 3 |
| Unweathered Lavery till | Dense, compact, and slightly porous clayey and silty till with some discontinuous sand lenses | Glacial ice deposits | 1 to 31.1 Lavery till thins west of WVDP Premises | 4.3 to 27.4 Lavery till thins west of WVDP Premises |
| Till-sand member of Lavery till | Thick and laterally extensive fine to coarse sand within Lavery till | Possible meltwater or lake deposits | 0.1 to 4.9 | May be present in one well near northeast corner of NDA |
| Kent Recessional Sequence | Gravel comprised of pebbles, small cobbles, and sand, and clay and clay-silt rhythmic layers overlying the Kent till | Proglacial lake, deltaic, and alluvial stream deposits | 0 to 21.3 | 0 to 13.4 |
| Kent till, Olean Recessional Sequence, Olean till | Kent and Olean tills are Clayey and silty till similar to Lavery till. Olean Recessional Sequence predominantly clay, clayey silt, and silt in rhythmic layers similar to the Kent recessional sequence overlying the Olean till | Mostly glacial ice deposits | 0 to 91.4 | 0 to 101 |
| Upper Devonian bedrock | Shale and siltstone, weathered at top | Marine sediments | > 402 | > 402 |

[a] Source: Geologic unit descriptions and origins from Prudic (1986) as modified by WVNS (1993a, 1993b). Thickness from lithologic logs of borings drilled in 1989, 1990, and 1993 (WVNS 1994); from Well 905 (WVNS 1993b); and from Well 834E (WVNS 1993a). Kent and Olean till thickness from difference between bedrock elevation (based on seismic data) and projected base of Kent recessional sequence (WVNS 1993a); upper Devonian bedrock thickness from Well 69 U.S. Geological Survey 1-5 located in the southwest section of the WNYNSC (WVNS 1993a).

[b] To convert meters to feet, multiply by 3.2808.

[c] Coarse sandy material was encountered in this well. It is unknown whether this deposit is equivalent to the sand and gravel layer on the North Plateau.

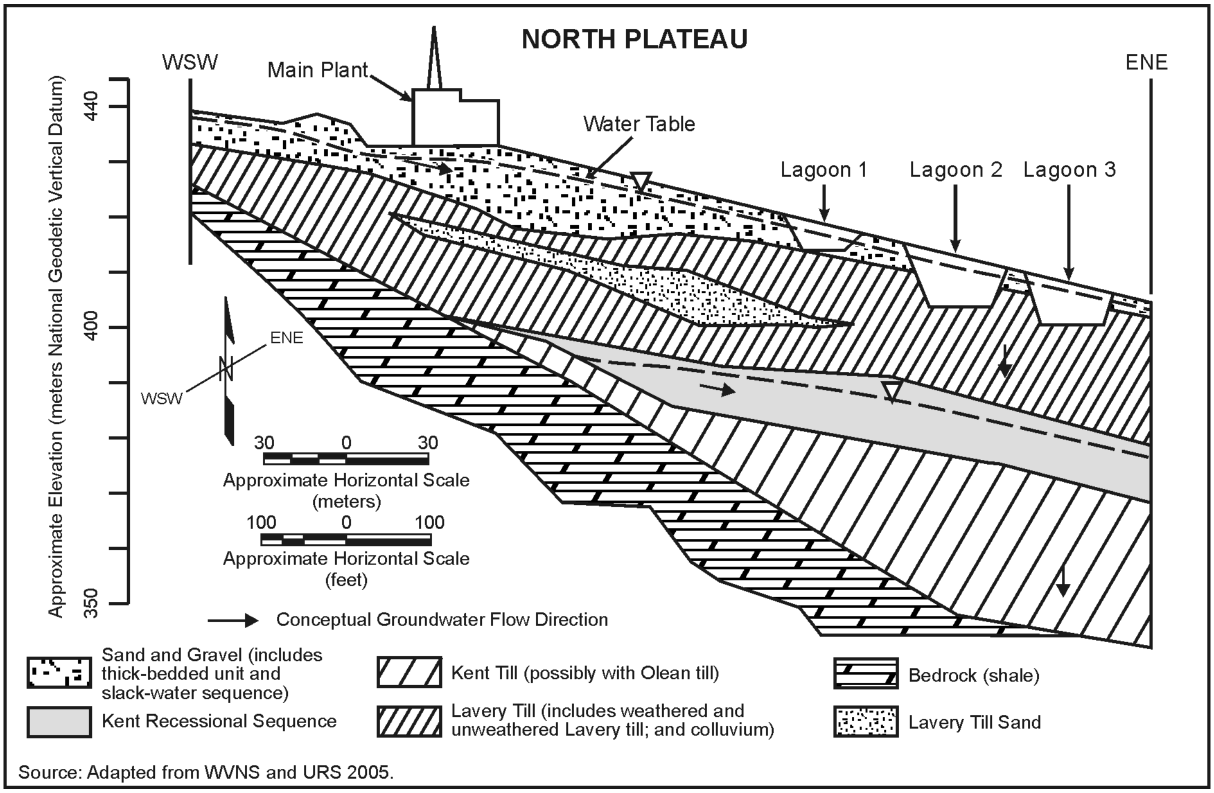


**Figure E–5 Geologic Cross-section through the North Plateau**

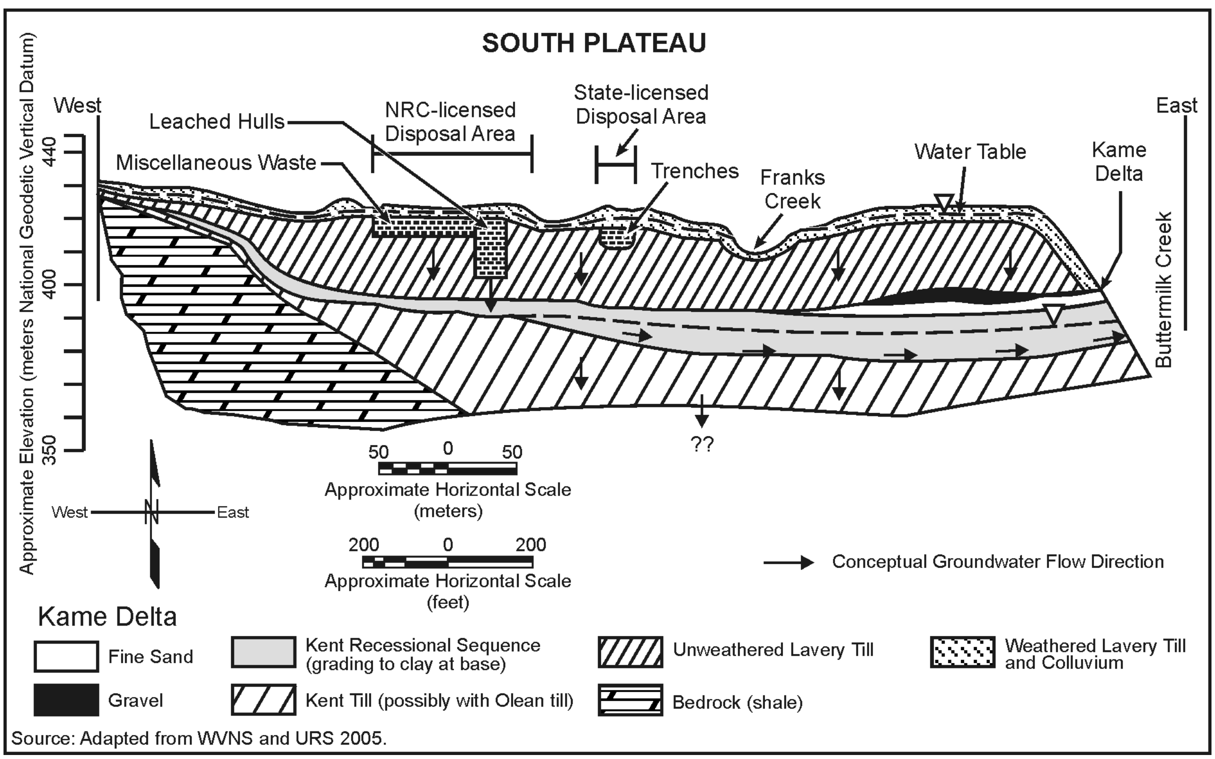


**Figure E–6 Geologic Cross-section through the South Plateau**

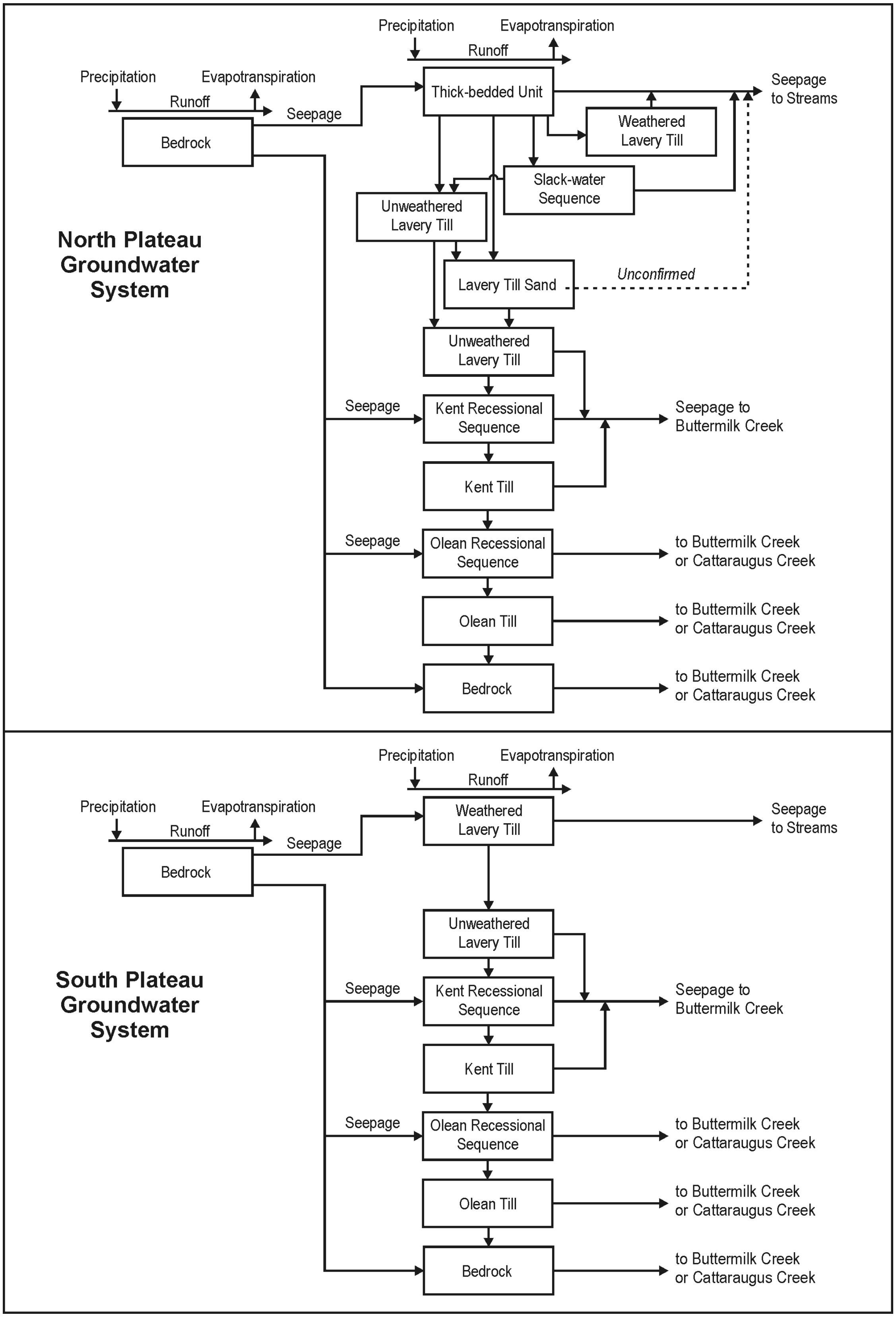


**Figure E–7 Conceptual Block Models of the North and South Plateau Groundwater Flow System at the West Valley Demonstration Project Site**

### E.2.2.1 Thick-bedded Unit Sand and Gravel and Slack-water Sequence

The thick-bedded unit is a Holocene-age alluvial fan that was deposited by streams entering Buttermilk Valley and which is the thicker and more extensive of the two deposits. The alluvial fan overlies the Lavery till over most of the North Plateau and directly overlaps the Pleistocene-age glaciofluvial slack-water sequence that occurs in a narrow northeast trending trough in the Lavery till (see **Figure E–8**). On steeper slopes, Holocene-age landslide deposits (colluvium) also blanket or are interspersed with the sand and gravel (WVNS 1993a). Fill material occurs in the developed portions of the North Plateau, and mainly consists of recompacted surficial sediment that is mapped as part of the sand and gravel (WVNS 1993b). The slack-water sequence is a Pleistocene age glaciofluvial gravel deposit that overlies the Lavery till in a narrow northeast trending trough across the North Plateau (WVNS 1993a, 1993b, 1994, 2007). The unit contains thin-bedded layers of clay, silt, sand, and fine-grained gravel deposited in a glacial lake environment (WVNS 1994). These subunits overlie the Lavery till on the North Plateau with localized amalgamation with the Lavery till-sand. Previous studies have combined the thick-bedded unit and slack-water sequence as the Sand and Gravel Unit. Investigators have used both the single and the two-subunit representations in past studies, depending on the purpose of the analysis. In this EIS, the two-subunit representation is used to account for the differences in hydraulic conductivity between the units for modeling purposes.

#### E.2.2.1.1 Thick-bedded Unit Sand and Gravel

The thick-bedded unit underlying the North Plateau has an areal extent of approximately 42 hectares (104 acres) with a thickness of up to 12.5 meters (42 feet) in the vicinity of the process building (WMA 1) and the wastewater treatment facility (WMA 2). The average textural composition of the surficial sand and gravel is 41 percent gravel, 40 percent sand, 11 percent silt, and 8 percent clay classifying it as a muddy gravel or muddy sandy gravel (WVNS 1993b). The sand and gravel unit is thickest, ranging from 9 meters (30 feet) to 12.5 meters (41 feet) along a trend oriented southwest to northeast across WMA 1. The locally thicker sand and gravel deposits correspond to erosional channels incised into the underlying Lavery till. The sand and gravel thins to the north, east, and south where it is bounded by Quarry Creek, Franks Creek, and Erdman Brook, respectively, and to the west against the slope of the bedrock valley (WVNS 1993a, 1993b; WVNS and URS 2006). At these boundaries, the thick-bedded unit is truncated by the downward erosion of the streams and groundwater discharges to surface water through seepage faces and underflow down stream valley walls through weather Lavery till or colluvium.

The thick-bedded unit on the North Plateau is recharged by inflow from direct contact with fractured bedrock west of the site and from infiltrating precipitation. Discharge from this unit flows into Erdman Brook, Franks Creek, and Quarry Creek from the North Plateau, and into Franks and Buttermilk Creek from the East Plateau. Prior studies indicate that a small fraction of the water flows downward from the surficial thick-bedded unit to the Lavery till (Prudic 1986, WVNS 1993b). The thick-bedded unit underlying the East Plateau is physically and hydrologically disconnected from the North Plateau.

Groundwater in the sand and gravel forms the upper aquifer beneath the WVDP site. The depth to the water table within the sand and gravel ranges from 0 meters (0 feet) where the water table intersects the ground surface and forms swamps and seeps along the periphery of the North Plateau, to as much as 6 meters (20 feet) beneath portions of the central North Plateau where the layer is thickest (WVNS 1993b). Groundwater in the sand and gravel generally flows to the northeast across the North Plateau from the southwestern margin of the unit near Rock Springs Road toward Franks Creek. Flow in the thick-bedded unit is predominantly horizontal (WVNS 1993b, WVNS and Dames and Moore 1997, WVNS and URS 2006).

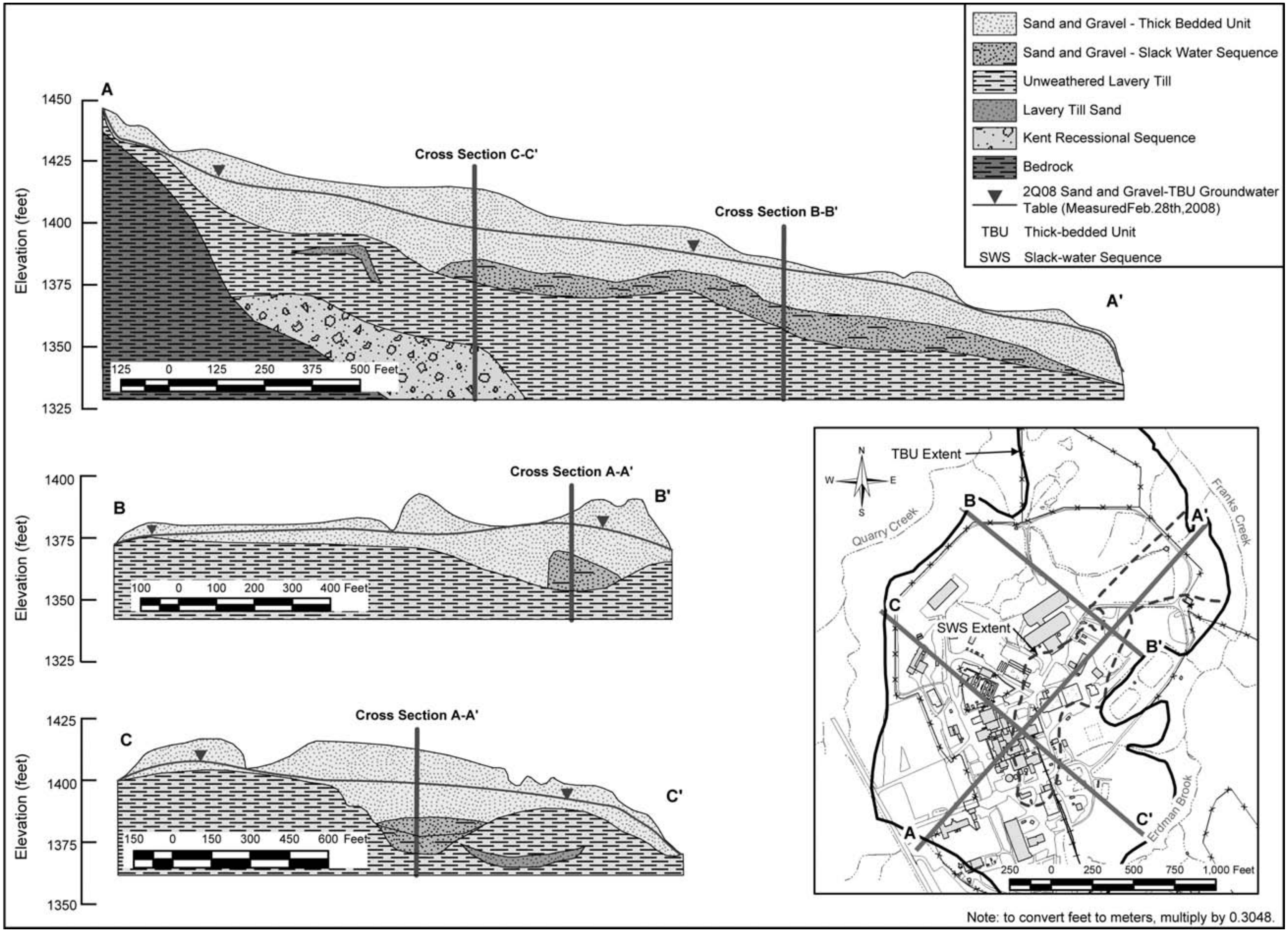


**Figure E–8 Surficial Sand and Gravel Showing the Extent of Both the Thick-bedded Unit and the Slack-water Sequence**

#### E.2.2.1.2 Slack-water Sequence

The slack-water sequence occurs at the base of the thick-bedded unit from the area of the cooling tower northeast to Franks Creek Valley (WVNS 1994). The slack-water deposits range in thickness up to 4.6 meters (15 feet). Numerous thin horizontal clay layers occur in the slack-water sequence. This can be seen in estimated slack-water sequence textures ranging from 95 percent clay and silt to 100 percent sand. Although the overlying thick-bedded unit aquifer is considered to be under unconfined conditions, localized confined conditions occur in the slack-water sequence.

### E.2.2.2 Lavery Till

The surficial units and the entire WVDP Project Premises are underlain by the Lavery till. The till underlying the North Plateau is predominantly unweathered, owing to the presence of the overlying sand and gravel (WVNS 1993a). Weathered zones in the till are generally less than 0.3 meters (1 foot) thick (WVNS and Dames and Moore 1997). The till consists of dense, pebbly silty clay to clayey silt. The unweathered Lavery till is typically olive-gray and calcareous (WVNS 1993a) and contains discontinuous and randomly oriented pods or masses of stratified sand, gravel, and rhythmically laminated clay-silt. The average textural composition of the unweathered Lavery till is 50 percent clay, 30 percent silt, 18 percent sand, and 2 percent gravel (WVNS 1993b). Across the site the thickness of the till ranges from 9 to 12 meters (30 to 40 feet) reaching a maximum thickness of approximately 31 meters beneath the North Plateau and 27 meters beneath the South Plateau.

The weathered Lavery till at the South Plateau is generally exposed at grade or may be overlain by a veneer of fine-grained alluvium (WVNS 1993a). The upper portion of the till beneath the South Plateau has been extensively weathered and is physically distinct from unweathered Lavery till. The weathered till has been oxidized from olive-gray to brown, contains numerous root tubes, and is highly desiccated with intersecting horizontal and vertical fractures (WVNS 1993b, WVNS and URS 2006). Vertical fractures extend from approximately 4 to 8 meters (13 to 26 feet) below ground surface into the underlying unweathered till. The average textural composition of the weathered Lavery till is 47 percent clay, 29 percent silt, 20 percent sand, and 4 percent gravel. The thickness of the weathered Lavery till ranges from 0.9 meters (3 feet) to 4.9 meters (16 feet) across the South Plateau (WVNS 1993b, WVNS and URS 2006).

Groundwater in the unweathered Lavery till generally infiltrates vertically toward the underlying Kent recessional sequence (Prudic 1986, WVNS 1993b, WVNS and Dames and Moore 1997). The till unit is perennially saturated with relatively low hydraulic conductivity in the vertical and horizontal dimensions and functions as an effective aquitard (WVNS and Dames and Moore 1997). The observed hydraulic gradient in the unweathered Lavery till is close to unity (Prudic 1986).

The weathered Lavery till variably weathered to a depth of 0.9 to 4.9 meters (3 to 16 feet) (see Section 3.3.1.1). Because of the weathered and fractured nature of the till, both horizontal and vertical components are active in directing groundwater movement (WVNS and URS 2006). Lateral groundwater movement in the weathered till is controlled by the availability of interconnected zones of weathering and fracturing, the prevailing topography on the weathered till/unweathered till interface, and the low permeability of the underlying unweathered Lavery till. The range of hydraulic conductivities and the variation in lateral gradients lead to horizontal velocity estimates on the order of tens of centimeters per year to meters per year. Flow may continue a short distance before slower vertical movement through the underlying unweathered till occurs, or in some circumstances, may continue until the groundwater discharges at the surface in a stream channel or a seep.

Research conducted by the New York State Geological Survey (Dana et al. 1979a, 1979b) studied the shallow till and associated joints and fractures as part of a hydrogeologic assessment of the Lavery till. Intrinsic till joints and fractures were classified as: (1) prismatic and columnar jointing related to hardpan soil formation; (2) long, vertical, parallel joints that traverse the entire altered zone and extend into the parent till, possibly reflecting jointing in the underlying bedrock; (3) small displacements through sand and gravel lenses; and (4) horizontal partings primarily related to soil compaction and secondarily from trench excavation. Prismatic and columnar jointing may represent up to 60 percent of all till fractures and were believed to have formed by alternating wet/dry or freeze/thaw conditions. Fracture density was determined to be a function of the moisture content and weathering of the till, with fracturing being more pervasive in the weathered and drier soil and associated till. Densely-spaced, vertical fractures with spacing ranging from 2 to 10 centimeters (0.8 to 3.9 inches) were limited to depths in the soil near the surface. However, vertically persistent fractures were observed to extend from the surface soils into the relatively moist and unweathered till. These long vertical fractures were systematically oriented to the northwest and northeast. Spacing between fractures ranged from 0.65 to 2.0 meters (2 to 6.5 feet) and generally extended to depths of 5 to 7 meters (16 to 23 feet). The fracture spacing increased with depth and the number of fractures were observed to decrease with depth. Trenching found one vertical fracture extending to a depth of 8 meters (26 feet) (Dana et al. 1979a).

Open, or unfilled, fractures in the upper portion of the Lavery till provide pathways for groundwater flow and potential contaminant migration. Tritium was not detected in two groundwater samples collected from a gravel horizon at a depth of 13 meters (43 feet) in New York State Geological Survey Research Trench #3, indicating that modern (post-1952) precipitation has not infiltrated to the discontinuous sand lens in the Lavery till. Analysis of physical test results on Lavery till samples by the New York State Geological Survey concluded that open fractures would not occur at depths of 15 meters (50 feet) below ground surface due to the plasticity characteristics of the till (NYSGS 1979, Dana et al. 1979a).

#### E.2.2.3 Lavery Till-Sand

The Lavery till-sand is a lenticular silty sand deposit localized in the southeastern portion of the North Plateau within the unweathered Lavery till. It is distinguished from the isolated pods of stratified sediment in the Lavery till because borehole observations indicate that the till-sand unit is laterally continuous beneath portions of the North Plateau (WVNS 1993b, WVNS and Dames and Moore 1997). The till-sand consists of 19 percent gravel, 46 percent sand, 18 percent silt, and 17 percent clay. The till-sand occurs within the upper 6 meters (20 feet) of the till and ranges in thickness from about 0.1 to 4.9 meters (0.4 to 16 feet).

Groundwater pathways through the till-sand travel to the east-southeast toward Erdman Brook. However, surface seepage locations from the unit into Erdman Brook have not been observed (WVNS and Dames and Moore 1997, WVNS and URS 2006). The lack of seepage suggests that the till-sand is largely surrounded by unweathered Lavery till. Fractures in the Lavery till may allow groundwater in the till-sand to discharge along the north banks of Erdman Brook, but at a slow rate. As a result, recharge to and discharge from the till-sand is likely controlled by the physical and hydraulic properties of the Lavery till (WVNS 1993b). Discharge occurs as seepage to the underlying Lavery till. Recharge occurs as leakage from the Lavery till and from the overlying sand and gravel unit, where the till layer is not present (WVNS 1993b, WVNS and Dames and Moore 1997).

The Lavery till-sand was reported in all previous studies as a water-bearing unit under semi-confined conditions that receives and transmits water to other units through vertical leakage from the thick-bedded unit as well as through the unweathered Lavery till. Hydraulic gradients average 0.01 in the general direction of flow, which indicates that some discharge occurs on the southeast boundary of the Lavery till-sand. This discharge is suspected to occur along an outcrop connected to Erdman Brook (WVNS 2002). In addition, downward gradients are recorded from the thick-bedded unit and slack-water sequence to the Lavery till-sand in the western upgradient area where recharge to the Lavery till-sand occurs. On the eastern side of the Lavery till-sand unit, piezometric heads exceed those in the thick-bedded unit, indicating possible upward flow. This is due to confined conditions in a portion of the Lavery till-sand and the proximity to thick-bedded unit discharge areas near Erdman Brook.

### E.2.2.4 Kent Recessional Sequence

The Kent recessional sequence is a sequence of interlayered, ice-recessional lacustrine and kame-delta deposits consisting of silt and clay that coarsens upward into sand and silt. The unit underlies the Lavery till beneath most of the site area, thinning to the southwest where it is truncated by the walls of the bedrock valley. The sequence receives recharge along a zone of contact with the fractured bedrock to the west, and also from downward seepage through the overlying Lavery till. The unit is not exposed on the WVDP Premises but crops out along Buttermilk Creek to the east of the site (WVNS 1993a, WVNS and URS 2005). The sequence is comprised of alluvial, deltaic, and lacustrine deposits with interbedded till (WVNS 1993b, 1993c). The upper Kent sequence consists of coarse-grained deposits of sand and gravel that overlie fine-grained lacustrine silt and clay (WVNS 1993b, WVNS and URS 2005). The basal lacustrine sediments were deposited in glacial lakes that formed as glaciers blocked the northward drainage of streams. Beneath the North Plateau, the Kent sequence consists of coarse sediments that either overlie the lacustrine deposits or directly overlie glacial till. The average textural composition of the coarse-grained deposits comprising the sequence is 44 percent sand, 23 percent silt, 21 percent gravel, and 12 percent clay. The average textural composition of the lacustrine deposits is 57 percent silt, 37 percent clay, 5.9 percent sand, with 0.1 percent gravel. The Kent recessional sequence attains a maximum thickness of about approximately 21 meters (69 feet) beneath the North Plateau.

Groundwater flow in the Kent recessional sequence is to the northeast and Buttermilk Creek (WVNS 1993b, WVNS and URS 2006). Recharge to the Kent recessional sequence comes from both the overlying till and the adjacent bedrock valley wall. Discharge occurs at seeps along Buttermilk Creek Figure E–6 and to part of the underlying Kent till (WVNS 1993b, WVNS and Dames and Moore 1997).

The upper interval of the Kent recessional sequence, particularly beneath the South Plateau, is unsaturated. However, the deeper lacustrine deposits are saturated and provide an avenue for slow northeast lateral flow to points of discharge (seeps) in the bluffs along Buttermilk Creek. The unsaturated conditions in the upper sequence are the result of very low vertical permeability in the overlying till, and thus there is a low recharge through the till to the Kent recessional sequence (Prudic 1986). As a result, the recessional sequence acts as a drain to the till and causes downward gradients in the till of 0.7 to 1.0, even beneath small valleys adjacent to the SDA (WMA 8) on the South Plateau (WVNS 1993b, WVNS and Dames and Moore 1997).

### E.2.2.5 Kent Till, Olean Recessional Sequence, and Olean Till

Older glacial till and periglacial deposits of lacustrine and glaciofluvial origin underlie the Kent recessional sequence beneath the North and South Plateaus, extending to Upper Devonian bedrock (WVNS 1993a, 2007). The combined thickness of these units ranges from 0 feet to more than 300 (see Table E–1). The Kent till and Olean Recessional Sequence are exposed along Buttermilk Creek southeast of the project. The Kent till has characteristics similar to the Lavery till. The estimated thickness of the till is 100 feet with thinning to the west where the unit is truncated by the walls of the bedrock valley. Field hydraulic conductivity testing has not been conducted in the Kent. The horizontal and vertical hydraulic conductivity is assumed to be approximately that of the lower values of the unweathered Lavery till.

The Olean Recessional Sequence underlies the Kent till and has characteristics similar to the Kent recessional sequence. The Olean Recessional Sequence is assumed to be a fully saturated unit and underlies the Kent till throughout most of the site with a thickness of approximately 30 feet, thinning out as it intersects the bedrock wall in the western portion of the site. Hydraulic conductivity testing has not been conducted in this unit, however, for modeling purposes it is assumed that the range is on the lower side of the values for the Kent recessional sequence. Vertical hydraulic conductivity is assumed to be one tenth of the horizontal values and some flow is assumed to migrate down to the Olean till. Recharge is assumed to come from the Kent till above and move horizontally within the unit to the north and northwest.

The Olean till contains more sand and gravel sized material than the Lavery and Kent tills. The Olean till is exposed near the sides of the valley overlying bedrock (Prudic 1986). The sequence of older glacial till and recessional deposits ranges up to approximately 91 meters (299 feet) in thickness beneath the North Plateau. The Olean till is a fully saturated unit and underlies the Olean Recessional Sequence throughout most of the site area. The unit thins as it intersects the bedrock valley wall in the western portion of the site. The hydraulic conductivity of the Olean till is assumed to be equivalent to the lower values of the unweathered Lavery till. The vertical hydraulic conductivity is assumed to be equivalent to the horizontal values. The unit receives recharge from the Olean Recessional Sequence unit above and the groundwater moves in a vertical direction to the weathered bedrock below.

#### E.2.2.6 Bedrock

Bedrock underlying the project area consists of Devonian shale and sandstone exposed in the upland stream channels along Quarry Creek northwest of the site, on hilltops west and south of the site, and in the steep-walled gorges cut by Cattaraugus Creek to the north and by Connoissarauley Creek to the west (Bergeron, Kappel and Yager 1987). The uppermost bedrock unit in the vicinity of the WVDP Premises and SDA is the Canadaway Group, which consists of shale, siltstone, and sandstone and totals approximately 300 meters (980 feet) in thickness. The regional dip of the bedrock layers is approximately 0.5 to 0.8 degrees to the south (Prudic 1986, WVNS 1993a). Locally, measurements of the apparent dip of various strata and two marker beds in selected outcrops along Cattaraugus Creek recorded a dip of approximately 0.4 degrees to the west near the northern portion of the WNYNSC (CWVNW 1993).

Regional groundwater in the bedrock flows downward within the higher elevation recharge zones, laterally beneath lower hillsides and terraces, and upward near major stream discharge zones. The upper 3 meters (10 feet) of bedrock in the shallow subsurface and in outcrop is weathered to regolith with systematically-oriented, joints and fractures. As cited by Prudic (1986) and others and observed in outcrop along Quarry Creek, the joints are not restricted to the upper 3 meters (10 feet) of the bedrock. They are developed throughout and continue at depth (Engelder and Geiser 1979). Recharge to bedrock is from precipitation on the upland areas west of the project area (outside the model area). Subsurface groundwater flow in the weathered bedrock follows the buried topography to the northwest. Wells completed in this zone yield approximately 40 to 60 liters per minute (10.6 to 15.9 gallons per minute).

### E.2.3 Flow Systems

Movement of contaminants in groundwater is largely controlled by the direction and speed of that groundwater. However, the groundwater is part of an interconnected flow system consisting of not only groundwater, but surface water bodies, recharge and seepage. Therefore, to understand groundwater flow patterns, it is important to understand the other mechanisms associated with the flow systems and how they interact at the site.

#### E.2.3.1 Surface Water and Seepage Faces

The WNYNSC lies within the Cattaraugus Creek watershed, which empties into Lake Erie about 43 kilometers (27 miles) southwest of Buffalo, New York. Buttermilk Creek, a tributary to Cattaraugus Creek, drains the WNYNSC site. The Creek exists primarily within the Kent recessional sequence geologic layer, with a small portion in the upstream segment flowing through the Kent till. The older materials are exposed along the creek's bed upstream because they were deposited on the upslope of the bedrock in the vicinity of the valley head, and hence, are tilted. Franks Creek joins Buttermilk Creek from the southwest approximately

3 kilometers (2 miles) upstream of the Cattaraugus-Buttermilk confluence. In this area, Franks Creek flows through the Kent recessional sequence. However, the majority of the Creek in the vicinity of the WVDP lies within the Lavery till. The drainage area for the site is about 13.7 square kilometers (5.3 square miles) and the total Buttermilk Creek drainage area is 79 square kilometers (29.4 square miles).

Quarry Creek and Erdman Brook are two important tributaries to Franks Creek because of their proximity to the WVDP grounds. Quarry Creek drains the largest area north and west of the active site operations, while Franks Creek and Erdman Brook drain the majority of the plant area and the state- and NRC-licensed waste disposal areas to the south. Both tributaries exist primarily within the Lavery till. However, portions of Quarry Creek do flow through areas of exposed bedrock. In addition to the streams described, there also exist a number of natural swamps and ponds within the WNYNSC site. Manmade water bodies consisting of drainage ditches and holding lagoons also have been constructed at the site. In other areas facilities eliminate or reduce infiltration and hence, recharge to the groundwater system. These features, natural and manmade, and the streams shown in **Figure E–9** are the surface hydrological features interacting with the groundwater system at the site.

All the creeks and brooks of interest at the WNYNSC site have seen very high levels of streambank erosion over the years. This has resulted in very steep slopes in the vicinity of each stream, yielding a set of observable seepage faces on the North Plateau occurring near the interface of the permeable surficial sand and gravel and the low permeability till underneath. These perimeter seeps occur on three sides of the plateau and have a profound influence on the near-surface groundwater hydrology in that area. The locations of observed seeps are indicated in **Figure E–10**.

There has been some characterization of seeps at the site as a result of a 1983 field investigation by the U.S. Geological Survey. The results of these analyses are presented in **Table E–2**. Kappel and Harding (1987) and others (Yager 1987, Bergeron, Kappel and Yager 1987) summarize various aspects of the investigation, describing both locations and flows recorded for each face during the investigation. They also report stream-discharge data collected at three continuous record stations (Lagoon Road, NP-1 and NP-3) and one partial record station (NP-2). Locations of the recording stations are also indicated in Figure E–10. Estimates of the discharge from springs and seepage faces along the northeast and northwest sides of the 42 hectare North Plateau, which drain to Quarry and Franks Creeks, indicated a total discharge of 20 cubic meters per day or an average application of 1.8 centimeters per year normalized to the surface area of the thick-bedded unit (Kappel and Harding 1987). Estimating the flow into Erdman Brook from the Main Plant at 500 cubic meters per day Yager also indirectly quantified the amount of discharge from the North Plateau into Erdman Brook as 180 to 260 cubic meters per day (16 to 23 centimeters per year) (Yager 1987).

**Table E–2 Observed Seep and Stream Flows**

| ***Location*** | ***Observed Discharge (cubic meters per day)*** |
|---|---|
| NP-1 | 29 |
| NP-2 | 6 |
| NP-3 | 113 |
| NP – Total | 148 |
| Quarry Creek and Franks Creek | 20 |
| Erdman Brook (Yager's estimate) | 220 (180-260) |
| Erdman Brook (Kappel and Harding) | 10 |
| French Drain (Kappel and Harding) | 23 |
| Total | 388 (178[a]) |

[a] Total using Kappel and Harding flow for Erdman Brook.
Note: To convert cubic meters per day to cubic feet per day, multiply by 35.314.

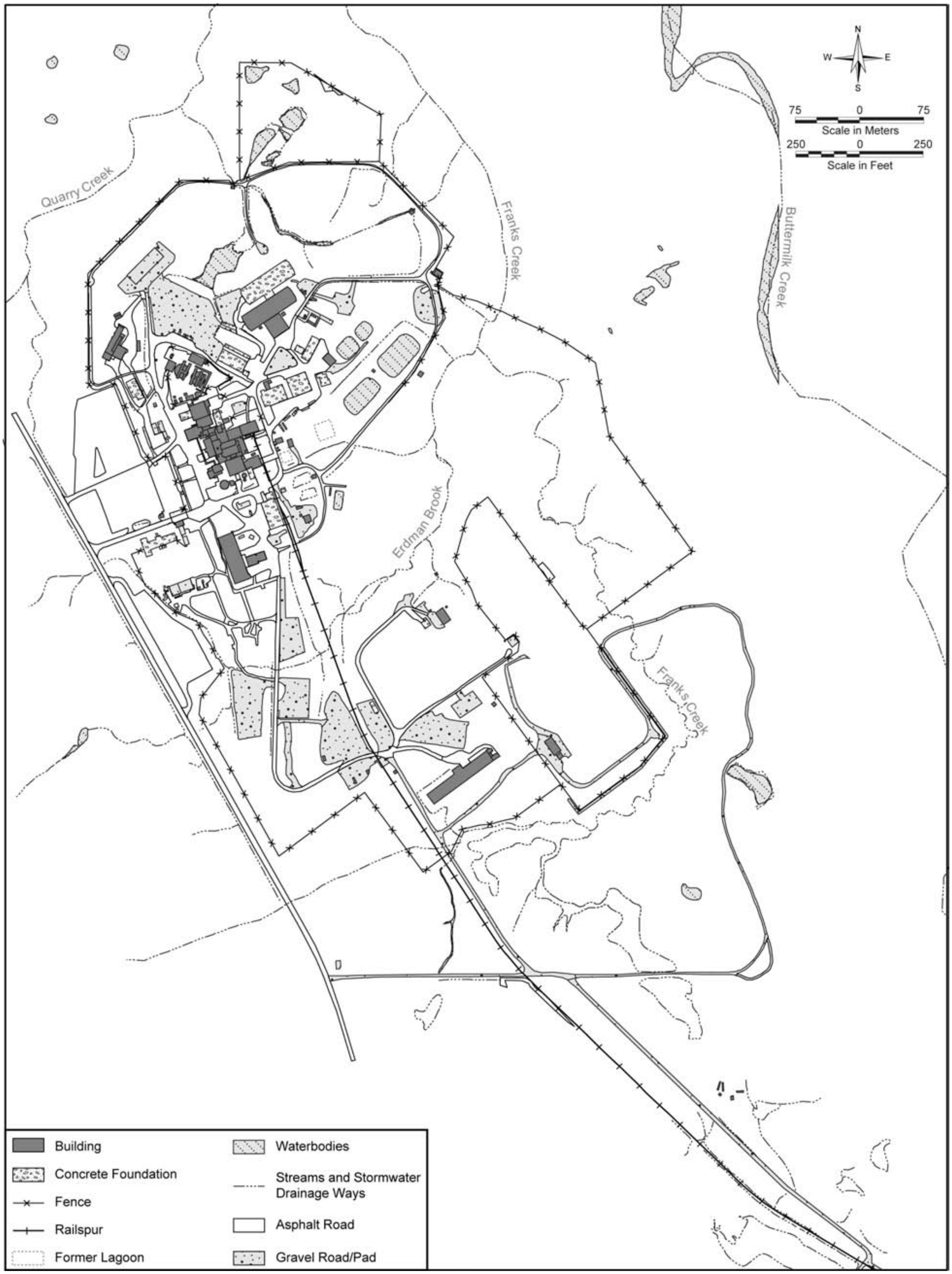


**Figure E–9 Site Surface Hydrology**

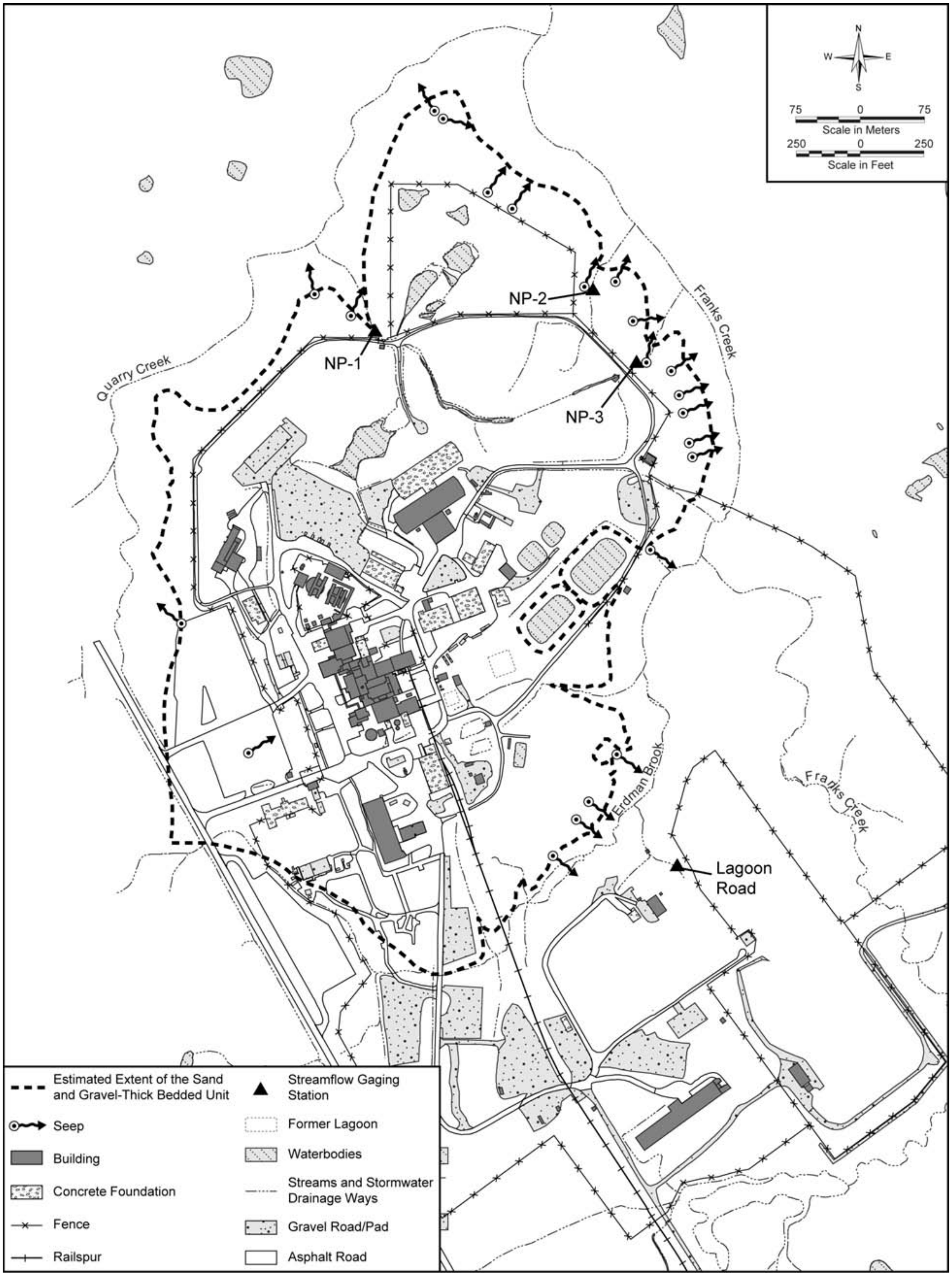


**Figure E–10 Locations of Perimeter Seeps and Stream Gauging Stations for the North Plateau**

The flows reported for the Erdman Brook seeps by Kappel and Harding (1987) are much lower. These authors estimate the seepage flow into that stream to be 10 cubic meters per day. One possible explanation for the large difference in the two estimates may lie in the indirect approach used by Yager and in particular, the need to subtract one large number (the estimated flow from the plant) from another (flow in Franks Creek).

The flows shown in Table E–2 are used in the calibration of the present groundwater model in Section E.3.5.

### E.2.3.2 Groundwater

#### Groundwater Flow Systems

The paragraphs that follow provide a composite description of groundwater flow at the site as extracted from the results and interpretations found in previous modeling studies of groundwater subsystems at the site (Bergeron and Bugliosi 1988, Kool and Wu 1991, Prudic 1986, Yager 1987). The groundwater flow system near the surface in the vicinity of the site consists of two aquifers, separated by an unsaturated zone. Both of these aquifers appear in Figures E–5 and E–6. The upper aquifer exists within the thick-bedded unit/slack-water sequence and Lavery till (weathered and unweathered). The upper aquifer is unconfined and is primarily fed by infiltration coming from precipitation and from surface water bodies. In addition, some inflow likely occurs into the thick-bedded unit where it interfaces with weathered bedrock at the western edge of the site near Rock Springs Road. The quantity of water coming into the thick-bedded unit from the bedrock has not been well characterized.

Permanent unconfined conditions extend over much of the unit. Groundwater exits the upper aquifer primarily through seeps, discharge into surface water, and some evapotranspiration. The material directly beneath the thick-bedded unit and slack-water sequence is the low permeability unweathered Lavery till. Vertical flow through the till appears to be limited because of its low hydraulic conductivity, and hence, flow within the saturated zone of the upper aquifer is predominantly horizontal.

The physical basis and hence the behavior of the flow in the southern portion of the upper aquifer is quite different. Here the aquifer material overlying the unweathered Lavery till is weathered Lavery till. The weathered Lavery till is less permeable and thinner than the thick-bedded unit. Infiltration into the weathered Lavery till is much reduced compared to the thick-bedded unit. In addition, the shallowness of the weathered Lavery till means that the upper aquifer is more susceptible to changes in topography. These factors lead to a picture of highly variable saturated flow regime sensitive to climatological and hydrological stresses. As such it is difficult to quantify and is difficult to model in detail. The current model, like previous models (Bergeron and Bugliosi 1988, Kool and Wu 1991, Prudic 1986), reflects this characteristic. While there is some lateral component to the flow in the weathered Lavery till, discharge to surface water is limited to those areas close to the discharge locations, and much of the water entering the system as infiltration will move downward. Wet periods do lead to more potential for lateral flow and discharge at the surface.

Much less is known about the lower aquifer, which is also a water table aquifer. It is situated within the Kent recessional sequence below the unweathered Lavery till. This aquifer has not been previously modeled and its behavior has been inferred from available groundwater monitoring and log data, expert opinion, and analogy with the thick-bedded unit, a unit having similar origins and composed of similar materials. The Kent recessional sequence water table likely exists due to a combination of low infiltration from above through the unweathered Lavery till and a source inflow from the weathered bedrock where the Kent recessional sequence and weathered bedrock interface (Prudic 1986)—a situation analogous to that for the thick-bedded unit in the upper aquifer.

Lying between the bottom of the upper aquifer and the unsaturated top of the lower aquifer, much of the unweathered Lavery till is saturated. Given these circumstances and the low permeability of the unweathered

Lavery till, flow through that unit is essentially vertical.

Other, deeper aquifer systems may exist at the site and in the Buttermilk Creek valley. Little is known about the Olean materials although the present model does have a recessional unit analogous to the Kent recessional sequence. The possibility of a continuous weathered bedrock aquifer has been considered. In a white paper, Zadins (Zadins 1997) summarizes this work and examines the question of connection with the Springville aquifer further to the north. The physical extent of the present model allows some rudimentary examination of the impacts of the deeper extended geohydrological units through the manipulation of the boundary conditions of those units involved.

Figure E–7 summarizes all of the aquifer systems discussed in the paragraphs above, relating known and assumed flows into and out of each system.

Groundwater level data dating from 1990 to the present are available for both WVDP and SDA wells. Since 1995, these data have been collected on a quarterly basis. Additional data are available at other well locations established for special projects. Water level data are collected and maintained in the site's Laboratory Information Management System, for over 220 locations and provide well elevation information for all of the principal units (thick-bedded unit and slack-water sequence, weathered Lavery till, unweathered Lavery till, Lavery till-sand, and Kent recessional sequence). This number includes locations where monitoring has been discontinued. **Figures E–11** and **E–12** show the fourth quarter 2007 groundwater contours for the upper aquifer at the North Plateau and the WVDP areas of the South Plateau, respectively. Levels for the SDA are monitored and reported annually by New York State independent of Project reporting. Contours based on posted water levels in the vicinity of the SDA have been added to Figure E–12.

The data were examined using both seasonal trend analyses and hydrographs to identify wells that had a trend over time and those that did not show a trend. Based on these analyses, a set of non-trending or low-trend wells was determined for use in initial model calibration in Section 3.

#### E.2.3.3 Water Balances

Water balances have been estimated for the surficial sand and gravel unit. Using data developed by Kappel and Harding (Kappel 1987), Yager developed a two-dimensional numerical model for the 42 hectare surficial sand and gravel on the North Plateau for the year 1983 (Yager 1987). As a part of the study Yager developed water budgets for the sand and gravel unit—one from the data and one from the model. Using the data of Kappel and Harding the total annual recharge to the sand and gravel was 66 centimeters per year with approximately 50 centimeters per year from precipitation, 12 centimeters per year from inflow from adjacent bedrock near Rock Springs Road, and 4 centimeters per year from leakage from the Main Plant's outfall channel discharging into Erdman Brook. The estimated total discharge was less at 59 centimeters per year. Discharge to seeps and springs accounted for 21 centimeters per year, streams and channels 13 centimeters per year, discharge to the french drain (now closed off) and low-level waste treatment system 2 centimeters per year, evapotranspiration 18 centimeters per year, vertical leakage into the Lavery till 1 centimeters per year and change in storage 4 centimeters per year. This water balance was calculated using the larger estimate, 220 cubic meters per day, for the seepage flow to Erdman Brook discussed in Section E.2.3.1.

Yager's steady-state flow model water budget estimated a total recharge of 60.1 centimeters per year with 46.0 centimeters per year from the infiltration of precipitation, 10.4 centimeters per year from the bedrock inflow, and 3.7 centimeters per year from the outfall leakage. Model-derived discharge estimates from the sand and gravel were evapotranspiration 20.0 centimeters per year, stream channels 12.2 centimeters per year, french drain and low-level-waste treatment system 4.3 centimeters per year, and seeps and springs 23.5 centimeters per year. Agreement between this water budget and the data-based water budget is good.

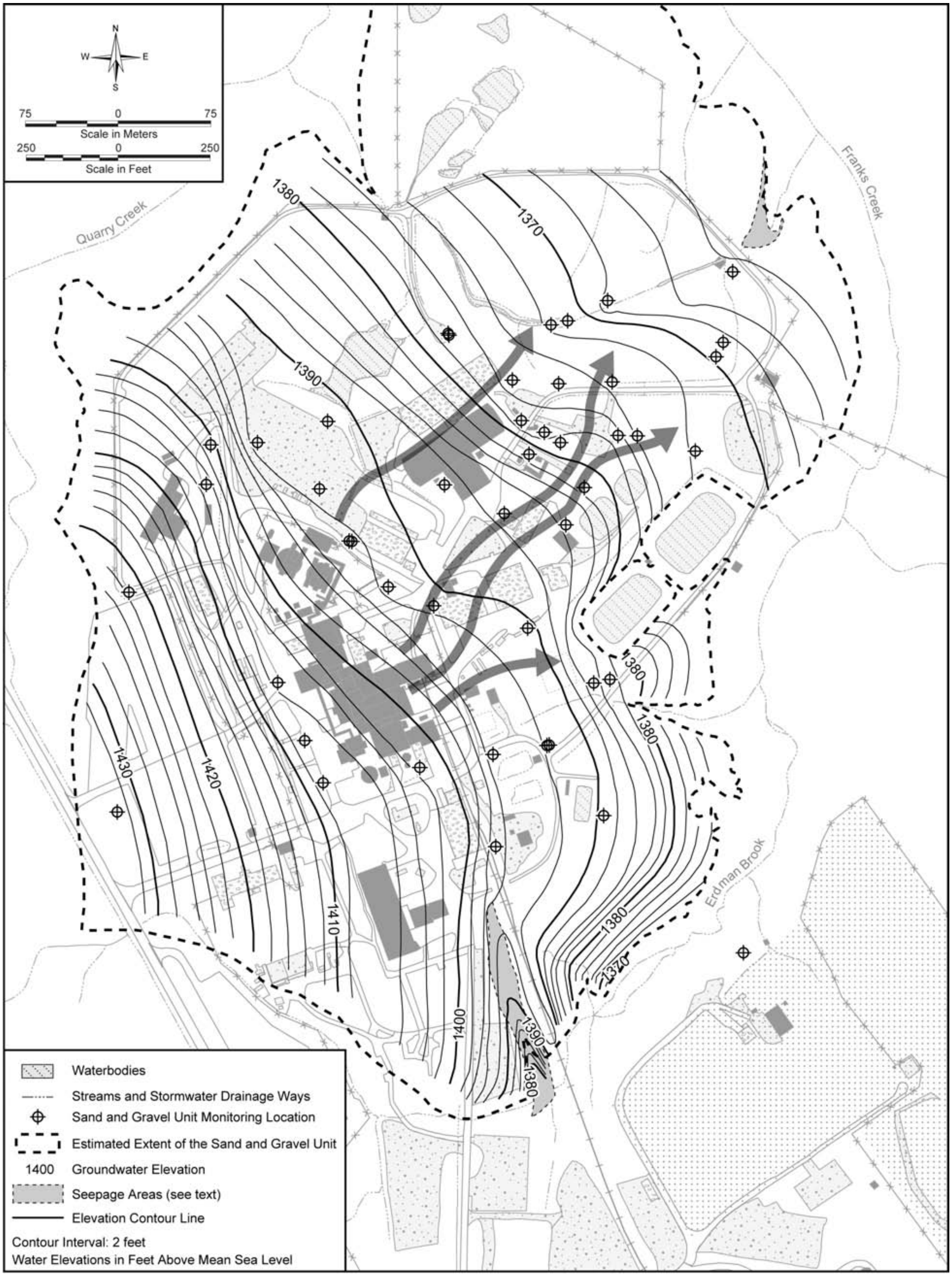


**Figure E–11 Fourth Quarter 2007 the Surficial Sand and Gravel Aquifer Groundwater Levels**

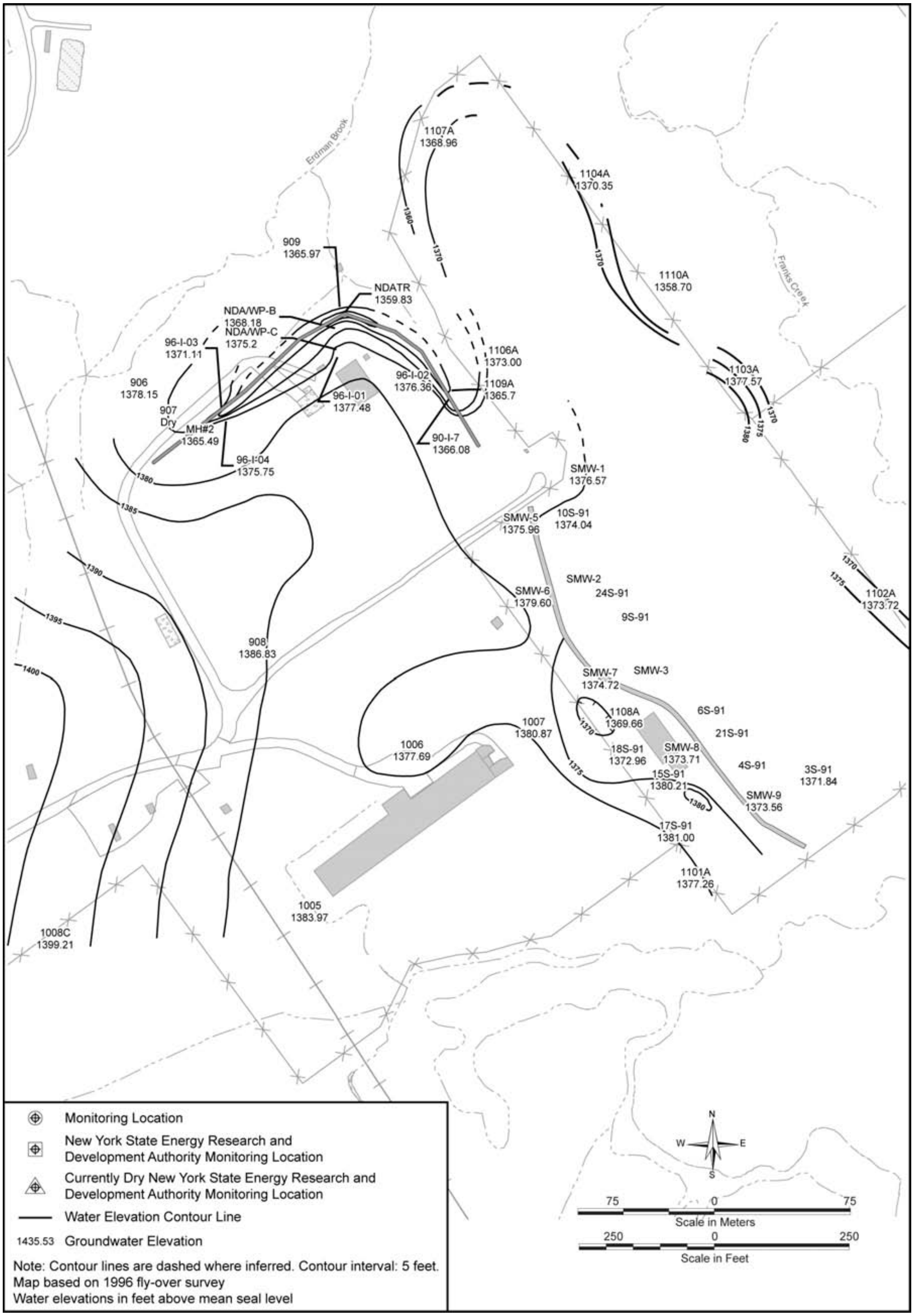


**Figure E–12 Fourth Quarter 2007 South Plateau Groundwater Levels**

In 1993 seasonal fluctuations from 35 wells installed in the sand and gravel unit were used to arrive at a spatially averaged annual recharge to the North Plateau (WVNS 1993b). The estimated recharge was 17.3 centimeters per year. The difference between this value and the recharge derived by Yager was attributed to differences in the hydraulic conductivities used in the calculations—Yager's model hydraulic conductivities (~0.001-0.01 centimeters per second) being greater by approximately an order of magnitude. In a review of the 1993 report Yager notes also that the 1993 calculations do not consider the effects of groundwater discharge from the North Plateau and hence, underestimate the recharge (Yager 1993). Also in 1993 water budget and hydrological analyses for the North Plateau arrived at a total steady-state annual precipitation of 100.1 centimeters per year, runoff 25.5 centimeters per year, infiltration 74.7 centimeters per year, drainage below 4 meters (recharge) 15.8 centimeters per year, and evapotranspiration 56.0 centimeters per year (WVNS 1993c). The estimate, 15.8 centimeters per year, of the recharge from precipitation in this study is also significantly less than those made by Yager—50 centimeters per year and 46 centimeters per year. Yager's 1993 review suggests that the runoff may have been over-estimated and recharge underestimated in these calculations (Yager 1993). Other analyses performed in the study produced North Plateau recharge estimates in the range of 5 centimeters per year to 12 centimeters per year (WVNS 1993b).

## E.3 Groundwater Flow Model

There were several objectives in the development of the present model:

- Examine how regional flow dynamics directly affect the flow patterns at the site.
- Provide context and guidance in the development of submodels, e.g., models for groundwater flow in the thick-bedded unit and slack-water sequence, used to evaluate EIS alternatives.
- Examine the validity of approximations used when developing submodels for specific areas on the site—both in a historical context and for EIS alternatives.
- Consider alternative conceptual models.

There is overlap in the objectives as stated. In the most direct context there is the need to develop models for use in evaluating EIS alternatives. However, review and discussion during the EIS process have also pointed to a need to examine the bases and limitations of models that have been used and are being developed. In addition, groundwater flow and transport modeling has evolved significantly over the past two decades. A significant trend is the move from deterministic models to stochastic models (Yoram Rubin's *Applied Stochastic Hydrogeology* provides a comprehensive overview of stochastic groundwater modeling); the present model is deterministic, thus the development of such a model in the present case had to be considered. The current view is that the essential need is to reasonably discriminate between alternatives, thereby informing the decision process, and that deterministic models coupled with sensitivity analyses are sufficient.

An important question that must be resolved is whether a single model is sufficient to model flow or even subsystem flow. In some cases two or more models of a system lead to equally acceptable representations of the system's behavior (known as equifinality). This situation often arises as the complexity of the modeled system increases. In these circumstances an understanding of all model uncertainties is essential to the assignment of equal behavior. These uncertainties include system conceptualization, structural uncertainty, uncertainties in model parameters values and uncertainties associated with the algorithms and implementations of the model. The geohydrology at the West Valley Site is complex and the physical extent of the present model allows for some examination of all of these factors short of a full Generalized Likelihood Uncertainty Estimation or GLUE implementation (Beven 2006).

The current model encompasses a larger area than previous models. The lateral extent of the model at the surface roughly includes both the North and South Plateau and extends eastward from the vicinity of Rock Springs Road to Buttermilk Creek. In the vertical dimension the model extends into the bedrock. This model domain was chosen based on the considerations above and based on discussion with professionals working on the project. Natural boundaries were chosen whenever possible.

This model domain incorporates not only the thick-bedded unit/slack-water sequence and unweathered Lavery till, used in previous site models, but also adds the Kent recessional sequence, Kent till, Olean Recessional Sequence, Olean till, weathered bedrock and bedrock. Choosing a model boundary above the bedrock assumes knowledge of the conditions at the intersection of the model layers, which is an approximation often made to reduce the computational time required to solve the problem. However, in light of present computer capabilities, possible insight gained in the larger domain and a need to explore the effects of deeper units, even if demonstrated to be negligible, justifies the increased computational effort.

The model was setup and run to a steady state solution. The assumption that the system is in a "steady state" is clearly an approximation that is further addressed in the Results section. The remainder of this section provides a discussion overview of how the model was implemented, calibration, base case results, and sensitivity analyses.

### E.3.1 Model Boundaries

The boundaries are the locations that define the physical extent of the model. Calculations are completed inside the domain, and the boundary supplies the interface with the model calculations and the known or presumed field conditions. In the present model, the project geohydrologist, engineers, and physicists interpreted and fused both the field data and the local geological interpretations into a conceptual site model that supports definition of the numerical model boundaries:

- **Northern Boundary**. The western side of the northern boundary is located along Quarry Creek. As the boundary moves eastward, it intersects and follows Franks Creek after the latter's confluence with Quarry Creek. The boundary then extends along Franks Creek to where it joins Buttermilk Creek.

- **Western Boundary**. The western boundary roughly follows the 440-meter (1,450-foot) surface contour. It is also near and runs approximately parallel to Rock Springs Road, extending from the vicinity of Quarry Creek in the north to the upper Franks Creek drainage.

- **Southern Boundary**. Beginning at the western boundary, the southern boundary follows the West-East trending reach of Franks Creek immediately south of the South Plateau until that creek bends north into the interior of the model. At that point the boundary becomes an imaginary line extending east perpendicular to Buttermilk Creek.

- **Eastern Boundary**. The eastern boundary is defined by Buttermilk Creek.

- **Top of Model Domain**. The upper surface of the model domain is the ground surface.

- **Bottom of Model Domain**. The bottom of the model is located at an elevation of 160 meters (525 feet) above sea level. The model bottom is assumed to be a no-flow boundary, i.e., there is no vertical flow across this boundary.

### E.3.2 Description of Model Grid

A plane view of the finite-element grid used for the model is shown in **Figure E–13**. The grid blocks are of uniform dimension in the x-y plane with each side having a length of 43 meters (140 feet). The irregular shape of the grid results from the boundaries of the model following the natural boundary lines (such as the creeks) described in the previous section. Each grid block has one node located in the center of the block, resulting in 955 nodes per model slice.

For the vertical discretization of the grid, the topographic surface is the upper boundary and the base of the bedrock is the lower boundary. The domain was broken up into 23 model layers to adequately represent the varying thicknesses of the 10 geologic materials found at the site. To avoid convergence problems in the simulations, the change in vertical discretization in moving from one model layer to an adjacent layer at any location was kept at or below 1.5. There are at total of 21,965 nodes in the model with 955 nodes in each model layer.

**Figure E–14** shows a schematic representation, aligned west to east through the North Plateau of these geologic layers. In the figure, the geologic unit occurs in one or more horizontal regions, delineated by heavy horizontal lines. Each of these regions, corresponds to one or more of the model layers, indicated on the far left side of the figure. However, the layers in the model are neither horizontal nor uniform in thickness, but instead change in elevation and thickness to better capture the disposition of the geologic units at the site. In addition, some features shown in Figure E–14 do not occur throughout the entire extent of the site or model. As examples, the bed of Buttermilk Creek is situated in geologic units other than the Kent till for different reaches along its course, and the Lavery till-sand is limited in extent to a portion of the North Plateau.

The creeks at the site are sharply incised and have very steep stream banks. Because numerical considerations require model layers to be reasonably level, some parts of the upper layers were extended by necessity across these stream banks, creating nodes that are located "in the air." These nodes are effectively "inactive" and though not removed from the total node numbering, are not a part of the study area.

### E.3.3 Boundary Conditions

To accurately simulate the hydrogeological conditions, the boundary conditions have to be properly defined. The numerical model uses Dirichlet (specified head), Neumann (specified flux), and Cauchy (variable) boundary conditions to simulate groundwater flow into or out of the modeled area. The boundary conditions imposed for the base model are qualitatively described in this section.

The upper surface of the model consists of flux boundary conditions applied over areas receiving a net infiltration, determined by slope and groundcover, in addition to a variety of boundary conditions depicting other hydrologic influences such as surface water bodies, seeps and inflow from the weathered bedrock. These boundary conditions are indicated in **Figure E–15**. In this figure, grid cells with a heavy border denote constant head conditions, grid cells with small squares denote seepage faces, and shaded cells denote fluxes into the model. Also, nodes where thick-bedded unit inflow is occurring are modeled as flux nodes; crosses are used to denote these nodes. No-flow conditions exist along the boundaries where there are no seep or constant head designations. Seepage nodes exist along much of Erdman Brook, Franks, Quarry and Buttermilk Creek consistent with seepage observed along the steep banks of those streams and discussed above. Some nodes along Quarry Creek and Franks Creeks are modeled as constant head nodes with the head values approximated by the surface elevations at those locations.

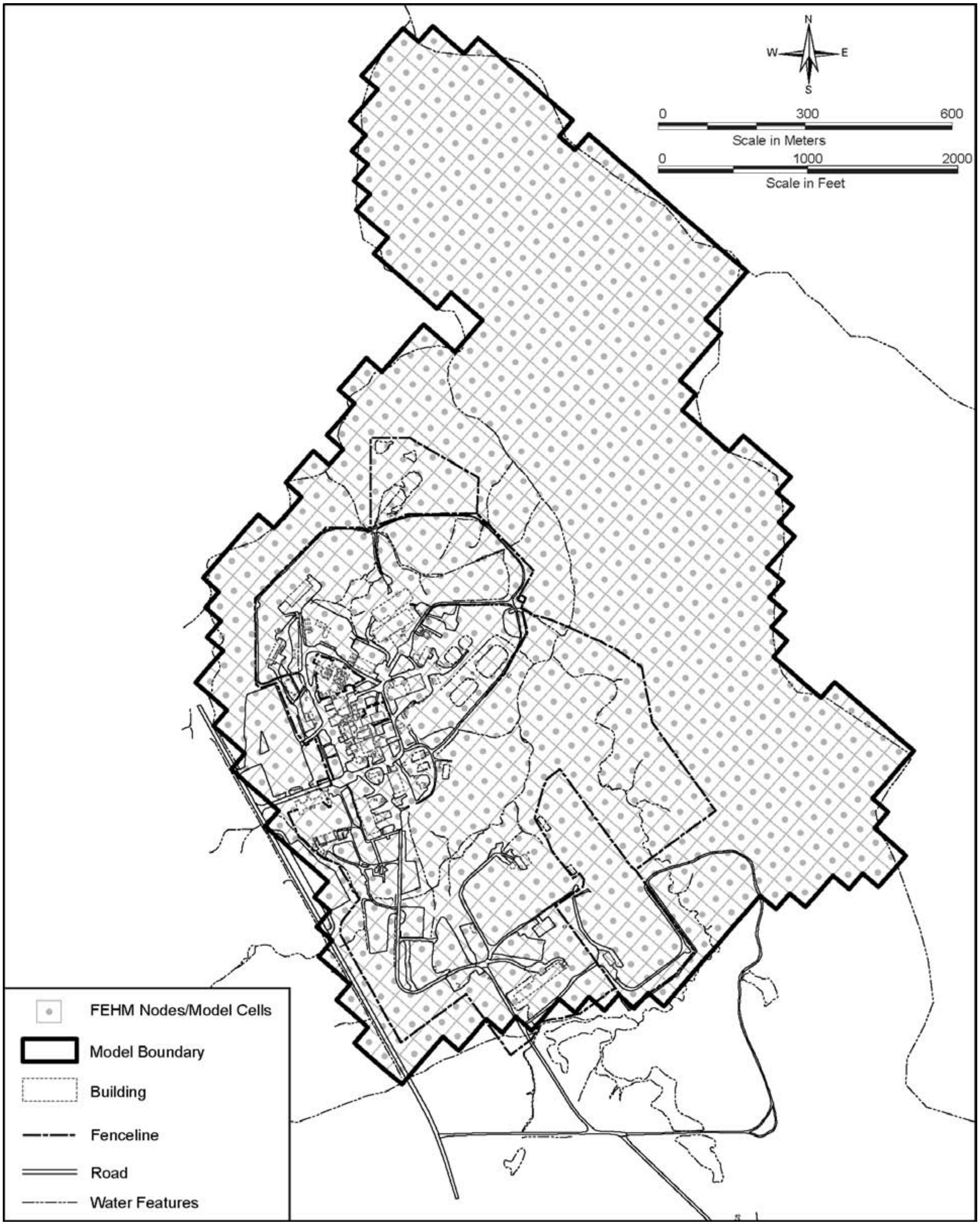


**Figure E–13 Plane View of Model Domain and Grid**

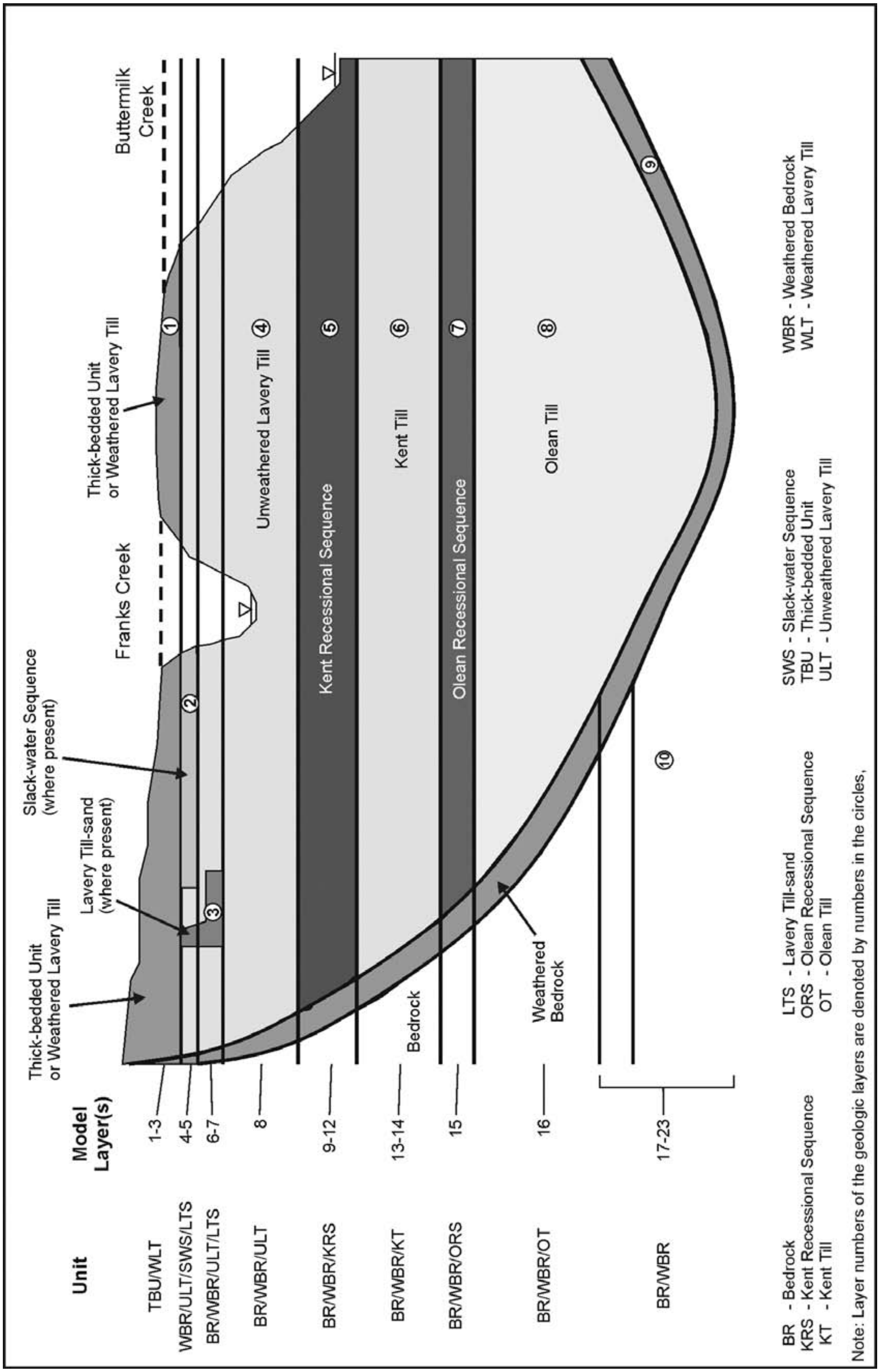


**Figure E–14 Schematic Representation of the Geologic Model in the Vicinity of the North Plateau**

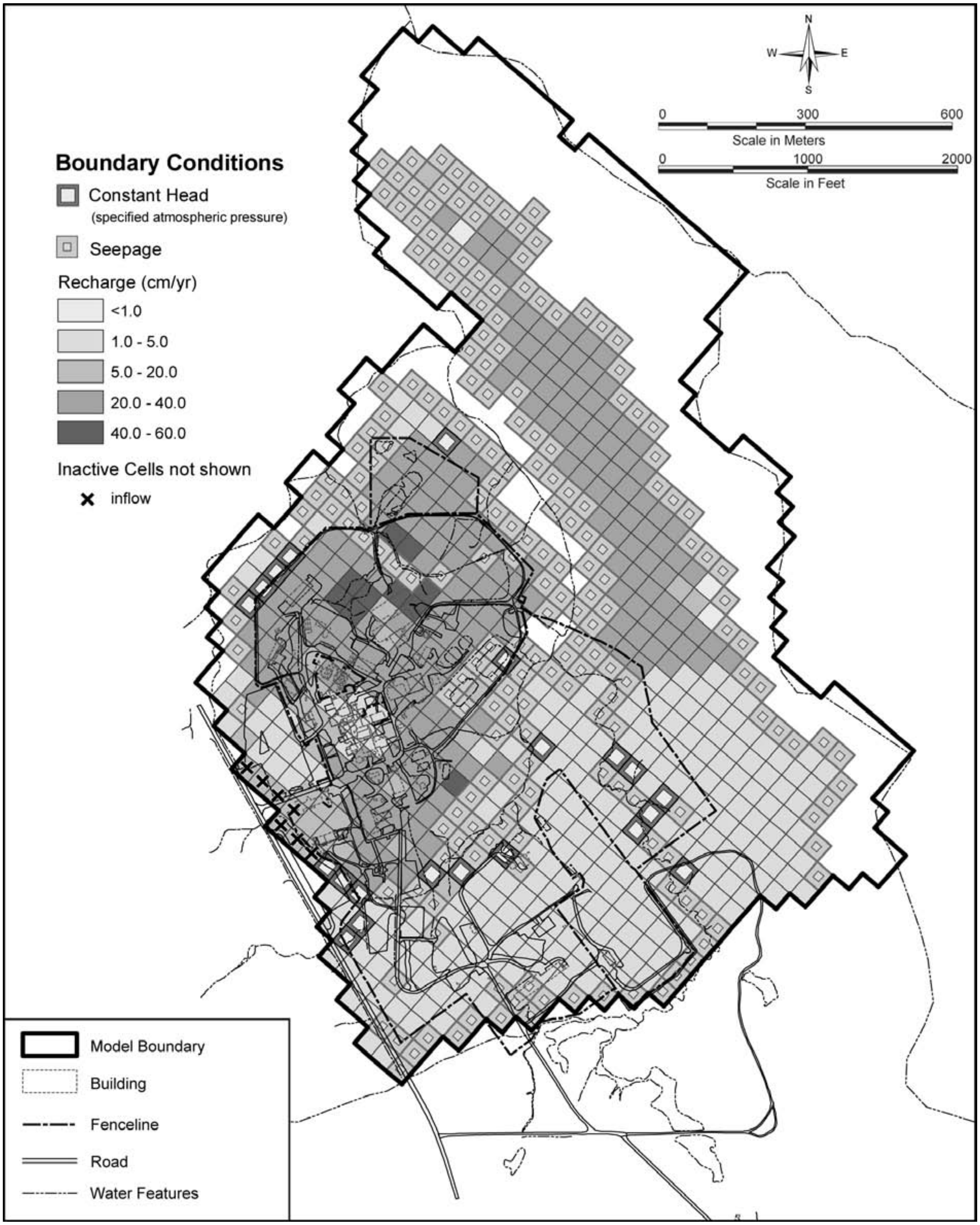


**Figure E–15  Surface Boundary Conditions for Model**

The initial estimate of the total inflow into the thick-bedded unit along the western boundary (the x's in Figure E–15) was the 142 cubic meters per day used by Yager (Yager 1987). Model runs with that value subsequently indicated that this inflow was excessive with the result that the predicted heads of wells (thick-bedded unit and Lavery till-sand) in the vicinity of the Main Plant Process Building were too high. The inflow was gradually reduced eventually to a value of 20 cubic meters per day, where the impacted head s appeared reasonable. Independent uncertainty calculations used estimated "low-medium-high" distributions for key parameters used by Yager to make his estimate for the inflow (hydraulic conductivity, height and length of the bedrock- thick-bedded unit interface, hydraulic gradient and porosity of the thick-bedded unit) provided an estimated an average inflow of 50 cubic meters per day and a median inflow of 37 cubic meters per day. The $5^{th}$ and $95^{th}$ quantiles were 12 and 150 cubic meters per day.

The unweathered Lavery till constitutes model layers 4 through 8 (see Figure E–14). Much of the western and southern boundaries for this layer are considered to be no-flow predicated on the assumption of vertical movement through this unit. Boundary conditions along Franks and Quarry Creeks vary based on model layer. Areas above the creeks receive seepage conditions. When the creek falls within the model layer, a constant head condition is used. Nodes located within the unweathered Lavery till below Quarry Creek and the lower reach of Franks Creek (after the confluence with Quarry Creek) are considered no-flow to account for the vertical flow up into the creek or the vertical movement downwards described above. Finally, seepage faces exist along the entire eastern boundary of the till to account for observations of water seen along the Buttermilk Creek valley.

Model layers 9 through 12 are made up of bedrock along the western boundary and Kent recessional sequence along the remaining boundaries. A no-flow boundary condition is imposed along the western boundary. The southern boundary and portions of the northern boundary (Kent recessional sequence) are also set as no-flow boundaries. The remaining boundaries vary based on model layer. Areas above the creeks receive seepage conditions. When the creek falls within the model layer, a constant head condition is used. Nodes within the Kent recessional sequence that fall below the lower reach of Franks Creek along the boundary are considered no-flow to account for vertical flow up into the creek.

Layers 13 and 14 are comprised of bedrock and Kent till. Flow is considered to be vertical through both of these units and hence, a no-flow condition is imposed at most locations along these boundaries. The only exception is the southeast corner of the model, where Buttermilk Creek intersects the unit. There, a constant head boundary condition is imposed in layer 13.

No-flow boundary conditions are applied along the entire perimeter of layer 15, consisting of the Olean Recessional Sequence and bedrock. The western boundary exists within the bedrock and groundwater flow is presumed vertical. The remainder of the boundary lies within the Olean Recessional Sequence. Little is known about the direction of flow within the Olean Recessional Sequence. The present base case model assumes that flow in the Olean Recessional Sequence is mostly vertical and thus, no-flow conditions are imposed for this layer along its perimeter.

Beginning in layer 16 and continuing in layer 17 and below, a constant head condition was applied along the western boundary of the model where those layers consist of bedrock. Formulated as the model evolved, this boundary condition was a key to achieving water levels near observed values in the Kent recessional sequence. The boundary condition is tied to an assumption that the water table existing within the Kent recessional sequence (to the east of the model boundary) occurs approximately 3 meters (10 feet) below the unit's highest and western-most extent on the bedrock valley upslope. To simulate that condition, a constant head condition was imposed at the model boundary (bedrock) directly west of the elevation of the Kent recessional sequence top less 3 meters (10 feet) (**Figure E–16**). Due to the variation in the Kent recessional sequence top elevation the constant head boundary condition was applied as appropriate in either layer 16 or 17. Horizontal movement is assumed for the regional aquifer, to the west of and outside the site model and the boundary conditions along that boundary remain constant at the upper elevation for the remaining deeper layers.

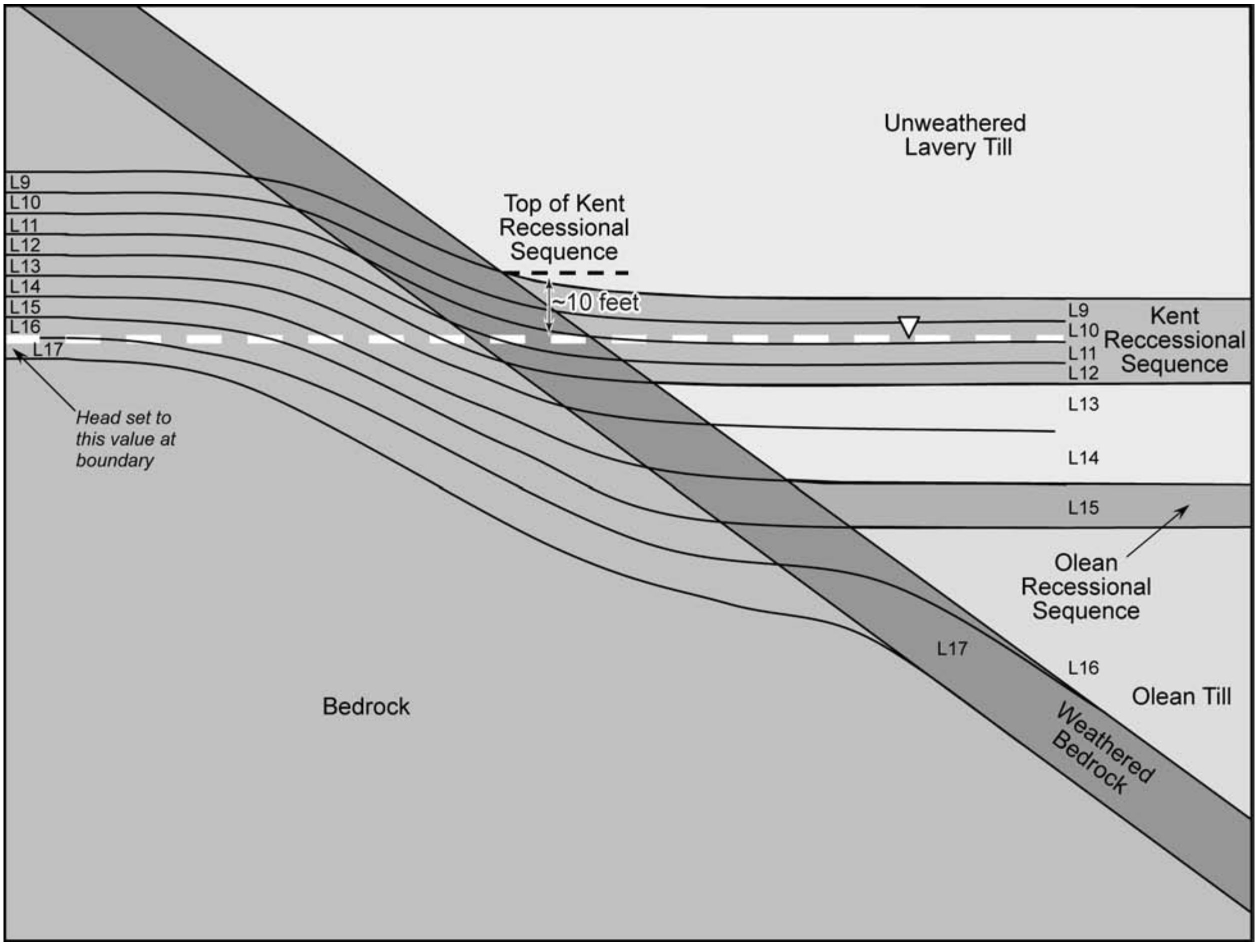


**Figure E–16 Boundary Condition Set Relative to Top of the Kent Recessional Sequence**

In the base case model, groundwater can effectively exit the system only by discharge to streams or seeps at the surface. However, there is some discussion in site literature of the weathered bedrock on site being part of a larger valley-wide weathered bedrock aquifer flowing to the north with discharge to Cattaraugus Creek or locations beyond (Zadins 1997). One of the primary uses of the present model is to examine alternative conceptual formulations. Related to this is a need to examine error in smaller, more manageable models based on surface and near surface units and decoupled from the deeper geology on site. Hence, an important sensitivity case boundary condition exists for layer 17. In an alternative conceptual model the assumption is made that water flows down through the weathered bedrock until it reaches the bottom of the bedrock valley. It then moves northward in the direction of the bedrock valley trough. This flow is implemented in a sensitivity (or equifinality) case below, as a constant head condition where the trough exits the northern boundary of the model. The constant head at each exit node is set equal to the elevation of the node.

### E.3.4 Input Parameters

This section provides a summary characterization of the physical properties of those materials comprising the geohydrological units found at the West Valley Site. Estimates of the properties are needed as input for all of the models used in this EIS to quantify the flow of groundwater and transport of contaminants at the site.

By nature each property described in this section is a distributed property. That is, the property's value varies from one location to another location. In models that approximate natural processes, these properties can be treated as either distributed or lumped (point-value), i.e., characterized by a single value. Statistical characterizations in terms of means, medians, etc., provide lumped parameter estimates, and geostatistical models provide spatially distributed estimates. The ability to develop the latter is at times constrained by the number of observations available, and/or by the distribution in space of those data. West Valley Site data are extensive in number but often are 1) the result of focused directed investigations, or 2) the product of routine monitoring at widely separated locations. Such data are informative for characterization but are not complete. Data sources used for the present compilation include both literature sources, typically appearing as document references in this appendix, and electronic data obtained from the site Laboratory Information Management System and provided by site personnel.

Reviews of site stratigraphy data and all well screening interval data came in the early phases of the modeling—before the quantitative characterization of hydraulic conductivities and before the determination of best target water levels for use in model calibration. A rating system was developed in which data from wells screened entirely in a single geohydrological unit were rated high whereas data from wells screened in more than one unit were rated lower, the exact rating depending on the relative amount screening in each unit, the relative hydraulic conductivities geologic materials involved, and their situation relative to one-another—low hydraulic conductivity over high, high over low, etc. These ratings were used to identify those well data retained for subsequent statistical characterization. The parameter values presented in this appendix are based on those data surviving both the initial stratigraphy-screen interval review and the follow-on statistical analyses.

There were two additional significant findings in the evaluations. First, in the case of the more permeable units, only hydraulic conductivity data collected after 1999 should be used for characterization. The reason is a distinctive change in conductivity data after 1999 likely due to the introduction of automated data-logging into the site groundwater protocols (**Figure E–17**). In Figure E–17(a), boxplots of the log-transformed data grouped by year clearly show how the hydraulic conductivity determinations are higher after 1999. The plot was constructed so that the horizontal line in each box is the median, and the lower and upper ends of the boxes indicate the 25$^{th}$ percentile and 75$^{th}$ percentile, respectively. In Figure E–17(b) median values for the "before 2000" data and median values for the "2000 and later" data at each well location were first plotted and then a line was drawn connecting the two points for that well location. Hence, a single line in the figure presents a visual comparison of the earlier and later hydraulic conductivities at the corresponding well location. A line increasing from left to right indicates that the more recent determinations of hydraulic conductivity at that location tend to be higher then the earlier determinations. Conversely, a line decreasing from left to right in the figure indicates that the later hydraulic conductivity determinations tend to be lower than those from earlier. Left-to-right increases in the location medians from through 1999 and after 1999, indicated by the gray lines in the figure, occur in 25 of the 27 locations where paired medians exist. That is, the more recent determinations are (collectively) higher than the earlier determinations at these 25 locations. There are only two locations, indicated with dashed lines for emphasis, where the median decreases, i.e., post 1999 hydraulic conductivities are lower than the corresponding earlier set (through 1999). This result, combined with the boxplot, suggests a significant difference exists between those thick-bedded unit hydraulic conductivity determinations made before 2000 and those determinations made during and after 2000.

The second finding for the evaluation of the hydraulic conductivities is that geostatistical characterization is practical only for the thick-bedded unit data. The data for the other units are too few and poorly distributed in space for the development of the statistical models (variograms) needed to estimate hydraulic conductivity in space, i.e., as a function of location and the set of observed values in the unit(s).

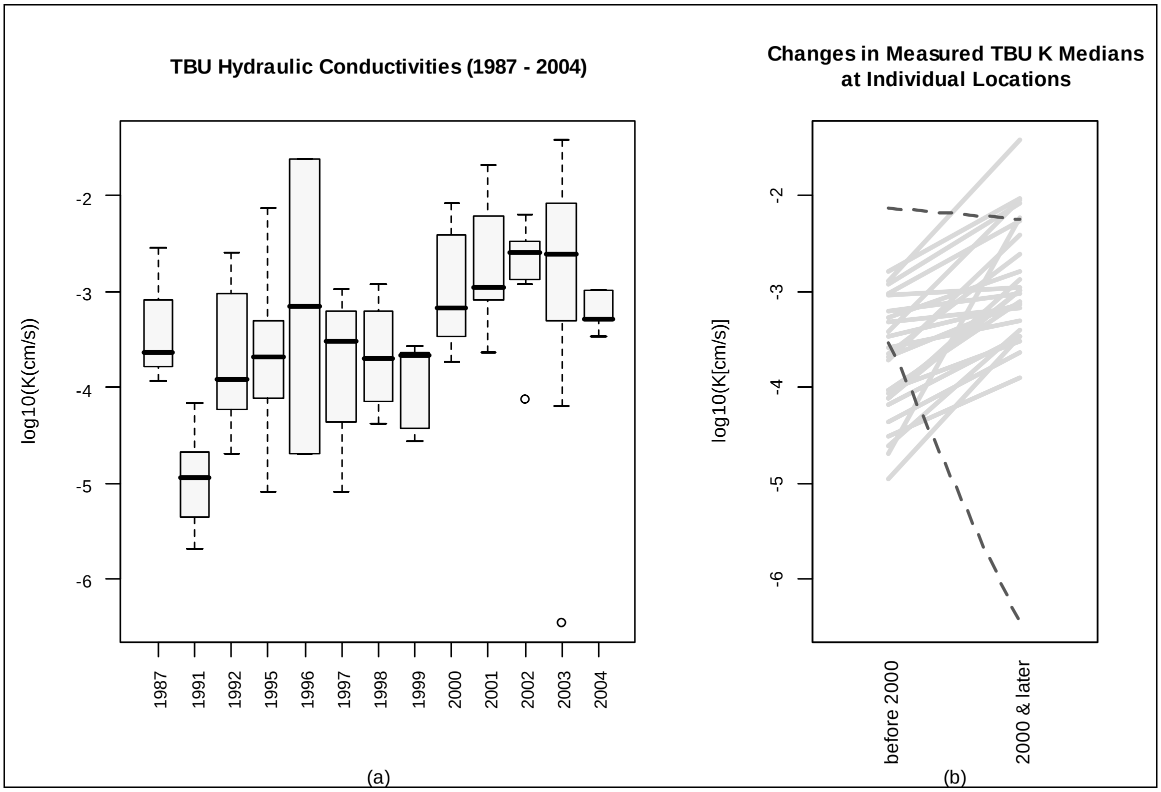


**Figure E–17 Changes in the Thick-bedded Unit Hydraulic Conductivity during the Period of 1987 to 2004**

### E.3.4.1 Hydraulic Conductivity

**Thick-bedded Unit**

The 27 hydraulic conductivity data of the thick-bedded unit are lognormally distributed with a mean of $4.43 \times 10^{-3}$ centimeters per second, and a median of $1.11 \times 10^{-3}$ centimeters per second. The observed minimum and maximum values are $1.25 \times 10^{-4}$ and $3.78 \times 10^{-2}$ centimeters per second, respectively.

The thick-bedded unit is the one unit for which geostatistical modeling is feasible. In the case of the geostatistical modeling those data remaining after screening and statistical evaluation were extended with hydraulic conductivity estimates derived from soil textures. These estimates employed artificial neural network methods. Data from locations with both hydraulic conductivity measurements and soil textures were used to train a Radial Basis Network or RBN network Soil texture data from locations without conductivity determinations were run then through the trained network to produce estimates for those locations. The soil textures used for training the network and subsequently predict addition hydraulic conductivities consisted of both laboratory determines textures extended by estimates from site geologists using boring log descriptions (Cohen 2006).

A spherical semi-variogram was fit to the log-transformed extended data (Englund and Sparks 1991). A kriged (interpolated) log-transformed hydraulic conductivity field was then developed (**Figure E–18**) using the U.S. Environmental Protection Agency (EPA) GEOEAS geostatistical software (*ibid.*). The kriged field covers a significant fraction of the thick-bedded unit on the North Plateau and hydraulic conductivity estimates are made in areas impacted by previous activities at the site. Locations of observed hydraulic conductivities used in the analyses are indicated by “+” symbols in the figure.

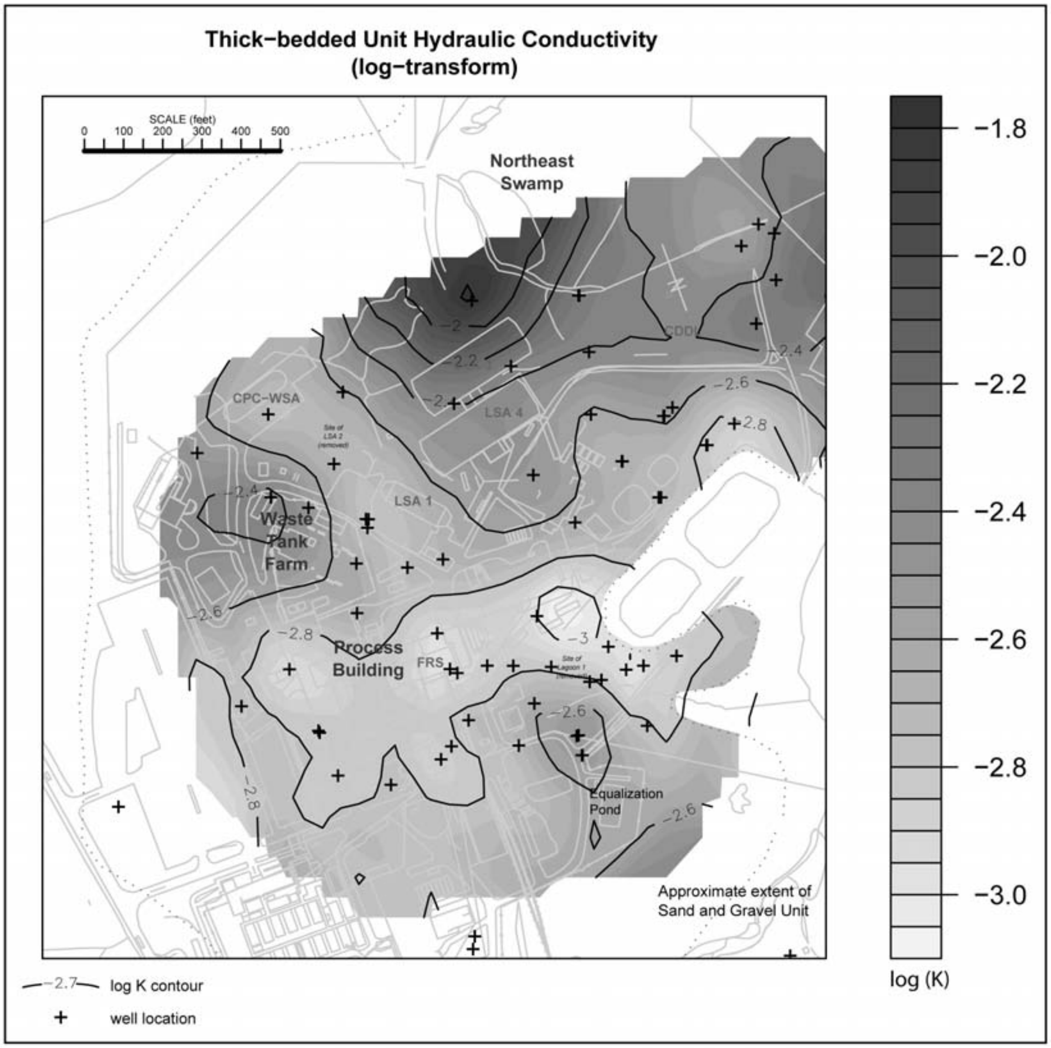


**Figure E–18 Kriged Thick-bedded Unit Hydraulic Conductivity (log-transformed)**

Improvement of the spatial model for the thick-bedded unit is limited by the current data density and distribution. The data do support development of (geostatistical) models showing intermediate range (200 to 400 foot) structure. As a part of the analyses, clustered data in the vicinity of the North Plateau Groundwater Recovery System and the Permeable Treatment Wall were removed from the data set during the development of the conductivity field seen in the figure. These clustered data have an average separation of approximately 1/10 that of the data in Figure E–18 and semi-variograms indicate some structure with a range on the order of tens of feet. This is suggestive of a hierarchical structure. Such structure in the thick-bedded unit and similar deposits at the West Valley Site would be consistent with the findings by researchers at other sites with glacio-fluvial deposits in buried bedrock valleys (Ritzi 2003). These structures are also discussed in Rubin's monograph.

The kriged field is incorporated into the FEHM mode by back-transforming the log field with bias correction (Weber 1992), and importing the corrected hydraulic conductivity field into the model cells as block averages. A large area of the thick-bedded unit is not included in the kriged field estimate. Kriging is an interpolation technique and there are no data in these areas. The present FEHM model uses an estimate of the mean hydraulic conductivity for these areas. Because the data are lognormally distributed the back-transformed estimate of the mean is used. Discussion of lognormal data can be found in the environmental literature, for example Gilbert's monograph. (See *Statistical Methods for Environmental Pollution Monitoring*.) That value is $2.48 \times 10^{-3}$ centimeters per second (6.3 feet per day). An anisotropy (horizontal to vertical hydraulic conductivity ratio) of 10 is assumed in the model. **Figure E–19** shows the thick-bedded unit hydraulic conductivity as imported into the model.

**Unweathered Lavery Till**

The predominant feature of the Lavery till hydraulic conductivity is a change with depth. At the shallowest depths, the hydraulic conductivity of the Lavery till is on the order of $10^{-4}$ centimeters per second (Prudic 1986, Bergeron and Bugliosi 1988, Kool and Wu 1991, WVNS 1993b). In the extreme this material is distinctly different from the till found deeper, and is even classified as a separate material—the weathered Lavery till—the deep material being known as the unweathered Lavery till. Alteration of till's chemical and physical properties is the result of the chemical/physical weathering due to infiltration of meteoric water. Fracturing of the till due to relaxation of the materials is also evident with fracture density decreasing with depth. In addition, the till material itself is subject to desiccation fracturing. At depth, observed field hydraulic conductivities approach laboratory values of $2 \times 10^{-8}$ to $8 \times 10^{-8}$ centimeters per second (Prudic 1986).

In **Figure E–20**, hydraulic conductivity, for wells screened at different depths in the unweathered Lavery till is plotted as a function of depth. Here the depth is defined as being from the top of the unweathered Lavery till to the top of the screened interval. In instances where more than one hydraulic conductivity determination has been made the arithmetic mean at that location is plotted. A decrease in the maximum hydraulic conductivity observed with depth is evident in the figure, particularly when the heavy gray line is included delineating the envelope of plotted values. This figure suggests that by the time a depth of 10 meters is reached the hydraulic conductivity is approaching values less than $1 \times 10^{-7}$ centimeters per second.

In light of the dependence on depth and the low number of data locations after screening, the emphasis in the unweathered Lavery till characterization for the model was on vertical change. A simple rule-based two-layered model for the unweathered Lavery till hydraulic conductivity was implemented:

- At depths of 3 meters or more, $K_h = 6.00 \times 10^{-8}$ centimeters per second.
- At depths of less than 3 meters, $K_h = 1.00 \times 10^{-6}$ centimeters per second.

The first rule is supported by the data. The second number is an interpolation between the weathered Lavery till and the deep unweathered Lavery till.

No descriptive statistics are presented for the unweathered Lavery till hydraulic conductivity because of the tendency toward lower values with increasing depth.

**Weathered Lavery Till**

The seven (7) hydraulic conductivity data for the weathered Lavery till are neither normally nor lognormally distributed. The mean is $3.36 \times 10^{-4}$ centimeters per second and the median is $1.72 \times 10^{-4}$ centimeters per second. The observed minimum and maximum values are $4.87 \times 10^{-7}$ and $1.50 \times 10^{-3}$ centimeters per second, respectively. The geometric mean is $4.95 \times 10^{-5}$ centimeters per second.

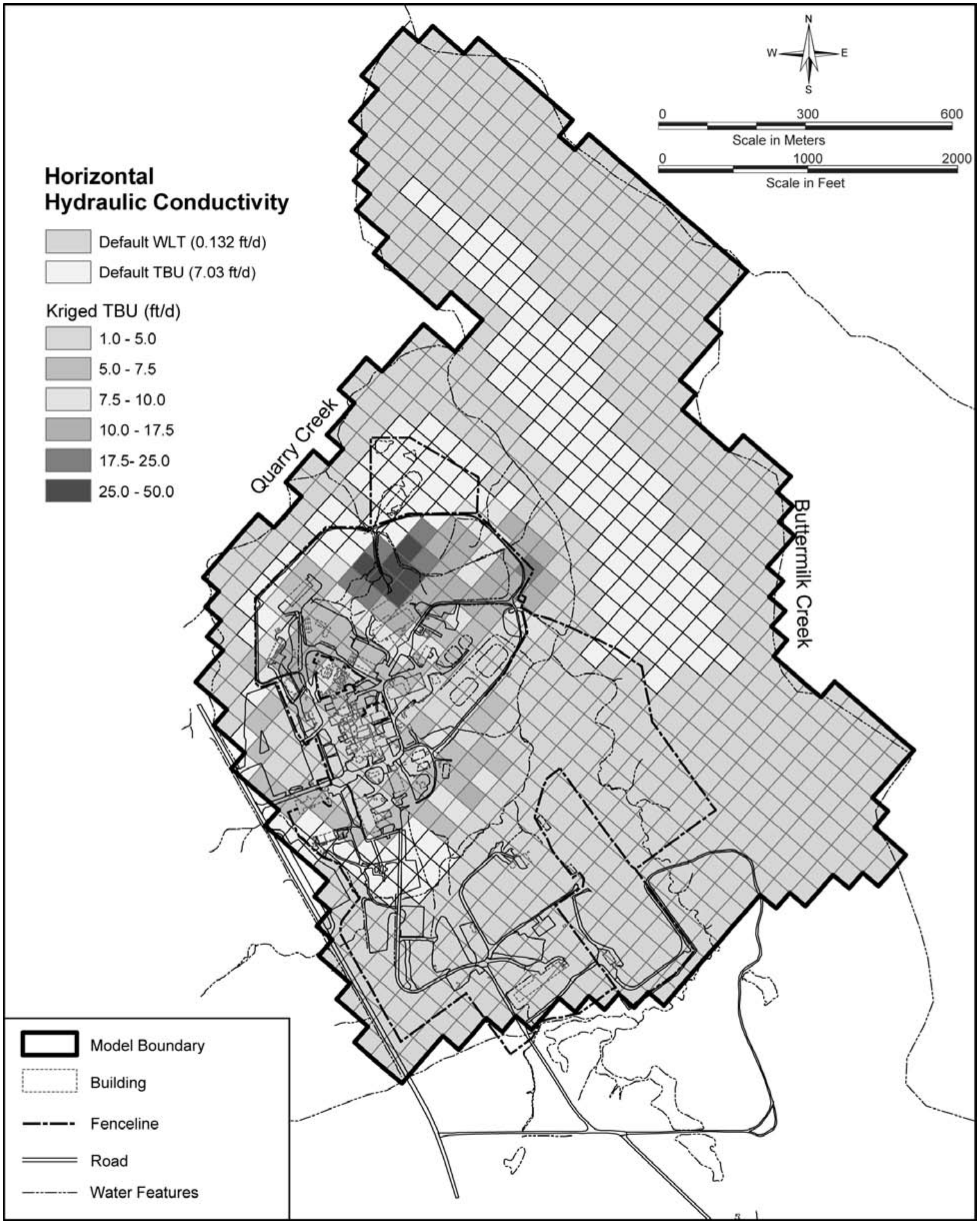


**Figure E–19 Horizontal Hydraulic Conductivity of the Thick-bedded Unit in Layers 1, 2, and 3**

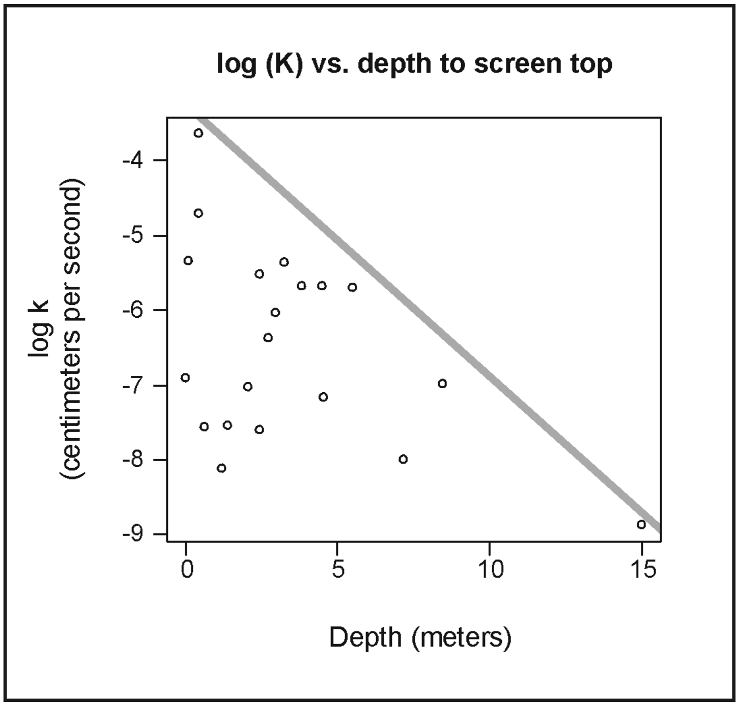


**Figure E–20 Unweathered Lavery Till Hydraulic Conductivity as a Function of Depth**

No structure was evident in weathered Lavery till semi-variograms. Well locations are scattered about the site, mostly on the South Plateau and the average distance between locations is hundreds of feet—likely exceeding the scale of spatial any structure in the unit. Observed weathered Lavery till hydraulic conductivities vary over several orders of magnitude. Based on the observed wide range in values an initial hydraulic conductivity of one tenth the back-transformed estimate ($4.65 \times 10^{-4}$ centimeters per second), or $4.65 \times 10^{-5}$ centimeters per second, was used in the FEHM model. Although not completely optimal, sensitivity of model results to changes in the parameter value appears low and the initial input value has not been changed.

**Slack-water Sequence**

The slack-water sequence is permeable and the observed hydraulic conductivities appear to change around 1999 in a manner similar to the thick-bedded unit. Twelve (12) post 1999 locations remained after the initial screening. However, the data are clustered, and three-quarters of the data locations are in the vicinity of the North Plateau Groundwater Recovery System and the Permeable Treatment Wall. The values at the three locations lying away from the cluster are interquartile values and are not much different than the observations at the cluster locations. The slack-water sequence hydraulic conductivity used in the model was initially set equal to the back-transformed estimate ($1.61 \times 10^{-2}$ centimeters per second), and the anisotropy set to 10. However, early runs of the model indicated that the slack-water sequence was effectively draining the thick-bedded unit, precluding any reasonable match to observed conditions in that unit. As a result, both the (horizontal) hydraulic conductivity and the anisotropy were adjusted as part of the calibration. The slack-water sequence hydraulic conductivity from that process was $5.29 \times 10^{-3}$ centimeters per second. The final anisotropy was 20.

The 12 hydraulic conductivity data of the slack-water sequence are lognormally distributed with a mean of $2.44 \times 10^{-2}$ centimeters per second, and a median of $1.11 \times 10^{-3}$ centimeters per second. The observed minimum and maximum values are $8.19 \times 10^{-4}$ and $1.13 \times 10^{-1}$ centimeters per second, respectively.

**Lavery Till-Sand**

The Lavery till-sand is similar to the thick-bedded unit in that there appear to be differences between the pre-2000 and post 2000 hydraulic conductivity determinations. Only the hydraulic conductivities determined after 1999 were included in the analyses used to estimate the Lavery till-sand hydraulic conductivity. The minimum variance unbiased estimate of those locations, $1.85 \times 10^{-3}$ centimeters per second, was used for the Laverty till-sand horizontal hydraulic conductivity in the model. An anisotropy of 10 was assumed.

The five (5) hydraulic conductivity data of the Lavery till-sand are lognormally distributed with a mean of $2.04 \times 10^{-3}$ centimeters per second, and a median of $2.21 \times 10^{-3}$ centimeters per second. The observed minimum and maximum values are $1.06 \times 10^{-4}$ and $4.54 \times 10^{-3}$ centimeters per second, respectively.

**Kent Recessional Sequence**

The Kent recessional sequence is similar to the thick-bedded unit with differences between the pre-2000 and the 2000 and later hydraulic conductivities. Hence, only those hydraulic conductivities determined after 1999 were included in the analyses. Data from seven locations were used. However, the data are problematic. Their values ranged over three order of magnitudes consistent with the complex structure—lacustrine and kame deposit—and the distances between sample or well locations. The Kent recessional sequence data have a back-transformed estimate of $6.39 \times 10^{-4}$ centimeters per second and a median of $1.78 \times 10^{-4}$ centimeters per second. The back-transformed estimate was used for the initial Kent recessional sequence hydraulic conductivity. Calibration and subsequent sensitivity reduced that number by a factor of four and the final hydraulic conductivity for the Kent recessional sequence became $1.60 \times 10^{-4}$ centimeters per second with an assumed anisotropy of 10.

The seven (7) hydraulic conductivity data of the Kent recessional sequence are lognormally distributed with a mean of $7.03 \times 10^{-4}$ centimeters per second. The observed minimum and maximum values are $2.98 \times 10^{-6}$ and $1.62 \times 10^{-3}$ centimeters per second, respectively.

**Kent Till**

Little is known about the Kent till. In the present model it is assumed to be similar to the unfractured unweathered Lavery till.

**Olean Till**

Little is known about the Olean till. In the present model it is assumed to be similar to the unfractured unweathered Lavery till.

**Olean Recessional Sequence**

Little is known about the Olean Recessional Sequence and it is assumed to be similar to the Kent recessional sequence. An initial Olean Recessional Sequence hydraulic conductivity estimate of $1.0 \times 10^{-4}$ centimeters per second was used in the model. Unlike the Kent recessional sequence, that value has not been varied as a part of calibration. An anisotropy of 10 was assumed.

**Weathered Bedrock**

The weathered bedrock hydraulic conductivity used in the model is $1.0 \times 10^{-5}$ centimeters per second. This value is taken from Prudic (Prudic 1986). An anisotropy of 10 was assumed.

### Unweathered Bedrock

The unweathered bedrock hydraulic conductivity used in the model is $1.0 \times 10^{-7}$ centimeters per second. This value is taken from Prudic (Prudic 1986). An anisotropy of 10 was assumed.

All of the hydraulic conductivities used in the groundwater models are collected in **Table E–3**. The hydraulic conductivities presented in the table are final values from the hand-calibrated model discussed below in Section 3.5 and take on a variety of forms including statistically derived values from this section, single empirical values, a rule set, and values resulting from the calibration.

**Table E–3 Final Hydraulic Conductivities for the West Valley Groundwater Models**

<table>
<tr><th colspan="2">Unit</th><th>Nominal $K_h$ (centimeters per second)</th><th>Nominal $K_v$ (centimeters per second)</th><th>Anisotropy ($K_h$ / $K_v$)</th></tr>
<tr><td colspan="2">Thick-bedded Unit</td><td>Variable [a]</td><td>$K_h$ / 10</td><td>10</td></tr>
<tr><td colspan="2">Thick-bedded Unit-outlying</td><td>$2.48 \times 10^{-3}$ [b]</td><td>$2.48 \times 10^{-4}$ [2]</td><td>10</td></tr>
<tr><td colspan="2">Slack-water Sequence</td><td>$5.29 \times 10^{-3}$</td><td>$2.65 \times 10^{-5}$</td><td>20</td></tr>
<tr><td colspan="2">Lavery Till-Sand</td><td>$1.85 \times 10^{-3}$</td><td>$1.85 \times 10^{-4}$</td><td>10</td></tr>
<tr><td colspan="2">Kent Recessional Sequence</td><td>$1.60 \times 10^{-4}$</td><td>$1.60 \times 10^{-5}$</td><td>10</td></tr>
<tr><td colspan="2">Olean Recessional Sequence</td><td>$1.0 \times 10^{-4}$</td><td>$1.0 \times 10^{-5}$</td><td>10</td></tr>
<tr><td colspan="2">Weathered Lavery Till</td><td>$4.65 \times 10^{-5}$</td><td>$4.65 \times 10^{-5}$</td><td>1</td></tr>
<tr><td colspan="2">Weathered Bedrock</td><td>$1.0 \times 10^{-5}$</td><td>$1.0 \times 10^{-6}$</td><td>10</td></tr>
<tr><td colspan="2">Bedrock</td><td>$1.0 \times 10^{-7}$</td><td>$1.0 \times 10^{-8}$</td><td>10</td></tr>
<tr><td colspan="5">Special Cases Unweathered Lavery Till, Kent Till, Olean Till:</td></tr>
<tr><td rowspan="5">Unweathered Lavery Till</td><td colspan="4">A set of rules</td></tr>
<tr><td colspan="4">1.) At depths of 3 meters or more, $K_h = K_v = 6.0 \times 10^{-8}$ (centimeters per second) (anisotropy = 1) – deep</td></tr>
<tr><td colspan="4">2.) At depths of less than 3 meters, $K_h = K_v = 1.0 \times 10^{-6}$ centimeters per second – shallow</td></tr>
<tr><td colspan="4">3.) The depth 3 meters and the shallow</td></tr>
<tr><td colspan="4">Use for Olean Till, Kent Till (lower number, $6.0 \times 10^{-8}$ centimeters per second, only) and anisotropy = 1 ($K_h = K_v$) [c]</td></tr>
</table>

[a] Kriged field.
[b] For use in areas where no thick-bedded unit hydraulic conductivity determinations have been made and extrapolation would be required.
[c] Depth measured from the top of the unweathered Lavery till.

### E.3.4.2 Infiltration

The recharge for the model evolved from a composite developed from a review taken from multiple sources including the groundwater and vadose zone hydrology Environmental Information Documents (WVNS 1993b, 1993c), and several modeling reports (Bergeron and Bugliosi 1988, Kool and Wu 1991, Prudic 1987, Yager 1987). In the initial phase of the modeling two infiltration rates were applied. Based on the information in these reports a net recharge of 32 centimeters per year was applied uniformly across the thick-bedded unit, and a rate of 3 centimeters per year was applied across the remainder of the site, where the surficial unit is the weathered Lavery till. For the North Plateau, as calibration proceeded, zones having other recharge reflecting differences in surface conditions were added into the model. The number of these zones, however, was kept low to avoid over-calibration. The South Plateau infiltration was adjusted during the calibration but not in zones. The final infiltration used in the base model is shown in Figure E–15 as shaded surface flux cells.

A few porosity data are available for the near surface units. Estimates for the deeper units are based on similarity of a material to the thick-bedded unit or unweathered Lavery till as appropriate, or adapted from literature values. Effective porosity has been assumed to equal the total porosity. Model porosities are shown in **Table E–4**.

**Table E–4 Porosities**

| *Geologic Unit* | *Total Porosity (dimensionless)* | *Reference* |
|---|---|---|
| Thick-bedded Unit | 0.22 | WVNS 1993b, Yager 1987 (Specific yield) |
| Weathered Lavery Till | 0.324 | Prudic 1986 |
| Slack-water Sequence | 0.35 | WVNS 1993b |
| Unweathered Lavery Till | 0.324 | Prudic 1986 |
| Lavery Till-Sand | 0.22 | Geology EID |
| Kent Recessional Sequence | 0.22 | Kent recessional sequence assumed to be like the thick-bedded unit |
| Kent Till | 0.324 | Kent till assumed to be like unweathered Lavery till |
| Olean Recessional Sequence | 0.22 | Olean Recessional Sequence assumed to be like thick-bedded unit |
| Olean Till | 0.324 | Olean till assumed to be like unweathered Lavery till |
| Weathered Bedrock (Shale) | 0.4 | Assumed |
| Bedrock (Shale) | 0.05 | Adapted from Domenico and Schwartz (Domenico 1990) |

### E.3.4.3 Soil Moisture Characteristics

Soil moisture characteristics were modeled as a function of the representative hydraulic conductivity, $(K_xK_yK_z)^{1/3}$. In this approach a lookup table (**Table E–5**) is used for setting the soil moisture (van Genuchten) parameters based on established empirical relationships and keyed to the representative hydraulic conductivity for the material. The parameterization of this table (Pantex 2004) stems from earlier statistical characterizations as documented in the EPA RETC manual and code (EPA 1991).

**Table E–5 Lookup Table for Soil Moisture Characteristics**

| $(K_xK_yK_z)^{1/3}$ *(feet per day)* | $S_r$ | $\alpha$ ($cm^{-1}$) | *N* |
|---|---|---|---|
| <0.0001 | 0.2 | 0.6 | 1.25 |
| 0.0001 - 0.001 | 0.2 | 1 | 1.3 |
| 0.001 - 0.01 | 0.2 | 1.5 | 1.5 |
| 0.01 - 0.10 | 0.15 | 1.9 | 1.6 |
| 0.10 - 1.0 | 0.15 | 2.2 | 1.8 |
| 1.0 - 5.0 | 0.15 | 2.4 | 1.9 |
| 5.0 - 10.0 | 0.1 | 3 | 2 |
| 10.0 - 30.0 | 0.1 | 3.5 | 2.2 |
| >30 | 0.1 | 3.7 | 2.5 |

### E.3.5 Model Calibration

The model has been calibrated both manually and using an automated calibration code, Parameter Estimation (PEST) (Doherty 2008). The manual calibration was accomplished by the comparison of model predicted head with the median of observed groundwater level elevations at each of 56 target well locations, and by the comparison of model predicted seepage flows with estimated flows from the field. The 56 target locations and median water level values are listed in **Table E–6**. Target well locations did not align with the node locations and hence, the model predicted heads at the well locations were estimated by linear interpolation between nodes.

**Table E–6 Groundwater Elevation Targets for Model Calibration**

| *Unit* | *Well* | *Median (feet amsl)* | *TIER* |
|---|---|---|---|
| Thick-bedded Unit | 103 | 1391.4 | 1 |
| | 104 | 1385.5 | 1 |
| | 111 | 1383.0 | 1 |
| | 116 | 1380.5 | 1 |
| | 203 | 1394.4 | 1 |
| | 205 | 1393.1 | 1 |
| | 301 | 1410.7 | 1 |
| | 307 | 1402.0 | 2 |
| | 401 | 1410.3 | 1 |
| | 403 | 1408.0 | 2 |
| | 406 | 1393.3 | 1 |
| | 601 | 1377.3 | 1 |
| | 602 | 1387.8 | 2 |
| | 603 | 1391.9 | 1 |
| | 604 | 1391.6 | 1 |
| | 801 | 1376.6 | 2 |
| | 804 | 1369.9 | 2 |
| | 8606 | 1392.8 | 1 |
| | 8608 | 1393.6 | 2 |
| | 8609 | 1391.8 | 1 |
| | 8612 | 1364.8 | 2 |
| | EW01 | 1377.8 | 2 |
| | EW04 | 1379.2 | 2 |
| | NB1S | 1435.7 | 2 |
| | WP04 | 1382.2 | 2 |
| Slack-water Sequence | 501 | 1391.3 | 1 |
| | 408 | 1391.8 | 1 |
| Sand and Gravel Unit | 502 | 1388.0 | 2 |
| | 802 | 1368.4 | 1 |
| Kent Recessional Sequence | 902 | 1283.3 | 2 |
| | 903 | 1264.0 | 2 |
| | 1002 | 1285.7 | 1 |
| | 1004 | 1291.4 | 1 |
| | 8610 | 1264.4 | 1 |
| | 8611 | 1264.3 | 1 |

| Unit | Well | Median (feet amsl) | TIER |
|---|---|---|---|
| Lavery Till-Sand | 202 | 1394.6 | 1 |
| | 204 | 1394.5 | 1 |
| | 206 | 1394.3 | 1 |
| | 208 | 1388.0 | 1 |
| | 302 | 1400.4 | 2 |
| | 402 | 1401.4 | 1 |
| | 404 | 1400.6 | 1 |
| | 701 | 1382.6 | 2 |
| Unweathered Lavery Till | 108 | 1361.6 | 2 |
| | 109 | 1374.7 | 2 |
| | 110 | 1375.4 | 1 |
| | 405 | 1400.8 | 1 |
| | 702 | 1365.0 | 2 |
| | 703 | 1382.8 | 2 |
| | 705 | 1394.7 | 1 |
| | 904 | 1363.9 | 2 |
| Weathered Lavery Till | 907 | 1378.2 | 1 |
| | 1007 | 1379.7 | 2 |
| | 1008C | 1398.9 | 1 |
| | 96-I-01 | 1378.0 | 2 |
| Bedrock | 83-4E | 1242.6 | 1 |

With one or two exceptions the wells on the list are represented by a large number of observed water levels, i.e., have been tracked over a number of years, exhibit no or little trend, and exhibit no anomalous behavior in their hydrographs. Targets designated as TIER 1 targets were judged to be more reliable in this respect than the TIER 2 targets. Initial calibration used only TIER 1 targets but was later extended to include TIER 2 targets.

Trending in the water levels was evaluated using the United States Geological Survey code KENDALL (USGS 2005). Trend testing accounted both for seasonal variation and for external influences, e.g., multi-year climatological variations.

The trend methodology employed was the seasonal Kendall with a LOWESS[1] smooth of precipitation. Four seasons were employed—reflecting the water level measurement schedules. The precipitation record was daily from January 1990 through February 2006 with some records missing in the first year. The daily data were summed as quarterly based numbers for the LOWESS. The analyses were performed over the maximum period for which data are available. Selection of the target levels was restricted to locations with more than 32 observations and in most cases more the 60 observations.

The occasional spiked or outlying water level occurs in the observed water level data at a number of locations. For this reason, the median water levels at the (TIER 1 or TIER 2) locations were selected as the representative target level values to be used in the calibration. However, the differences between the median and arithmetic mean or average water levels were small, particularly when compared to the observed water level versus predicted water level residuals. **Figure E–21** shows the locations of the target wells used in the calibration.

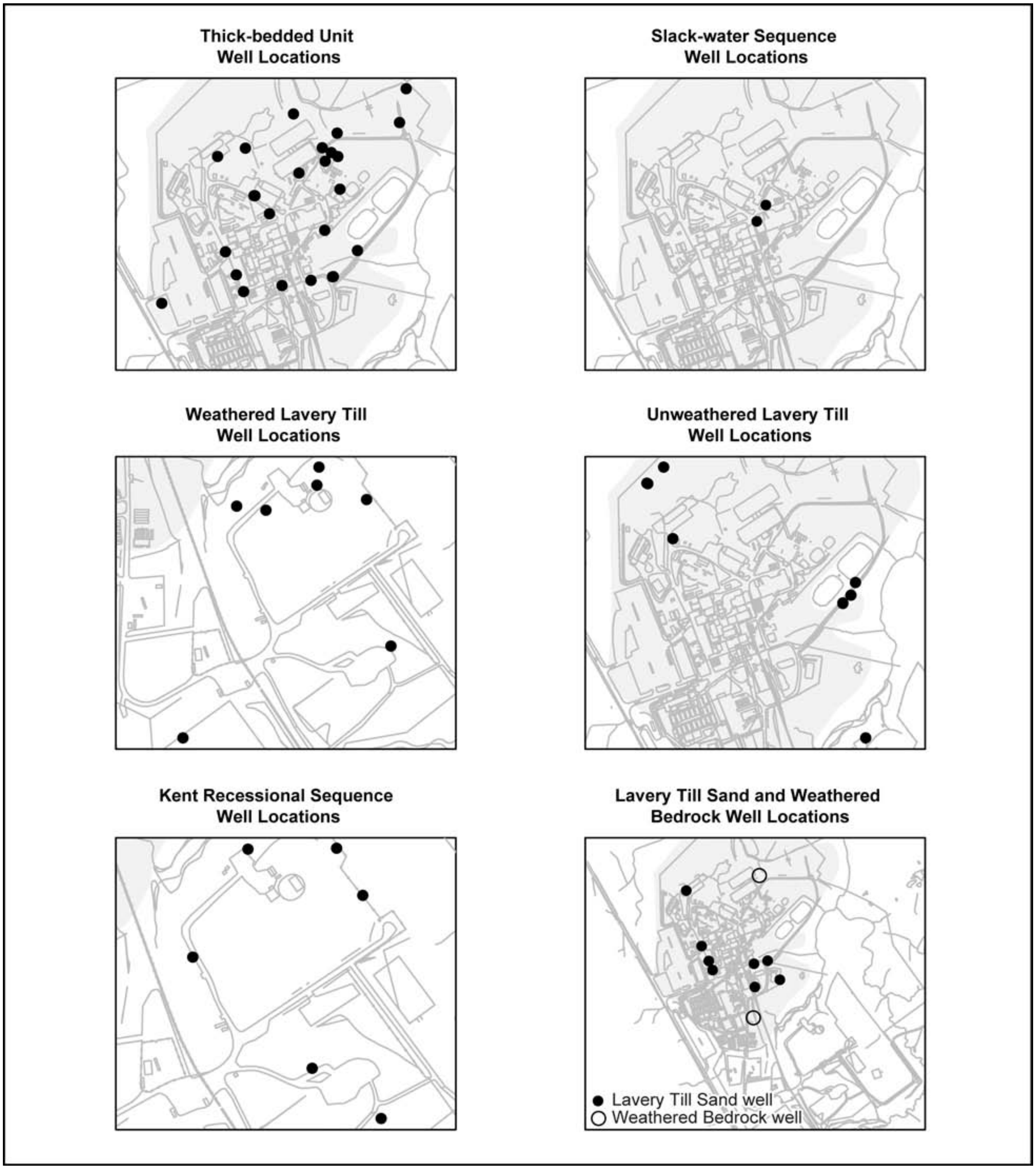


**Figure E–21 Locations of Target Wells Used in Calibration of the Site Model**

*[1] LOWESS or LOESS, is a locally weighted polynomial regression used here to account for precipitation, an external variable that potentially confounds the trend analysis.*

**Manual Calibration**

Calibration to the target levels was an iterative process using both qualitative and quantitative procedures. It began with a visual fit obtained by iterating between modification of one or more parameters, running the model, and visual/quantitative inspection of predicted head versus observed water-level plots. The visual inspection used two criteria to determine the goodness of a run with a given combination of parameters. First, all of the points in the observed versus predicted head scatter-plot should center around the one-to-one line. Second, all of the points should lie within +/- 3 meters (10 feet) of that line. As calibration improved, a quantitative measure was used: regression of observed versus predicted head should result in an adjusted square of the correlation coefficient ($R^2$) equal to or greater than 0.95.

The seep comparisons used in the calibration were more informal than the head comparisons. Seeps were modeled for nodes in the vicinity of those seep and spring locations identified in Figure E–10 in Section 2.3.1. The discharges from these nodes were then compared with the tabulated observed values in Table E–2. Comparisons were semi-quantitative imposing the constraint that modeled discharges reasonably approximate the reported discharges. Model gridding and a significant uncertainty in the observed discharges provide the rationale for this approach.

The manual calibration focused on infiltration, inflow into the thick-bedded unit from the west, and deeper head boundary conditions as the varying model parameters. This tacitly gave preference to the hydraulic conductivity data which with one exception were treated as fixed by observation. That one exception was the hydraulic conductivity for the slack-water sequence. That parameter had to be adjusted in the present calibration, because the slack-water sequence, was effectively draining the thick-bedded unit, precluding any fit between observed and predicted heads at a large number of target locations.

Final observed versus predicted head scatter-plots of the manually calibrated model are shown in **Figures E–22** and **E–23**. Figure E–22 presents the results for all target well locations. This figure shows how the target locations fall into two (2) natural groupings, an upper aquifer and a lower aquifer. The upper aquifer system is comprised of the thick-bedded unit, slack-water sequence, weathered Lavery till, unweathered Lavery till, and Lavery till-sand. The geohydrological units found in the lower units are the Kent recessional sequence, Olean till, Olean Recessional Sequence, weathered bedrock and bedrock. The soils and groundwater contamination and source areas are found at or near the surface at the site, and most of the data characterizing groundwater at the site are from units in the upper system. For these reasons the focus of this calibration was on the upper system, and hence, Figure E–23.

The adjusted $R^2$ for the upper aquifer plot is 0.953. The adjusted $R^2$ for all target locations, Figure E–22, is 0.992, but the high value reflects the high-low grouping of the data, i.e., predicted-observed pairs, more than goodness of fit. Other useful indications in these figures include the 95 percent confidence band (shaded dark gray), the 95 prediction band (shaded light gray), the one-to-one line (heavy solid line) and the +/- 3-meter (10-foot) band about that line (dotted lines). The confidence and prediction bands are centered about the regression lines (not shown). In both figures, the one-to-one line lies within the confidence band. While no statistical inference can be drawn from this, the fact that the confidence band—an entity constructed to contain the true observed-versus predicted regression line—also contains the one-to-one line does provide a degree of confidence in the calibration with respect to the heads.

The observed (see Section E.2.3.1) and modeled values for the drainage base flows and seep discharges are listed in **Table E–7**. The match between the two sets of values is good in light of the uncertainties in the observed flow estimates as evidenced by the Erdman Brook numbers. The model discharge to Erdman Brook is higher than the Kappel and Harding number but much lower than Yager's indirect estimate.

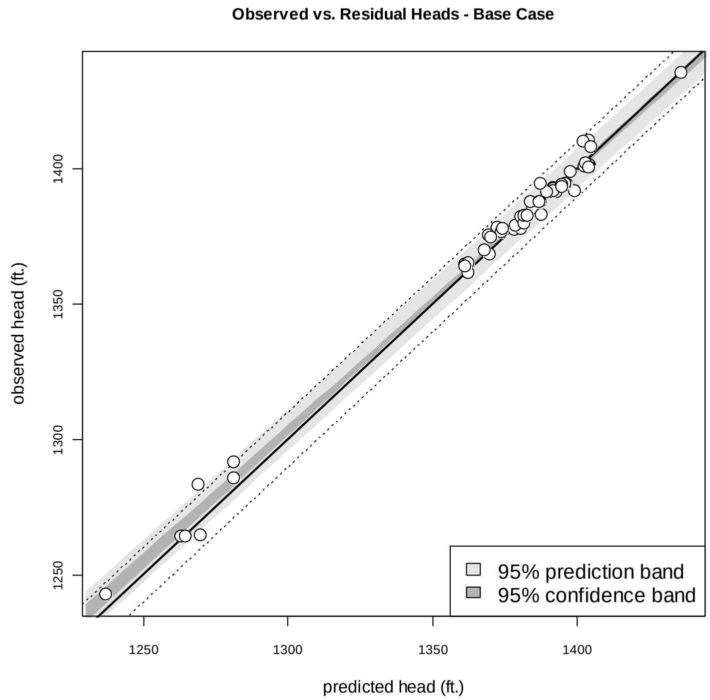


**Figure E–22 Observed Versus Predicted Heads in the Base Case Model (all well locations)**

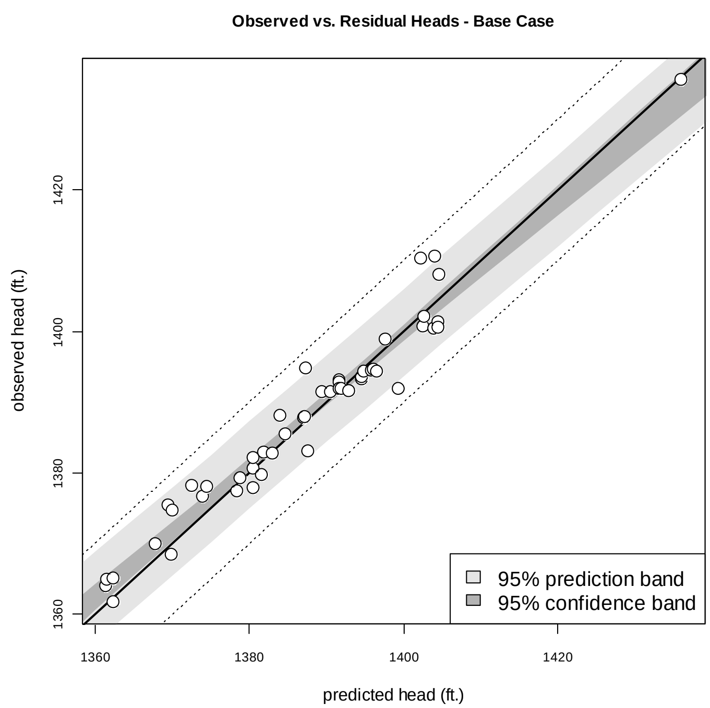


**Figure E–23 The Observed Versus Predicted Heads in the Base Case Model (upper aquifer only)**

**Table E–7 Comparison of Observed and Modeled Seep and Stream Discharges**

| *Location* | *Observed Discharge (cubic meters per day)* | *Predicted Discharge (cubic meters per day)* |
|---|---|---|
| NP-1 base flow | 29 | 8 |
| NP-2 base flow | 6 | 20 |
| NP-3 base flow | 113 | 86 |
| NP – Total | 148 | 114 |
| Quarry Creek and Franks Creek | 20 | 36 |
| Erdman Brook (Yager/Kappel and Harding) | 220/10 | 61 |
| Total | 388/178 [a] | 211 |

[a] Total using Kappel and Harding flow for Erdman Brook.
Note: To convert cubic meters per day to cubic feet per day, multiply by 35.314.

An understanding of the conceptual changes introduced by the new geological interpretations—a realignment of the slack-water sequence and Lavery till-sand—should contribute to a better understanding of the North Plateau seepage faces along Erdman Brook.

The predicted channel base flows (NP-1, NP-2, and NP-3) agree reasonably well with the observed values but, the total predicted flow is low and the observed and predicted distributions of the flow among the three channels differ. The flow at NP-3 is the largest for both the observed and predicted cases, accounting for 76 percent and 75 percent of the total channel base flow in each case, respectively. The split of the remaining 24 percent (25 percent) between the NP-1 and NP-2 channels is approximately reversed in the observed and predicted cases.

**Automated Calibration**

Sandia National Laboratories evaluated the hand-calibrated flow model with respect to the improvement at predicting contaminant transport subject to vis-à-vis automated calibration (Sandia 2008a). The Laboratory reported that the hand-calibrated model achieved a root-mean-square-error (RMSE) for heads of 4.6 meters and for seeps of 0.98 kilograms per second (weighted RMSEs of 5.5 meters and 1.05 kilograms per second, respectively), which are quite reasonable.

This model, combined with the latest utilities available in the Parameter ESTimation software, PEST (Doherty 2008), then was used to perform a preliminary uncertainty analysis investigating the ability of the model to match both observed (steady-state) heads and seep flows, in addition to approximating a 330 meter travel-time estimate of 1.6 years. Results indicated that, given the current estimable parameters and their admissible ranges, the predictive utility of this model would increase after an automated calibration effort.

Because better matches to weighted site data could be achieved, PEST then was used to perform a preliminary automated calibration. The automated-calibrated model yielded the a head RMSE of 4.2 meters and a seeps RMSE of 1.04 kilogram per second, but weighted RMSEs were 5.2 meters and 1.11 kilograms per second, respectively. However, the estimated travel time was reduced from 5.7 years for the hand-calibrated model to 1.6 years for the to automated-calibrated model.

The non-trending constraint applied to the hand-calibration was relaxed increasing the number of observed (median) heads to 162, thus augmenting both the observation data set and calibration parameter set (Sandia 2008b). The calibration was further simplified when multiple median head observations corresponding to a single FEHM node were averaged and the maximum weight from constituent wells applied in the calibration.

Weights for each observation were set inversely proportional to the range of heads measured at that well and a Gaussian distribution was assumed for the measurement error with the range in heads assumed to approximate the 95 percent confidence interval. This yielded weights inversely proportional to the standard deviations. Head observation weights were also evaluated with regard to the confidence to be placed in each (i.e., *excellent*, *good*, *fair*, *poor*, and *eliminate*). Wells rated as *excellent*, *good*, or *fair* did not have their weights adjusted. Those two rated as *poor* had their weights cut in half. Wells rated as *eliminate* had zero weight applied. This resulted in 87 non-zero-weighted head observations, a factor of 2.6 increase in the original TIER 1 hand-calibrated observation data set's size.

In this case the automated calibrated model has a higher RMSE and weighted RMSE for heads than the hand-calibrated model. However, incorporation of the seepage flow rates and transport time as calibration targets in the Phase II-calibrated model has resulted in a model where these "soft" observations are more closely matched than with the hand-calibrated model. The simulated transport time with the Phase II-calibrated model is near the middle of the estimated range of values; whereas, the simulated value with the hand-calibrated model is greater than the upper bound (5.0 years) of the estimated range. In addition, the simulated seepage from *Seep* 3 (Erdman Brook) is significantly higher than in the hand-calibrated model, although it is still somewhat lower than the lower bound of the estimated range of values.

Sandia concluded that it is reasonable that the match between simulated heads and observed heads be sacrificed to some degree, if the ultimate objective of the flow model is to simulate accurately the migration of contaminants and groundwater flow rates on the North Plateau of the West Valley Site. Further, there is no strictly objective or rigorous method for the relative weighting of different types of observations, such as heads, seepage rates, and transport times. As a consequence, professional judgment and subjective assessment of the relative importance of various model predictions (e.g., simulated heads versus contaminant transport times) are required to define the objective function used in the automated calibration process in a meaningful way.

The increased RMSE for heads in the PEST-calibrated model relative to the hand-calibrated model highlight structural and/or conceptual uncertainties in the West Valley flow model. By adding the constraints of the seepage rates and transport time to the automated calibration process, the flow model is less able to compensate for simplifications associated with these uncertainties and the RMSE for heads is forced to be higher than for the hand-calibrated model, even for an optimized model. These structural or conceptual uncertainties could be related to the zonation of hydraulic conductivity, the continuity of hydrogeologic units in the subsurface, the zonation of recharge, the location of underflow at the lateral boundaries, or zonation of seepage.

### E.3.6 Sensitivity and Uncertainty

A series of sensitivity analyses were carried out after the manual calibration. Using the sum of the square of the head residuals as the measure of fit, the values of fourteen parameters were varied about their base values in the model one at a time to determine 1) the sensitivity of the model to changes in the parameter value, and 2) the extent to which a locally optimum solution has been achieved.

The sum of the square of the residuals SSR is given by

$$SSR = \sum ( h_i - WL_i )^2$$

where

$i$ is an index denoting one of the target wells in Table E–6,

$WL_i$ is the Table E–6 median observed groundwater elevation for target well $i$,

$h_i$ is the model predicted head at the target well location.

The parameters examined include two (2) flux boundary condition parameters and 12 material properties, i.e., hydraulic conductivities. The flux parameters are the inflow into the thick-bedded unit along the western boundary (thick-bedded unit inflow) and infiltration at the surface (recharge). The hydraulic conductivities considered are the horizontal and vertical components for the six (6) geohydrological units found in the upper aquifer system: the thick-bedded unit (TBUKxKy, TBUKz), the slack-water sequence (SWSKxKy, SWSKz), the Lavery till-sand (LTSKxKy, LTSKz), the weathered Lavery till (WLTKxKy, WLTKz), the unweathered Lavery till (ULTKxKy, ULTKz), and the Kent recessional sequence (KRSKxKy, KRSKz).

In each case, the parameter is varied about its base case value using a multiplicative factor while the others are kept at their base case values. The multiplicative factors applied to the base value were 0.25, 0.5, 2, and 4. The results are summarized in **Figure E–24** in the form of bar graphs showing SSR (square feet) versus multiplicative factor for each of the flux boundary conditions and hydraulic conductivities. The base case is also included in each graph.

The change in a bar graph is indicative of a sensitivity of the model vis-à-vis the SSR to changes in the parameter. A flat appearance suggests little or no sensitivity of the model to a parameter. A large U or V shape indicates sensitivity with the low point representing the approximate best fit. Continually increasing or continually decreasing plots indicate situations where the best parameter value lies outside the range considered. If the change across the plot is judged significant, then this sensitivity should be addressed and the parameter's range should be extended with the analysis continued. If the change across the plot is judged not to be significant, no further analysis is performed on that parameter.

Evaluation of the plots in Figure E–24 in this manner pointed to one significant case where the range of analysis was extended—the Kent recessional sequence horizontal hydraulic conductivity (KRSKxKy). Here the SSRs in the original set of analyses continuously increased as the value of the Kent recessional sequence horizontal hydraulic conductivity was increased, suggesting that the best fit lay somewhere below the range used. The range was extended on the low end demonstrating the shallow minimum or best fit occurs in the vicinity of the 0.25 case—the lower bound of the original range.

The general conclusions of the sensitivity analyses on the base case model as determined in the head calibration are that the model was reasonably parameterized although lowering the Kent recessional sequence horizontal hydraulic conductivity is indicated. In addition, the particular set of sensitivities expressed tend to corroborate some of the assumptions regarding flow at the site that are key in decoupling schemes used when smaller domain models are implemented—horizontal flow, vertical flow, etc.

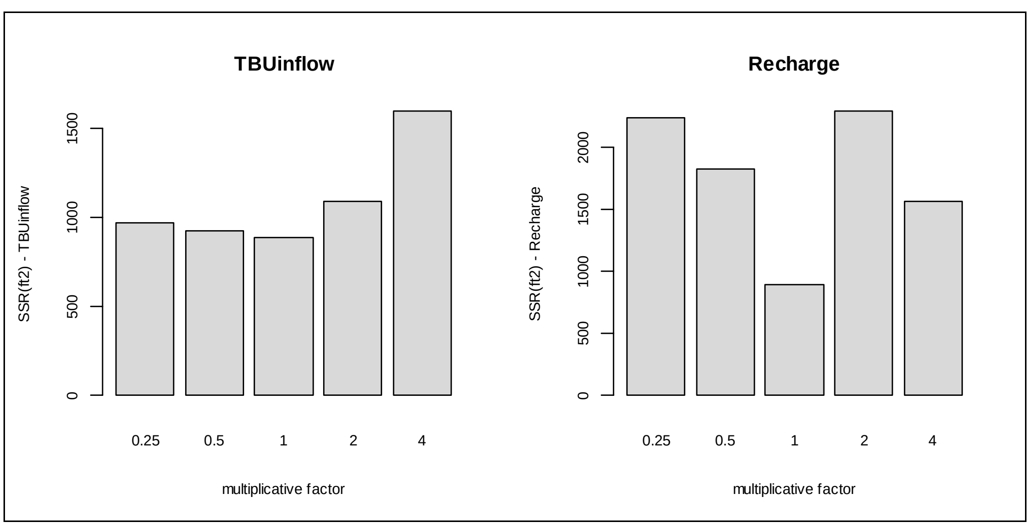


**Figure E–24 Results of Sensitivity Analysis of Base Case Model**

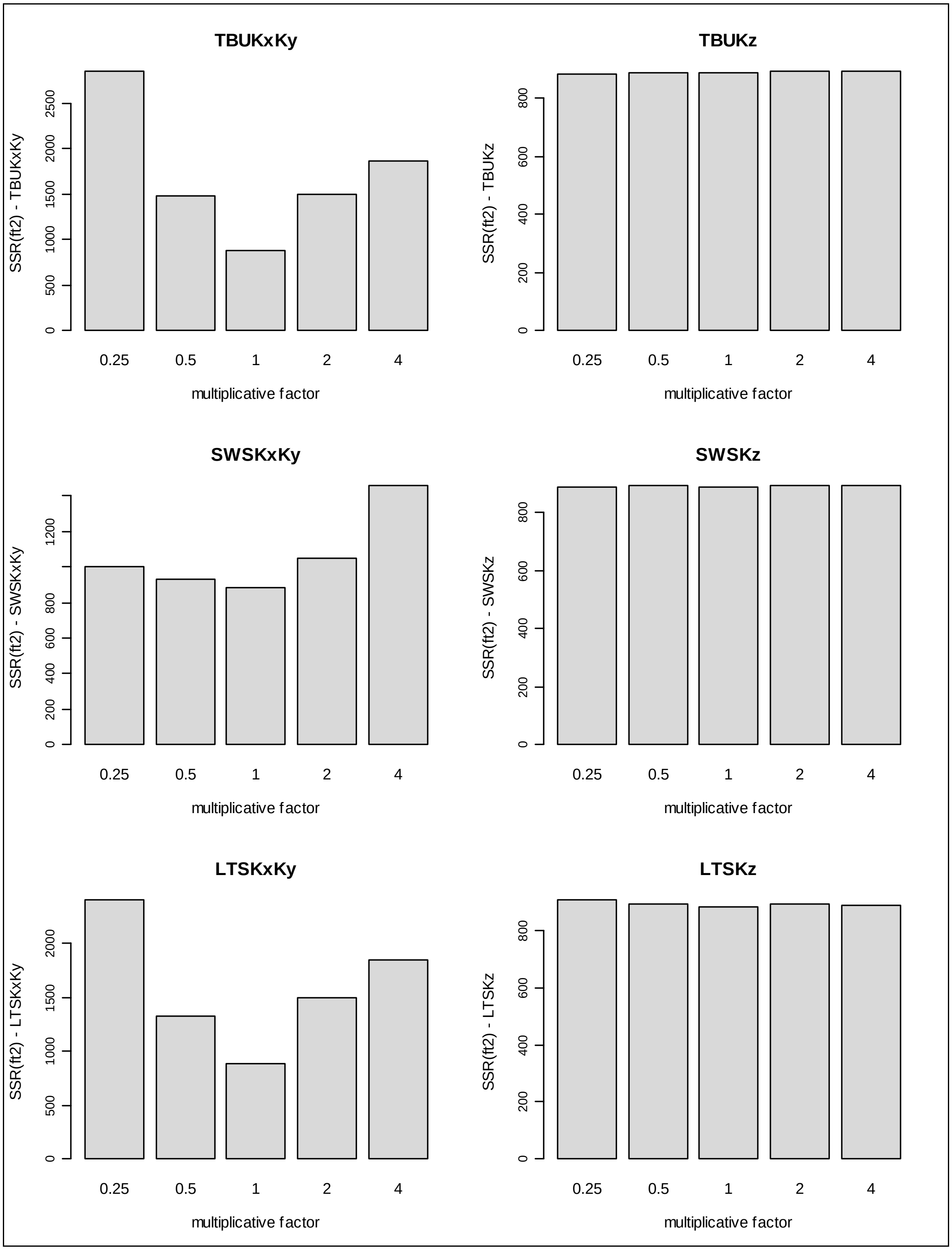


**Figure E–24 Results of Sensitivity Analysis of Base Case Model (continued)**

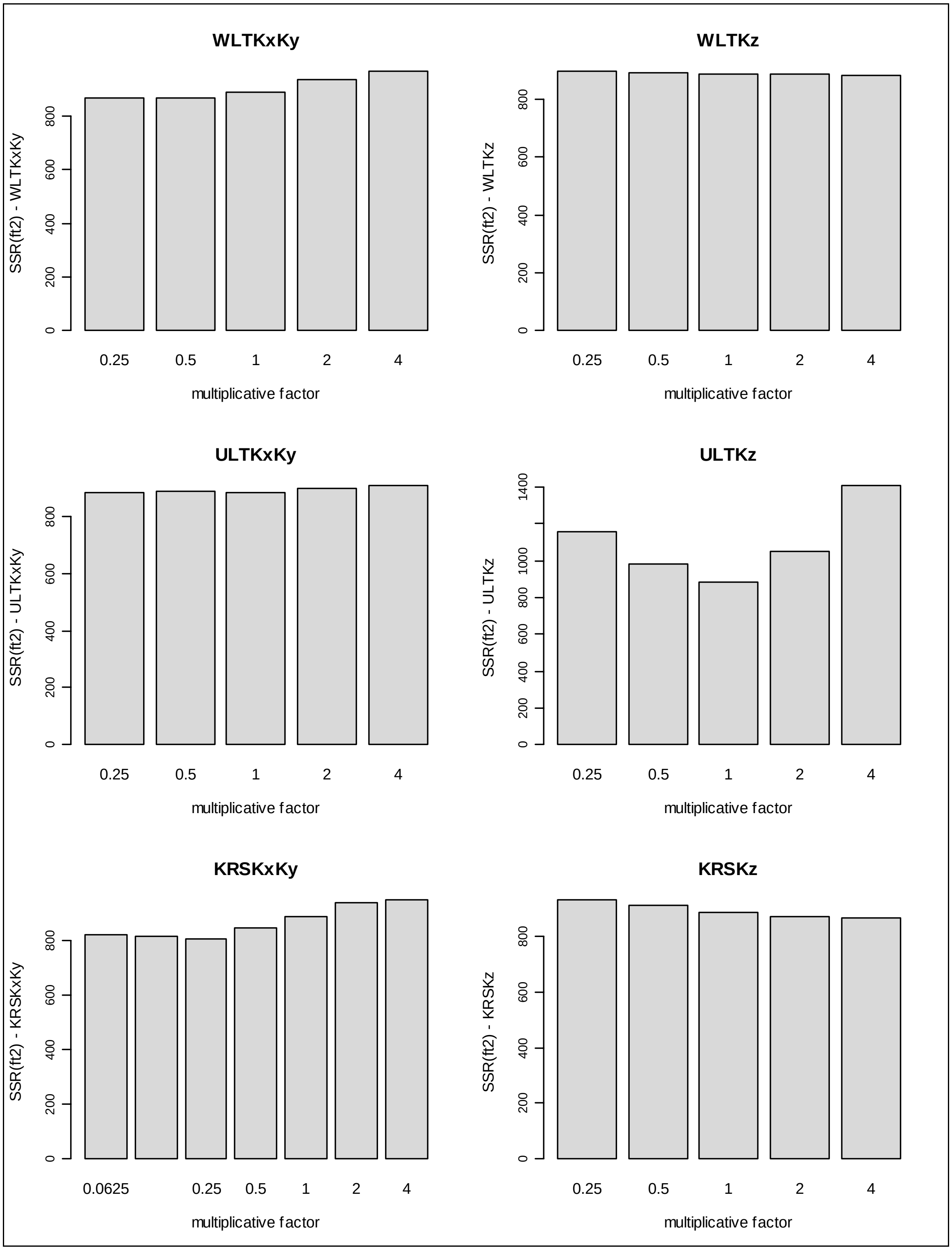


**Figure E–24 Results of Sensitivity Analysis of Base Case Model (continued)**

### E.3.7 Results

#### E.3.7.1 Predicted Water Tables

Automated water table contours for the upper aquifer are presented in **Figure E–25**. These contours are based on the calculated head in model layer 3 of the manually calibrated model. This approximation works well because flow in the upper aquifer is largely horizontal. This layer corresponds to the bottom of the thick-bedded unit at the North Plateau and the bottom of the weathered Lavery till at the South Plateau. Units in the next layer down are the unweathered Lavery till, the slack-water sequence, and the Lavery till sand.

Comparison of the contours in this figure with the fourth quarter 2007 observed North Plateau water table in Figure E–10 indicates close agreement in most areas of the North Plateau. The comparison is between the results of a steady-state calculation and a single snapshot in time of a dynamic system, the observed water table. Reasonable agreement between the contours in the two figures follows because the aquifer behaves as a steady-state system with small fluctuations over time and space. Exceptions occur, of course, when a major hydrologic stress is added to or removed from the system. An example of this includes tying off the french drain to the northwest of the lagoons in 2002 (WVNS and URS 2007). However, the target water levels (heads) used in the calibration were selected because they exhibit little or no trend over a time period that includes the introduction of and removal of stresses. That is, the model was fit to those portions of the aquifer that have been constant over time.

There are several minor differences between the two sets (observed and modeled) of North Plateau contours that can be seen. These include contours in the immediate vicinity of the process building and contours north of the lagoons. In the first case differences arise due to limitations inherent in both figures. In the case of Figure E–25, the impact of the building on infiltration has been incorporated into the model, but any restriction of flow due to subsurface building structure has not been incorporated. This is in part due to the size of the grid. In Figure E–11 only a limited number of locations provide control for contouring, whether done manually or automated. The difference in the contours north of the lagoons in the two figures is that the predicted contours are as a group slightly lowered than the observed contours, suggesting more water is needed in the modeled system in that area. This is also seen in observed versus predict heads plot (Figure E–23) where the cluster of locations near the 1370 elevation lie above the one-to-one line.

The contours along the perimeter of the plateau directly across Erdman Brook from the NDA and SDA exhibit features that are the result of the model implementation. Perimeter seeps have been included in the model but the grid spacing is large at 43 meters (140 feet). This part of the North Plateau is also the area where the prediction of water elevations above actual surface occurred during calibration of the model (Section 3.5). Yager had a similar result and subsequently refined his model grid in the area (Yager 1987). A physical factor impacting flow in the area is the evolving new hydrostratigraphy. Because the slack-water sequence extends further upslope in the new interpretation, a possible effect of the new slack-water sequence /Lavery till-sand is more of the flow in the surficial sand and gravel being directed through the slack-water sequence, diverted away from the perimeter seeps along Erdman Brook and Quarry Creek. A more refined interpretation of flow in this area would require further characterization of the Lavery till-sand. However, at present this is not expected to be a critical factor in the prediction of contaminant transport at the site.

A similar comparison can be made between modeled and observed South Plateau water tables. The observed South Plateau water table is in the bottom half of Figure E–12 and the modeled water table is shown in Figure E–25. Like the contours for the North Plateau the contours in the two figures are similar, but the differences between the two figures are more noticeable. The differences again reflect the absence of some structures in the model and insufficient control for contouring the observed data. Unperturbed subsurface

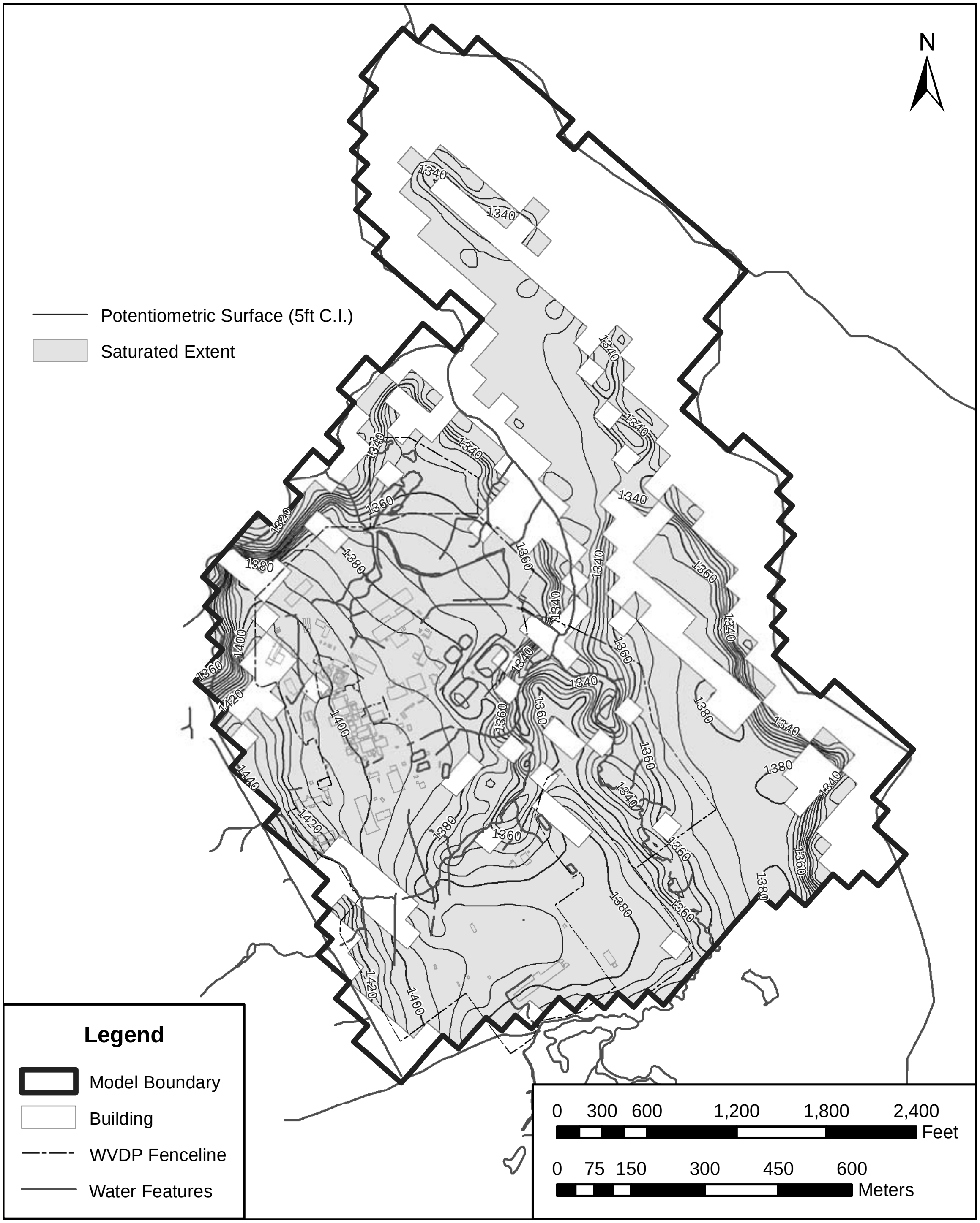


**Figure E–25 Simulated Upper Aquifer Water Table in the Thick-bedded Unit and Weathered Lavery Till (Model Layer 3 Head)**

conditions are presently modeled. Structures present but not included in the model are the actual disposal facilities. These consist of disposal pits, disposal trenches, the NDA interceptor trench, and the groundwater diversion barrier between the NDA and SDA. These clearly impact the system and any modeled or observed water table contours. The lack of explicit incorporation of these structures into the model may appear to be a limitation of the model but, when considered from the perspective of performance assessment and migration pathways, this limitation may not be too severe.

Two potential groundwater pathways may be proposed for the materials disposed in the NDA and SDA. The first pathway is a downward migration through the unweathered Lavery till from the disposal pits and trenches to the Kent recessional sequence and on from there. The second pathway is the result of the bathtub effect. Infiltration and interflow into the trenches and pits eventually raise the water levels in them until the water reaches the interface between the low permeability unweathered Lavery till and more permeable weathered Lavery till. From there the water and any contaminant with it begins to move laterally through weathered Lavery till saturated zone. That movement continues until the material either reaches a discharge location at a nearby stream or eventually turns down moving vertically through the unweathered Lavery till. The distance from the release area and the downgradient weathered Lavery till discharge location determines which path is taken.

The first pathway, movement downward through the unweathered Lavery till, is probably not significantly impacted by the exclusion of the pits and trenches from the model. This is because in their present configuration these facilities contain standing water. The difference between the top elevation of that water and the top of the unsaturated zone in the Kent recessional sequence provides the driving force for the downward movement. In the case of the unperturbed model, a very similar driving force is imposed by the water table in the weathered Lavery till and the top of the Kent recessional sequence. Hence, little difference is expected. In analyzing the second pathway, the lateral transport can be approximated in the current model by simply placing the release at the weathered Lavery till/unweathered Lavery till interface, i.e., at the bottom of layer 3 in the weathered Lavery till.

Only a few controls are available for construction of the observed contours seen in Figure E–12 and multiple sets of contours—most similar—could be obtained from the data. Expert and site specific knowledge applied to the task do not appear explicitly in the figure but do shape it. In light of these considerations and the model-side limitations mentioned above, comparison of the figures is valid only up to a point. The two sets of contours are qualitatively and quantitatively similar—both echoing the topography of the South Plateau.

In addition to showing the head contours, Figure E–25 also provides an indication of the extent of the upper aquifer. Shading is included to identify those areas that are fully saturated. The figure shows much of the North Plateau and South Plateau model layer 3 to be saturated. The partially saturated areas occur along or near the steep banks of the stream valleys. The fingerlike East Plateau lying between Franks Creek and Buttermilk Creek is interesting because of the partial saturation along part of its crest. The cause of this effect was not determined, but flow in this area is not considered critical to the estimates of contaminant transport at the site.

**Figure E–26** shows the head contours and saturation for model layer 12, which includes the bottom of the Kent recessional sequence. The narrow saturated area running along the western boundary is comprised of bedrock and weathered bedrock. The belt of partial saturation to the east of the bedrock and along the southern model boundary is the Kent recessional sequence, as is the large area of saturation over the remainder of the site to the east. The picture of the lower aquifer as it emerges from the present model is one where the zone of saturation does not extend through all of the Kent recessional sequence. In saturated areas the horizontal flow is in the direction of the Buttermilk Creek valley, where the aquifer discharges either through seeps along the valley wall or directly into the creek itself.

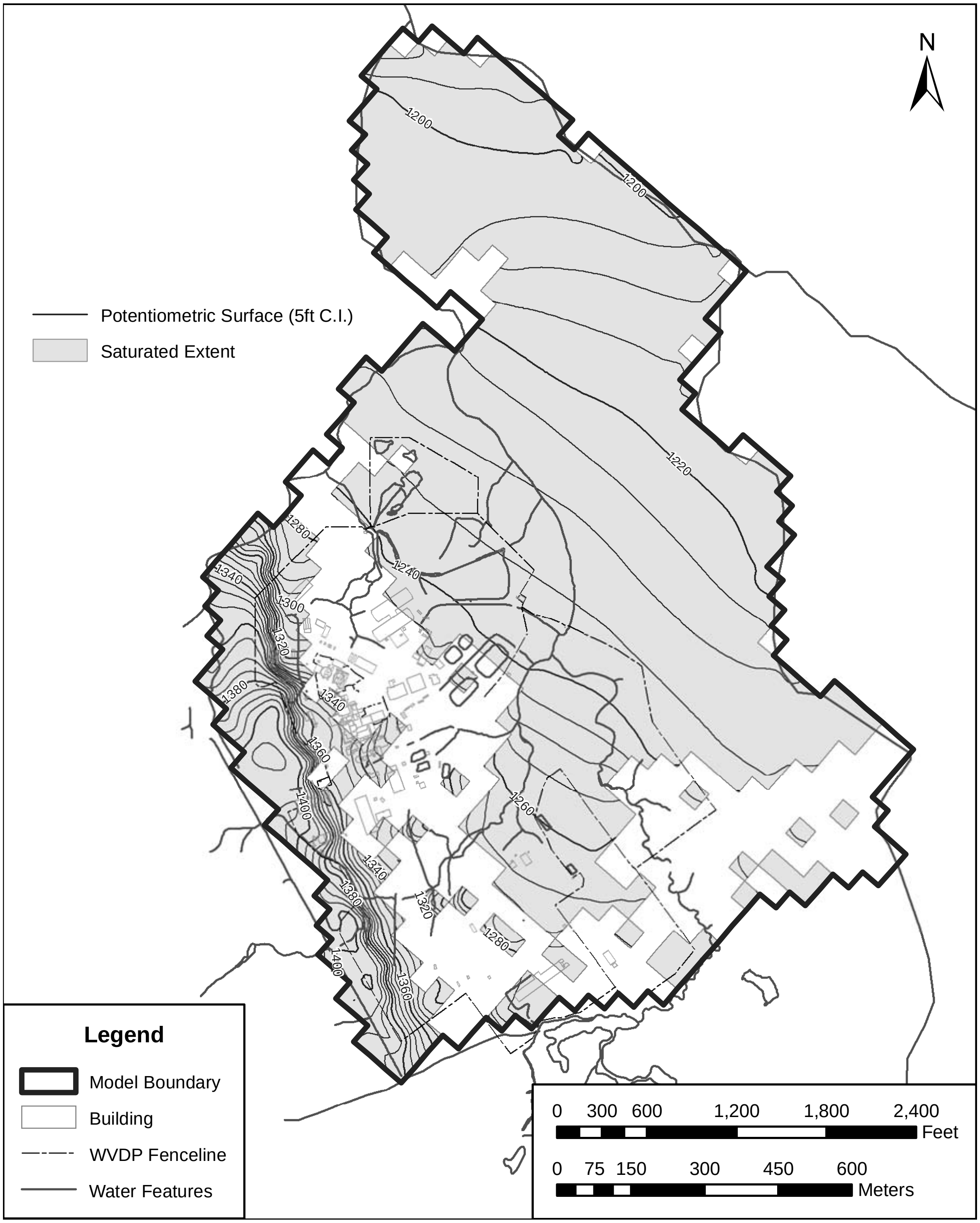


**Figure E–26 Simulated Lower Aquifer Water Table in the Kent Recessional Sequence (Model Layer 12)**

**Figure E–27** is a cross section through the North Plateau showing all of the geohydrologic units found in the model and the water tables for the upper and lower aquifers. Median water level observations for a number of wells screened in the upper system are also shown in the plot. Consistent with the calibration, the observed water levels and the computed water table show good agreement. The profile view in Figure E–27 also aids in understanding the limited extent of the lower aquifer in the Kent recessional sequence. Areas where the aquifer pinches out, becoming partially saturated, correspond to locations where the Kent recessional sequence and those glacial materials (Kent till, Olean Recessional Sequence, Olean till) underneath it thin out as bedrock rapidly rises to the west.

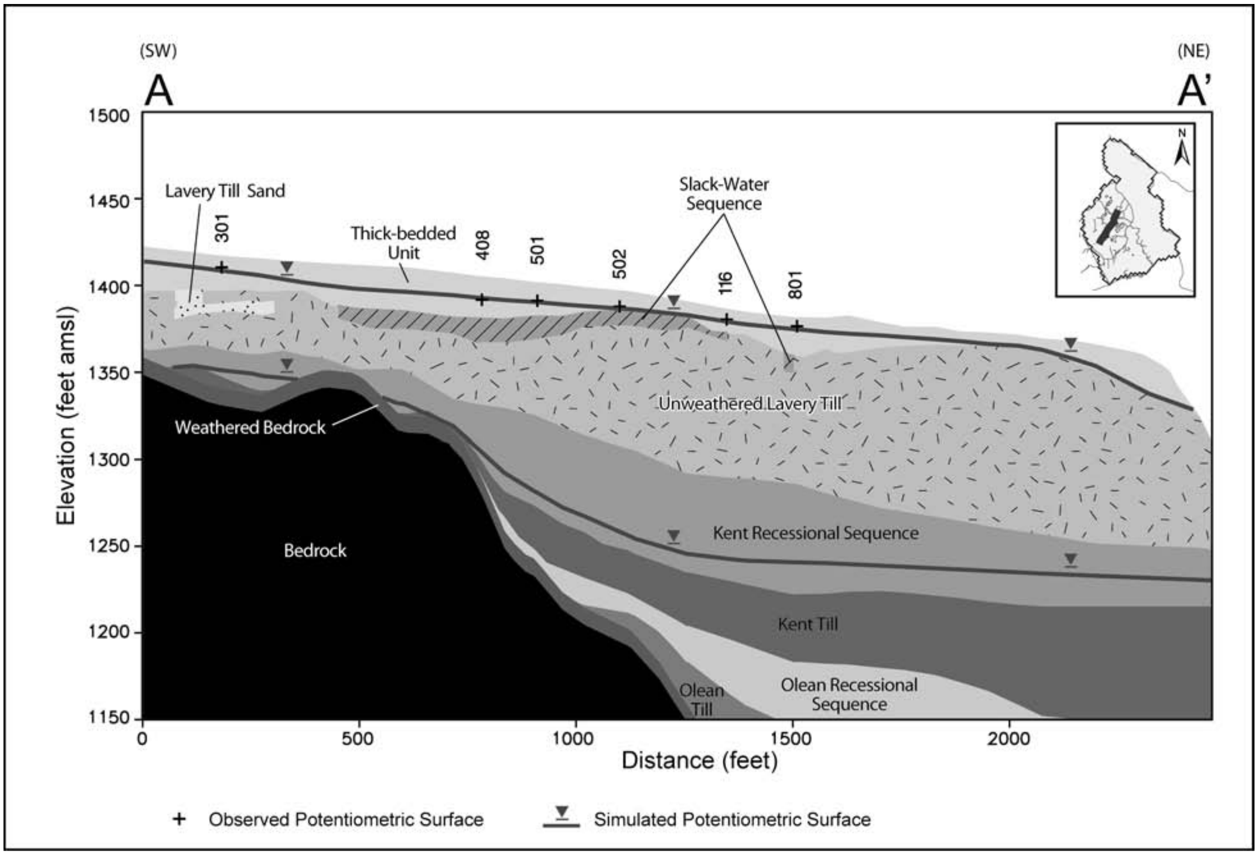


**Figure E–27 Upper and Lower Aquifers Tables at the North Plateau**

### E.3.7.2 Groundwater Flow Directions

**Figure E–28** shows the head contours and saturation in model layer 5. This layer consists mostly of unweathered Lavery till and slack-water sequence. The figure shows that most of this layer is saturated and in particular the unweathered Lavery till in the South Plateau is saturated. In the model the saturation is maintained down to the top of the Kent recessional sequence and is consistent with descriptions summarized in previous characterizations and modeling studies of the South Plateau (Bergeron, Kappel and Yager 1987, Kool and Wu 1991, Prudic 1986, WVNS 1993b). Calculated vertical nodal Darcy velocities in layer 5 beneath the NDA and SDA are on the order of $5 \times 10^{-8}$ centimeters per second and the estimated linear velocities are about 5 centimeters per year. This is in good agreement with estimates made in the past studies. While this result is expected, it is worth noting because the calculations are made within the much larger model domain and the nodes are located far from any boundary condition nodes.

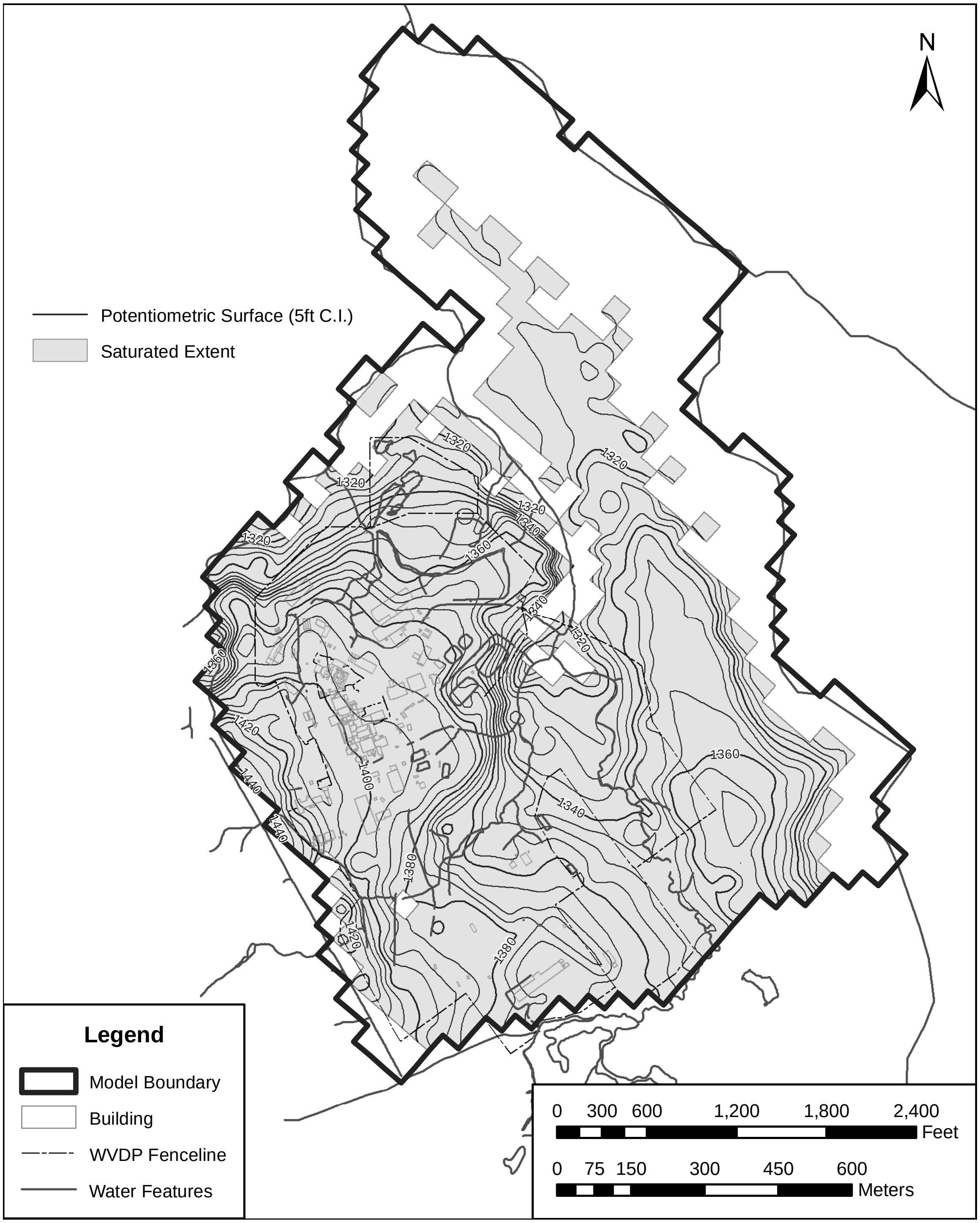


**Figure E–28 Saturation in the Unweathered Lavery Till**

**Figures E–29** and **E–30** show vertical profiles of the velocity field for the North Plateau and the South Plateau, respectively. In Figure E–29 the horizontal flow in the surficial sand and gravel is indicated by the mostly horizontal vectors in model layers 3 through 5, the bottom of the thick-bedded unit and the slack-water sequence. The length of each vector is an indication of the flow velocity at that location. The direction of the vector shows the direction of the groundwater flow at that location. The lower downward flow of groundwater through the unweathered Lavery till is indicated by the shortened vectors (heads only) pointing to the bottom of the figure. Horizontal flow in the lower Kent recessional sequence aquifer appears as the "row" of horizontal vectors in the lower mid portion of the figure. Figure E–30 presents similar information except that the uppermost geohydrologic unit is the weathered Lavery till. Flow through the unweathered Lavery till in the South Plateau profile is vertical and flow along the bottom of the Kent recessional sequence is horizontal.

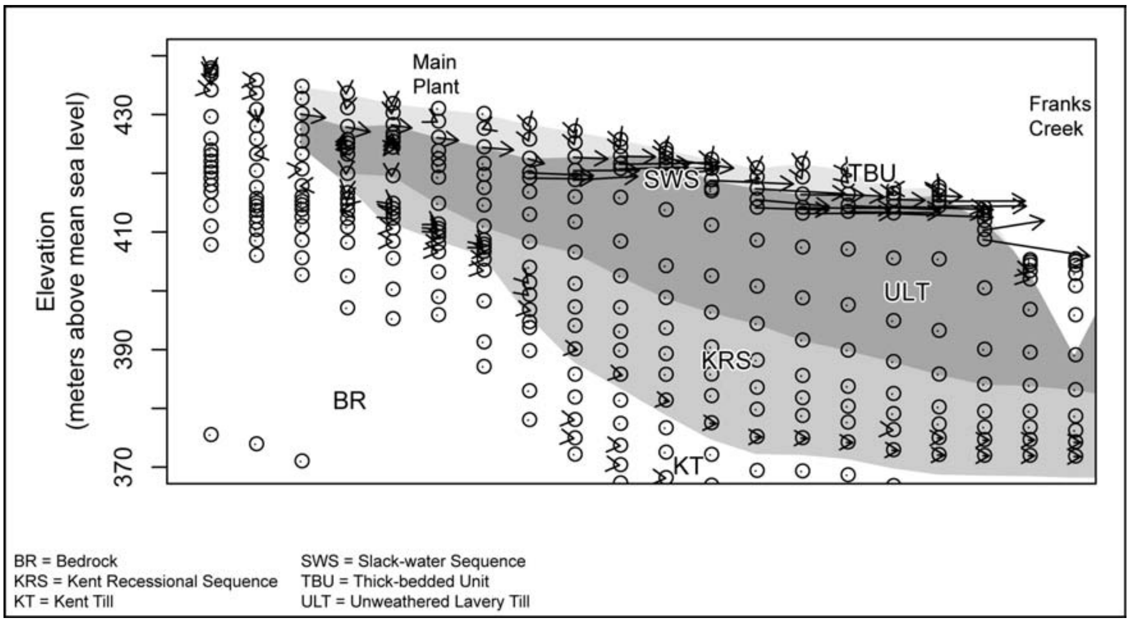


**Figure E–29 North Plateau Velocity Field in Profile**

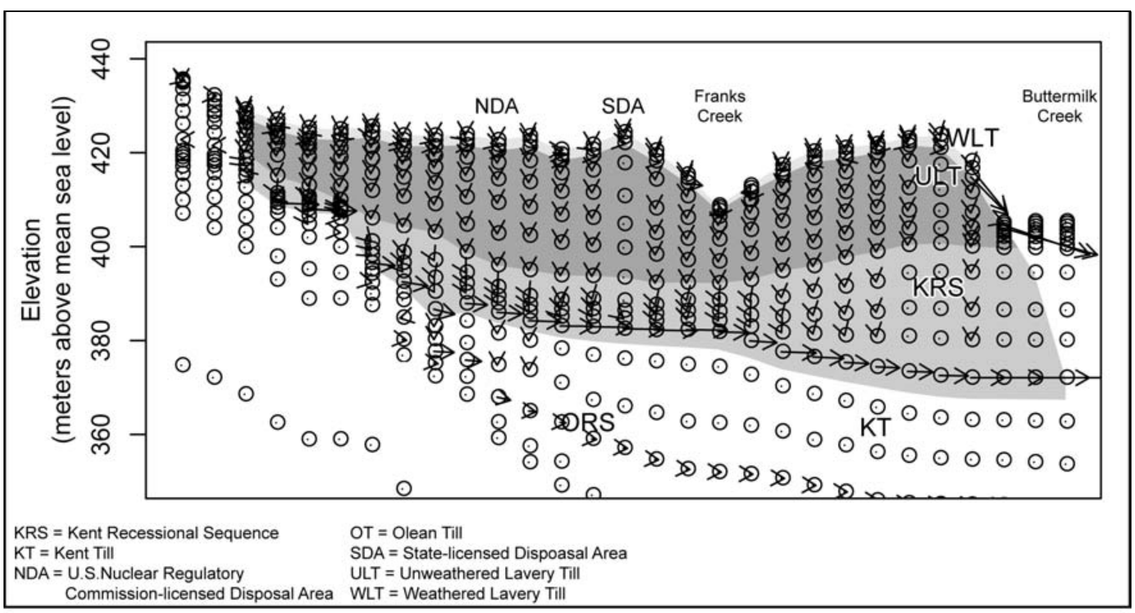


**Figure E–30 South Plateau Velocity Field in Profile**

### E.3.7.3 Alternative Conceptual Model – Weathered Bedrock Outlet

One of the modeling questions to be addressed by the current effort is to explore how flow out of the system by way of the weathered bedrock might impact flows in the upper units down to and including the Kent recessional sequence. That is, can the geohydrology below the Kent recessional sequence safely be ignored when modeling the impacts of surface and near-surface facilities at the site? To examine that aspect, the base case model was modified to allow flow out of the system to the north from the weathered bedrock. This was accomplished by setting constant head boundary conditions in a small segment of the boundary weathered bedrock cells near the bedrock valley axis located in that unit approximately beneath the northernmost reach of Buttermilk Creek in the model.

The weathered bedrock constant head used at these locations was varied in several runs, in each case using a single value ranging from 1,160 feet to 1,210 feet. A comparison of predicted target heads and predicted seep values in the different runs and the base case model reveals very little differences for the heads in the `upper units (through the Kent recessional sequence). Drawing on these results and on the velocity fields seen for the base case (Figures E–29 and E–30) the implication is that the deeper aquifer systems in the Buttermilk Creek basin can be ignored with little consequence when modeling impacts of near-surface facilities.

## E.4 Near-field Groundwater Flow Models

The three-dimensional site-wide groundwater flow model provides a basis for understanding of the rates and directions of groundwater flow for current conditions but does not provide information for Sitewide Close-In-Place or Phased Decisionmaking Alternative conditions. In addition, the scale of engineered features is small with respect to the scale of the site-wide flow model. For these reasons, three three-dimensional near-field groundwater flow models have been developed to supplement simulation of conditions on the North and South Plateaus. The models have been implemented using the STOMP computer code developed at Pacific Northwest National Laboratory (PNNL 2000). STOMP uses the integrated volume finite difference approach to solve flow and transport equations for unsaturated and saturated conditions. The approach for development of the near-field model is to use the stratigraphy and boundary conditions incorporated into the site-wide model to the extent possible with the STOMP computer code. Flow and transport calculations of the near-field models are used to establish directions and velocities of flow through and away from sources on the north and South Plateaus. To provide understanding of the nature of one-dimensional flow models used in estimation of human health impacts, description of use of a one-dimensional groundwater transport model is presented in the discussion of historical conditions. The following sections describe the near-field models for the North and South Plateaus.

### E.4.1 North Plateau

The model developed for the north plateau has the shape of a rectangular block oriented from the southwest to the northeast that extends from the ground surface to the top of the Kent recessional sequence. The exterior horizontal boundaries of the model are depicted in **Figure E–31**. The model boundaries on the south, west and east sides are consistent with the extent of the thick-bedded unit but on the northern end the model is terminated near the North Plateau ditch where groundwater is observed to discharge to surface drainage prior to the northern extent of the thick-bedded unit. Geohydrologic units represented in the model are the thick-bedded unit, the slack-water sequence and the unweathered Lavery till. Together, the thick-bedded unit and the slack-water sequence comprise the Surficial Sand and Gravel Unit. As described above, the thick-bedded unit comprises glaciofluvial gravel and alluvial deposits that range from 1 to 5 meters in thickness overlying the unweathered Lavery till. The slack-water sequence is a depositional sequence with layers of gravel, sand and silt filling a southwest-to-northeast trending channel in the upper portion of the unweathered Lavery till.

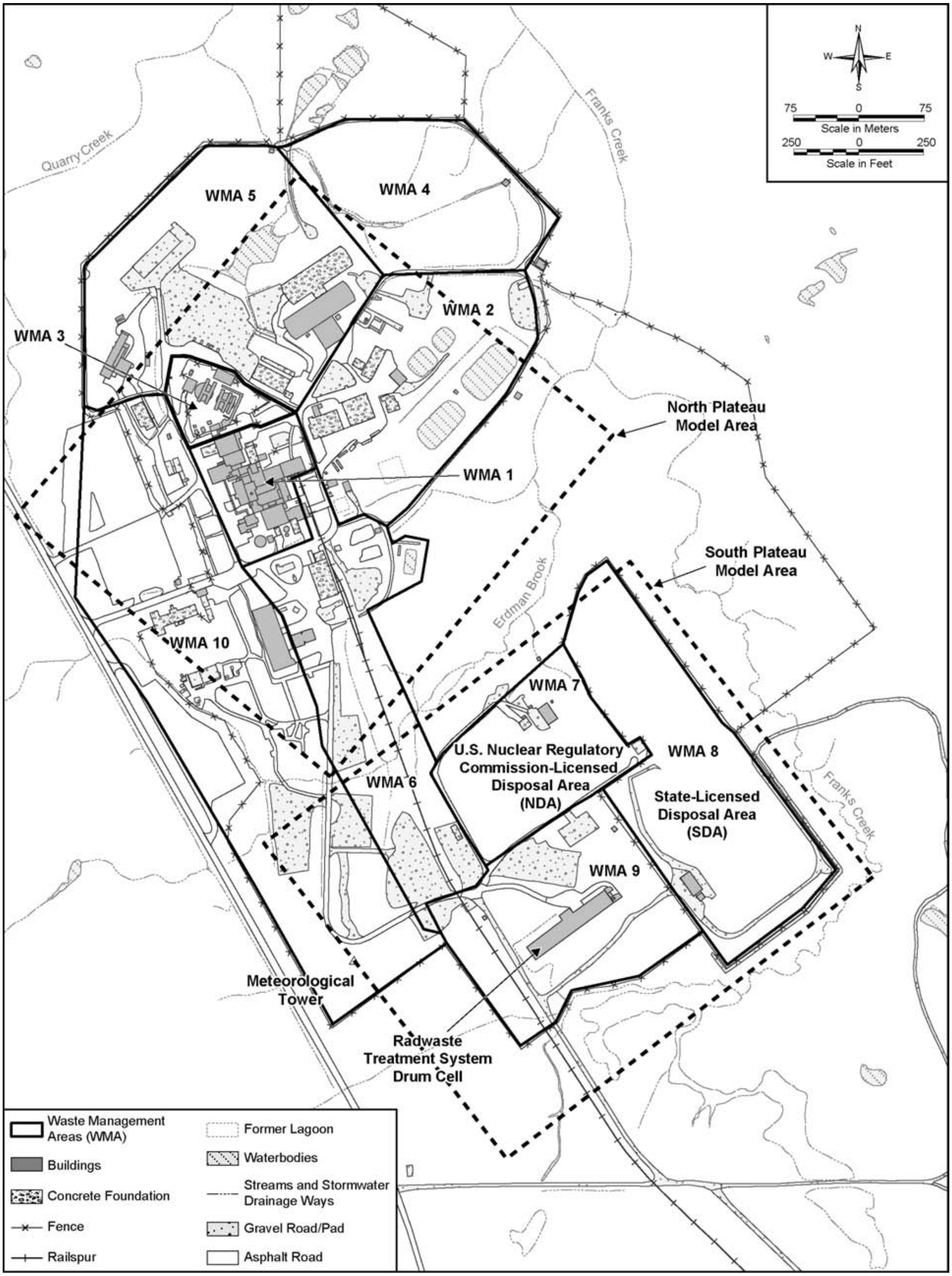


**Figure E–31 Boundaries of Model Areas for the North and South Plateau Near-field Groundwater Flow Models**

The slack-water sequence varies in thickness from 0 to 5 meters with the thickest portions at the southwest end of the unit below the Main Plant Process Building. The unweathered Lavery till is a glacial till with lenses of silt and sand with a range of thickness of 10 to 17 meters in the model volume. The Waste Tank Farm tanks are located in an excavation of the unweathered Lavery till located at the west side of the model volume. The cross-sectional structured encoded into the North Plateau near-field flow models is represented in **Figures E–32** through **E–36**. The slack-water sequence appears in the units and northern portions of the model as shown in Figure E–34 through E–36. The Waste Tank Farm excavation appears in the center portion of the model as shown in Figure E–35. Hydraulic conductivities of geohydrologic units are assumed constant over the model domain with values of $2.5 \times 10^{-3}$, $5.3 \times 10^{-3}$ and $6.0 \times 10^{-8}$ centimeters per second for the thick-bedded unit, slack-water sequence and unweathered Lavery till, respectively. These general elements of the model were developed further into three variants, the first developed for historical conditions as appropriate for the No Action Alternative, the second incorporated engineered features as appropriate for the Sitewide Close-In-Place Alternative, and the third incorporated the slurry walls percent for the Phased Decisionmaking Alternative.

### E.4.1.1 Historical Conditions (No Action Alternative)

To simulate historical conditions, the horizontal portion of the model grid comprises uniform, rectangular 10-meter blocks with 49 blocks in the southwest-to-southeast direction and 54 blocks in the southwest-to-northwest direction. For the vertical direction, the upper 3 meters were represented using 15, 0.2-meter-thick layers, the next 3 meters were represented using 6, 0.5-meter-thick layers, and the bottom 17 meters were represented using 17, 1.0-meter-thick layers. Thus, this variant of the model utilizes approximately 100,000 grid blocks.

Boundary conditions applied for the near-field model are consistent with site observations and with those applied for the site-wide model. At the bottom of the unweathered Lavery till, atmospheric pressure was applied representing the presence of a water table in the Kent recessional sequence. On the south, north, west and east sides of the model, no flow conditions were applied for the unweathered Lavery till. On the south side of the model, lateral recharge into the thick-bedded unit of 20 cubic meters per day was applied. On the east side of the model, atmospheric pressure conditions were applied for the thick-bedded unit to represent seepage to Erdman Brook. At the north end of the model, elevation of the water table was specified to represent discharge to the North Plateau drainage ditch.

For recharge at the surface, uniform spatial distribution was applied but varied in a parametric fashion to provide the best match to site conditions.

Pressures simulated with the North Plateau near-field model are summarized in **Table E–8** along with measured conditions at target wells. The results indicate that a uniform recharge of 26 centimeters per year produced the closest match to observed conditions. A plot of elevation of the water table in the thick-bedded unit for recharge of 26 centimeters per year is presented in **Figure E–37**. The results are consistent with both the measured heads and with the predictions of the site-wide model.

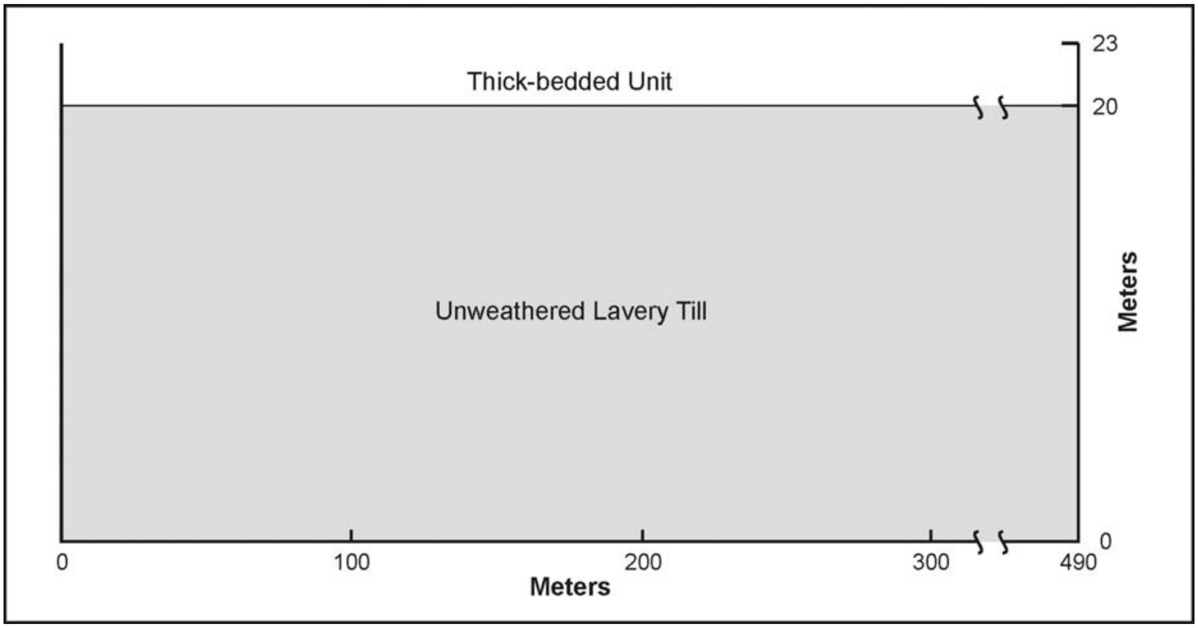


**Figure E–32 Cross-section of the Near-field Groundwater Flow Model of the North Plateau: Southwest to Northeast Distance of 0 to 80 Meters**

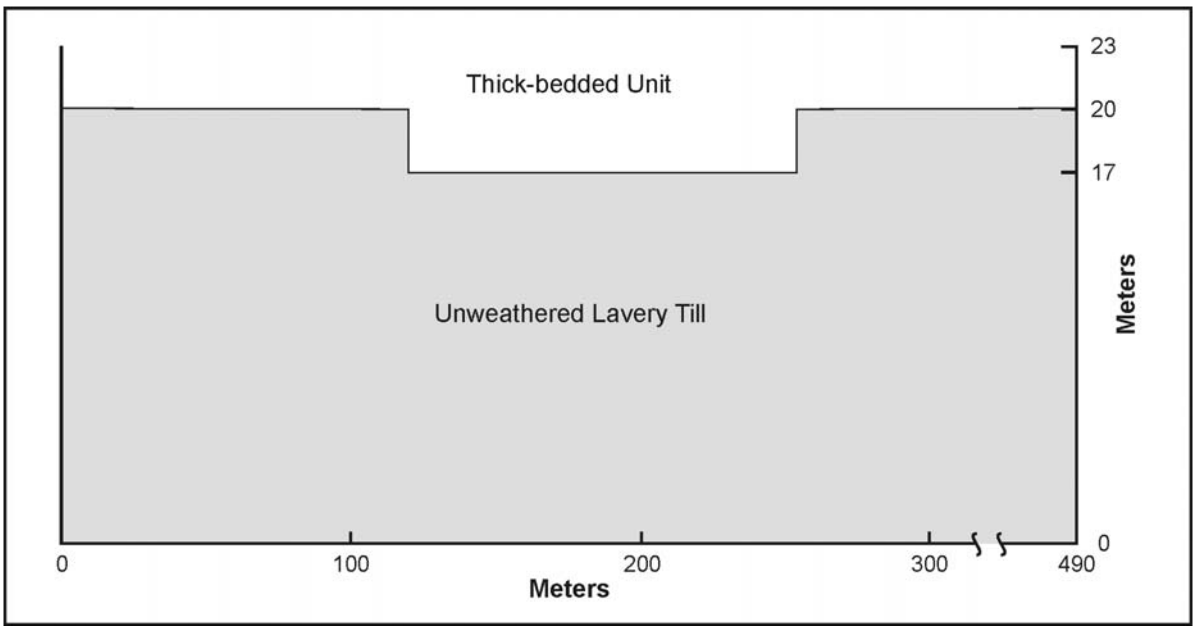


**Figure E–33 Cross-section of the Near-field Groundwater Flow Model of the North Plateau: Southwest to Northeast Distance of 80 to 200 Meters**

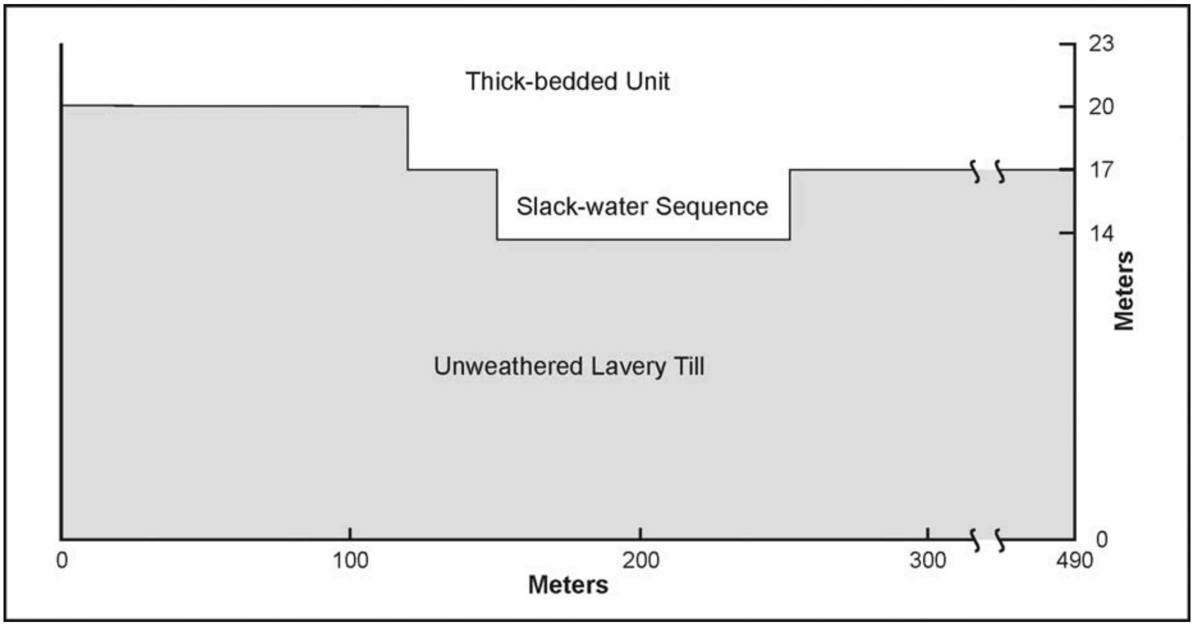


**Figure E–34 Cross-section of the Near-field Groundwater Flow Model of the North Plateau: Southwest to Northeast Distance of 200 to 260 Meters**

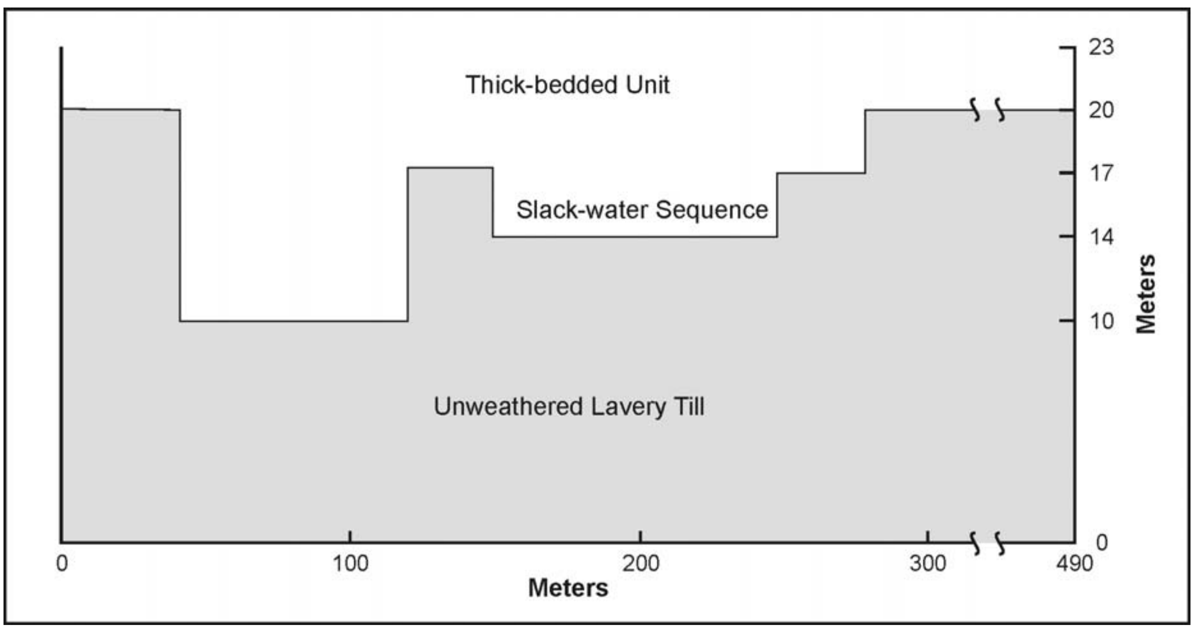


**Figure E–35 Cross-section of the Near-field Groundwater Flow Model of the North Plateau: Southwest to Northeast Distance of 260 to 320 Meters**

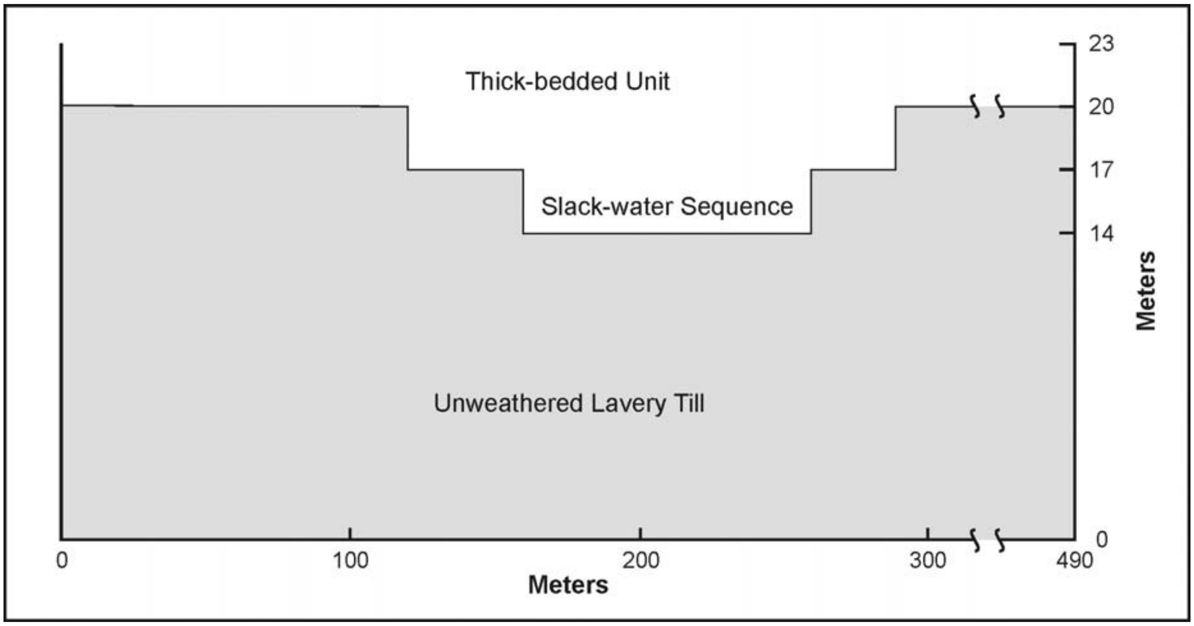


**Figure E–36 Cross-section of the Near-field Groundwater Flow Model of the North Plateau: Southwest to Northeast Distance of 320 to 540 Meters**

**Table E–8 North Plateau Near-field Flow Model Calibration for Head**

| *Well* | *Measured Head (feet)* | *Predicted Head (feet)* | | |
|---|---|---|---|---|
| | | *Recharge = 22 centimeters per year* | *Recharge = 26 centimeters per year* | *Recharge = 30 centimeters per year* |
| 103 | 1391.4 | 1387.9 | 1389.9 | 1391.2 |
| 104 | 1385.5 | 1380.2 | 1381.5 | 1382.9 |
| 116 | 1380.5 | 1375.5 | 1376.2 | 1376.8 |
| 203 | 1394.4 | 1402.0 | 1402.6 | 1403.3 |
| 205 | 1393.1 | 1398.5 | 1399.1 | 1400.4 |
| 301 | 1410.7 | 1408.0 | 1409.6 | 1410.8 |
| 401 | 1410.3 | 1406.8 | 1408.4 | 1409.6 |
| 406/86-08 | 1393.45 | 1394.1 | 1396.0 | 1397.4 |
| 601 | 1377.3 | 1376.8 | 1377.5 | 1378.1 |
| 603 | 1391.9 | 1394.2 | 1395.5 | 1396.8 |
| 604 | 1391.6 | 1390.0 | 1391.3 | 1392.6 |
| 86-09 | 1391.8 | 1392.7 | 1394.0 | 1395.9 |
| 408 | 1391.8 | 1391.5 | 1392.8 | 1394.7 |
| 501 | 1391.3 | 1387.9 | 1389.2 | 1391.2 |
| 403 | 1408.0 | 1400.3 | 1403.6 | 1404.7 |
| 801 | 1376.6 | 1372.5 | 1372.5 | 1373.2 |
| Sum of Squared Residuals (square feet) | | 268.88 | 210.81 | 242.42 |

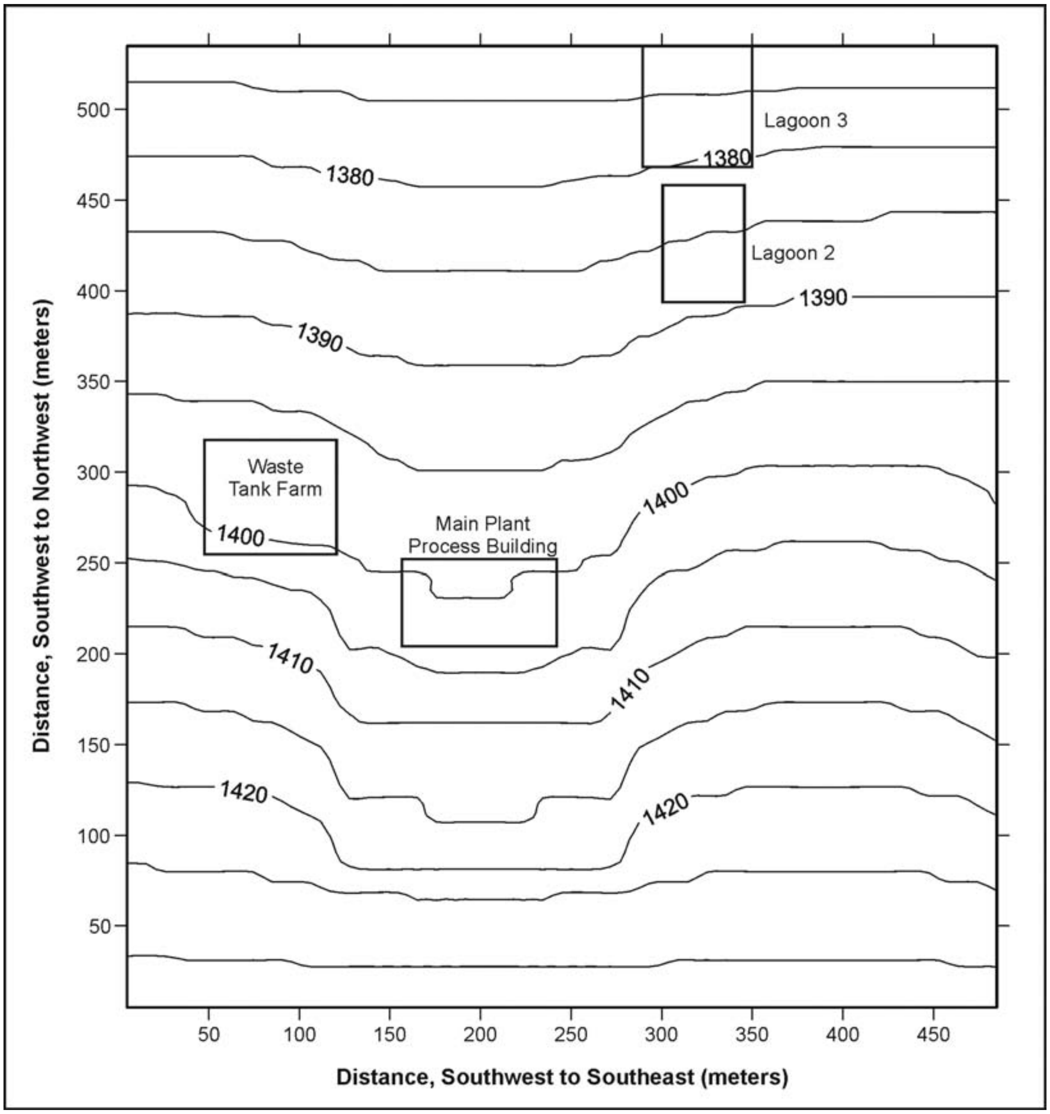


**Figure E–37 Water Table Plot for the North Plateau Near-field Flow Model, Historical Conditions**

As an additional check of validity of the model, transport calculations were performed for comparison to GeoProbe measurements of concentration of strontium-90 in the North Plateau plume (WVNS 1995). The major source for the plume is believed to be a leak in 1968 from the Main Plant Process Building into the underlying sediments. For this analysis, the leak was represented as injection of 200 curies of strontium-90 into the central portion of the thick-bedded unit. Two versions of the analysis were performed to evaluate the range of adsorption of strontium onto the sediments of the thick-bedded unit and slack-water sequence. In the first case, the thick-bedded unit and slack-water sequence were assumed to have values of distribution coefficient of 5.0 milliliters per gram. In the second case, the distribution coefficients for the thick-bedded unit and slack-water sequence were 2.7 and 5.0 milliliters per gram, respectively. These values are within the range observed in site-specific laboratory measurements (Dames and Moore 1995) and using GeoProbe measurements (WVNS 1999). The results presented in **Table E–9** indicate that the combination of values of distribution coefficient ($K_d$) produces the best match to measured concentrations, and that the model predictions for the center of mass of the plume are consistent with observed conditions.

**Table E–9 Comparison of North Plateau Near-field Flow Model Predictions With Observed North Plateau Plume Concentrations of Strontium-90**

| *GeoProbe Number* | *Distance from Source (meters)* | *Concentration of Strontium-90 (picocuries per liter)* | | |
|---|---|---|---|---|
| | | *Observed* [a] | *Predicted* [b] *TBU* $K_d$ *= 5 ml/g* *SWS* $K_d$ *= 5 ml/g* | *Predicted* [b] *TBU* $K_d$ *= 2.7 ml/g* *SWS* $K_d$ *= 5 ml/g* |
| 75 | 25 | $1.5 \times 10^5$ | $7.0 \times 10^5$ | $3.8 \times 10^5$ |
| 30 | 50 | $7.8 \times 10^5$ | $9.4 \times 10^5$ | $8.1 \times 10^5$ |
| 72 | 65 | $7.9 \times 10^5$ | $8.5 \times 10^5$ | $8.6 \times 10^5$ |
| 23 | 80 | $2.0 \times 10^5$ | $5.6 \times 10^5$ | $7.9 \times 10^5$ |
| 66 | 150 | $7.5 \times 10^4$ | $2.6 \times 10^4$ | $1.1 \times 10^5$ |
| 14/67 | 170 | $4.6 \times 10^4$ | $8.2 \times 10^3$ | $4.8 \times 10^4$ |
| 11 | 270 | $1.2 \times 10^4$ | 5.6 | 110 |
| 3 | 330 | $3.2 \times 10^2$ | 0.1 | 2.7 |

ml/g = milliliters per gram, SWS = Slack-water Sequence, TBU = Thick-bedded Unit.
[a] The reported observed values are the arithmetic average of Geoprobe measurements reported (WVNS 1995) for one or more depths below the ground surface at the given location.
[b] The predicted values are the average values estimated for the saturated portion of the Thick-bedded Unit and Slack-water Sequence.

The vertical distributions of moisture content and of concentration of strontium-90 for the three locations down-gradient of the source on the center line of the plume are presented in **Table E–10**. Mass balance analysis of predicted levels of strontium-90 for calendar year 1995, 27 years after the release, indicate that greater than 90 percent of the remaining radionuclide is in a volume with a width of 40 meters in horizontal extent (WVNS 1995).

**Table E–10 Near-field Groundwater Flow Model Predictions of Concentration of Strontium-90 in the North Plateau Plume for Calendar Year 1995**

| *Distance Below Ground Surface (meters) (unit)* | *Distance from Source (meters)* | | | | | |
|---|---|---|---|---|---|---|
| | *50 meters* | | *100 meters* | | *150 meters* | |
| | *Aqueous Moisture Content* | *Concentration of Strontium-90 (picocuries per liter)* | *Aqueous Moisture Content* | *Concentration of Strontium-90 (picocuries per liter)* | *Aqueous Moisture Content* | *Concentration of Strontium-90 (picocuries per liter)* |
| 2.3 (TBU) | 0.099 | $6.6 \times 10^5$ | 0.109 | $4.0 \times 10^5$ | 0.225 | $9.9 \times 10^4$ |
| 2.7 (TBU) | 0.101 | $7.2 \times 10^5$ | 0.225 | $5.0 \times 10^5$ | 0.225 | $1.0 \times 10^5$ |
| 3.75 (TBU) | 0.225 | $8.1 \times 10^5$ | 0.225 | $5.5 \times 10^5$ | 0.225 | $1.1 \times 10^5$ |
| 5.75 (TBU) | 0.225 | $8.1 \times 10^5$ | 0.225 | $4.1 \times 10^5$ | 0.225 | $1.3 \times 10^5$ |
| 6.5 (SWS) | 0.350 | $8.1 \times 10^5$ | 0.350 | $6.3 \times 10^5$ | 0.350 | $1.4 \times 10^5$ |
| 8.5 (SWS) | 0.350 | $8.4 \times 10^5$ | 0.350 | $6.3 \times 10^5$ | 0.350 | $1.3 \times 10^5$ |
| 13.5 (ULT) | 0.324 | 370 | 0.324 | 22 | 0.324 | 0.9 |
| 18.5 (ULT) | 0.324 | 0 | 0.324 | 0 | 0.324 | 0 |

SWS = slack-water sequence, TBU = thick-bedded unit, ULT = unweathered Lavery till.

For sources originating in the saturated portion of the thick-bedded unit below the Main Plant Process Building, transport analysis indicates that the solute reaches the North Plateau ditch along a southwest-to-northeast path centered on the release point. The entirety of the solute reaching the northeast edge of the model reaches the boundary within 50 meters of the centerline of the source with vertical movement downward into the slack-water sequence. Solute flux at the discharge is summarized in **Table E–11**. A plot of predicated contours of the plume is presented in **Figure E–38**.

**Table E–11 Cumulative Solute Flux at the Model Boundary for a Source Below the Main Plant Process Building Centered Above the Slack-water Sequence**

| *Unit* | *Cumulative Solute Flux at the Aquifer Outlet [a] (curies)* |
|---|---|
| Slack-water Sequence | 2.63 |
| Thick-bedded Unit | |
| Within 50 Meters West of Source Grid Block | 0.64 |
| In Line with Source Grid Block | 0.44 |
| Within 50 Meters East of Source Grid Block | 0.31 |

[a] Total solute flux at the aquifer outlet = 4.02 curies.

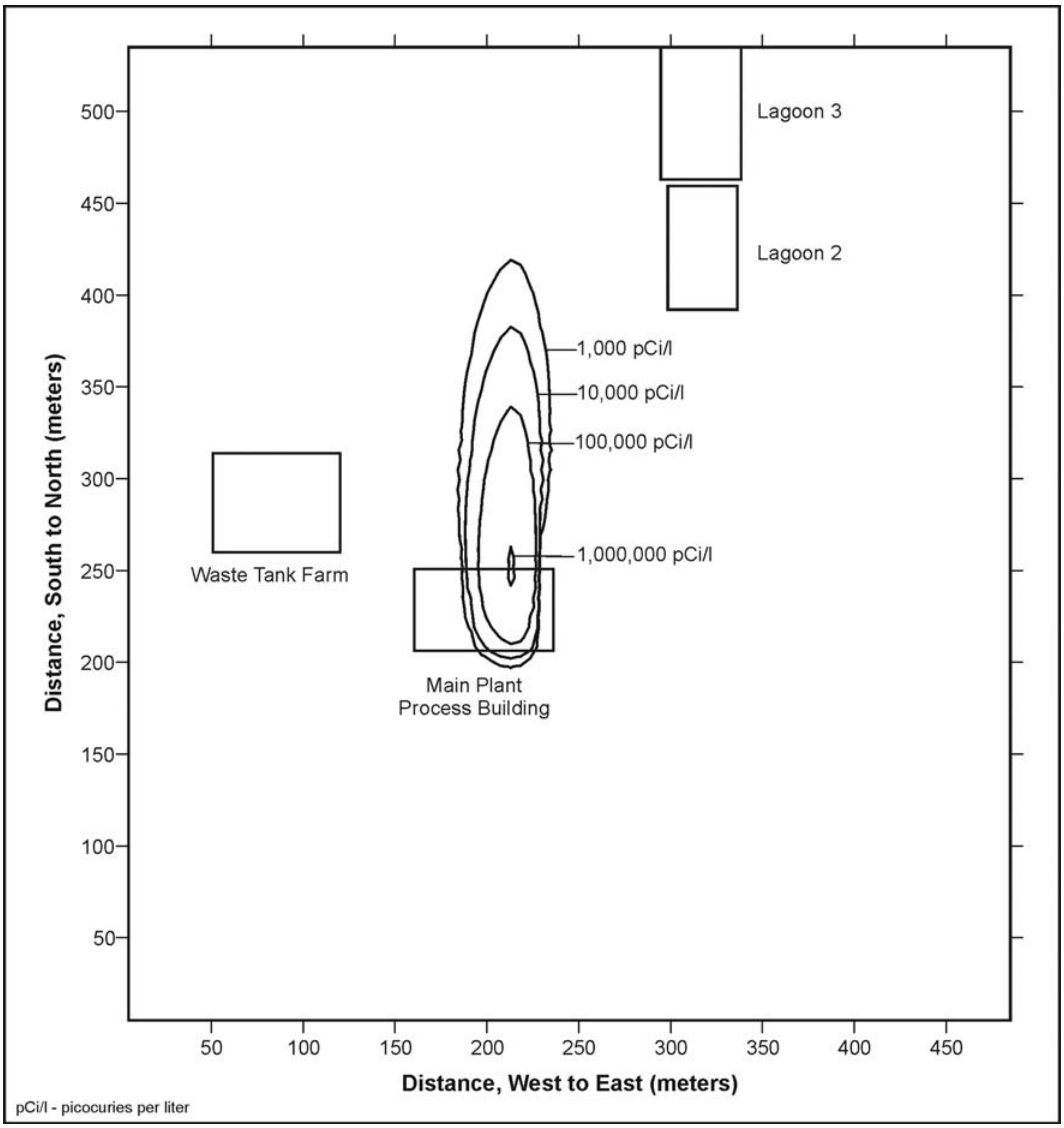


**Figure E–38 Near-field Groundwater Flow Model Prediction of Concentration of Strontium-90 in the North Plateau Plume 27 Years After Release**

The relation between rate of flow in the slack-water sequence and the thick-bedded unit above the slack-water sequence was investigated through tabulation of groundwater velocities along a flow path extending from the location of the Main Plant Process Building to the North Plateau ditch. Average linear velocities predicted by the near-field model for this path are presented in **Table E–12**. Values of effective porosity of 0.225 and 0.35 were used for the thick-bedded unit and slack-water sequence, respectively. For the slack-water sequence and thick-bedded unit above the slack-water sequence, the travel time and average velocity along the flow path are 2.77 years and 115 meters per year and 4.04 years and 79 meters per year, respectively.

**Table E–12 Average Linear Velocity for Flow Path Originating at the Main Plant Process Building**

| *Distance Along Flow Path (meters)* | *Average Linear Velocity (meters per year)* | |
|---|---|---|
| | *Slack-water Sequence* | *Thick-bedded Unit* |
| 0 to 40 | 89.7 | 51.0 |
| 40 to 80 | 106.2 | 67.1 |
| 80 to 120 | 117.4 | 85.8 |
| 120 to 140 | 129.9 | 95.6 |
| 140 to 180 | 139.9 | 102.1 |
| 180 to 220 | 147.6 | 108.6 |
| 220 to 260 | 155.6 | 114.2 |
| 260 to 300 | 162.1 | 119.3 |
| 300 to 340 | 165.6 | 122.2 |

Note: To convert meters per year to feet per year, multiply by 3.2803.

The direction of flow through sources at the Main Plant Process Building was investigated using aqueous fluxes produced by the near-field flow model. For sources at the Main Plant Process Building beginning at the ground surface and extending downward into the thick-bedded unit such as the General Purpose Cell, the primary direction of flow is downward into the underlying thick-bedded unit and slack-water sequence at the specified rate of recharge as indicated by the flow balance presented in **Table E–13**.

**Table E–13 Aqueous Flow Balance for the General Purpose Cell, Historical Conditions**

| *Direction of Flow* | *Aqueous Flow (cubic meters per year)* |
|---|---|
| In | |
| Top | 4.00 |
| South | 0.53 |
| West | $5.5 \times 10^{-5}$ |
| East | $1.0 \times 10^{-5}$ |
| Out | |
| Bottom | 4.30 |
| North | 0.23 |

Note: To convert cubic meters per year to cubic feet per year, multiply by 35.314.

Aqueous flux and solute flux were also investigated for sources at the Waste Tank Farm Tanks located in an excavation on the west side of the model area slightly north of the Main Plant Process Building.

The direction of flow towards the northwest end of the model volume was investigated for a conservative solute (100 curies of technetium-99) released from a location near the bottom of the Waste Tank Farm Tanks. The location of arrival of solute at the model boundary relative to the location of the source is summarized in **Table E–14**. The results indicate that solute moves eastward from the southwest-to-northeast centerline of the source towards the area of the slack-water sequence. This interpretation is also indicated in the concentration contours plotted in **Figure E–39** for a limit of 2 years after release. The time series of arrival at the thick-bedded unit west of the slack-water sequence and the thick-bedded unit above the slack-water sequence and slack-water sequence are presented in **Figure E–40**. The peak of the pulses occurs at approximately 5 years after traveling approximately 270 meters. The related estimate of average linear velocity of approximately 75 meters per year is consistent with movement primarily through the thick-bedded unit to reach the slack-water sequence and the northeast boundary.

**Table E–14 Location of Arrival at the Aquifer Boundary for Solute Released at the Waste Tank Farm Tanks**

| *Location of Arrival* | *Cumulative Solute Flux (curies)* |
|---|---|
| Thick-bedded Unit West of High Level Waste Tank Excavation | 0.16 |
| Thick-bedded Unit In Line With High Level Waste Tank Excavation | 3.58 |
| Thick-bedded Unit East of High Level Waste Tank Excavation, West of the Slack-water Sequence | 33.6 |
| Thick-bedded Unit Above the Slack-water Sequence and Slack-water Sequence | 38.0 |
| Thick-bedded Unit East of Slack-water Sequence | $1.2 \times 10^{-5}$ |

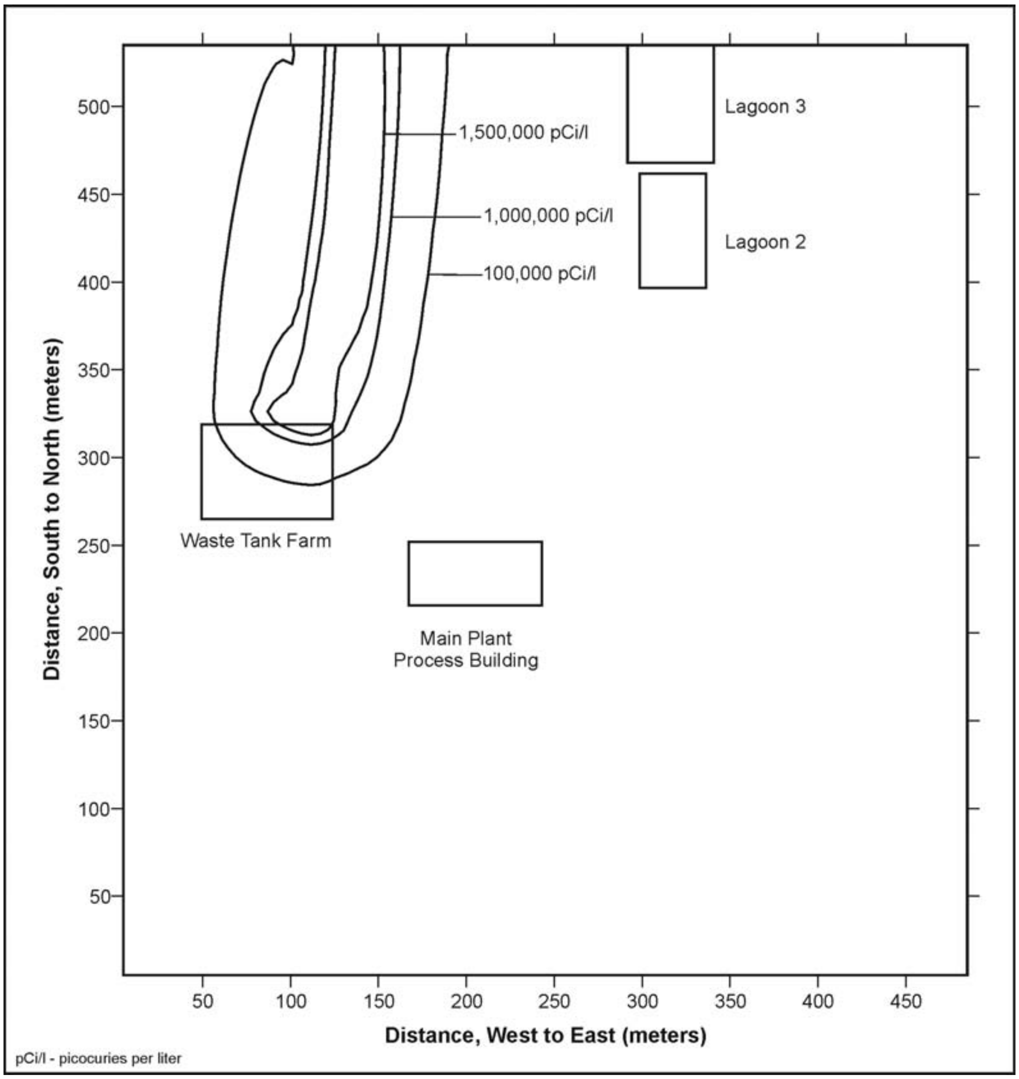


**Figure E–39 Near-field Groundwater Flow Model Prediction of Concentration of Technetium-99 for a Release at the Waste Tank Farm 5 Years After Release**

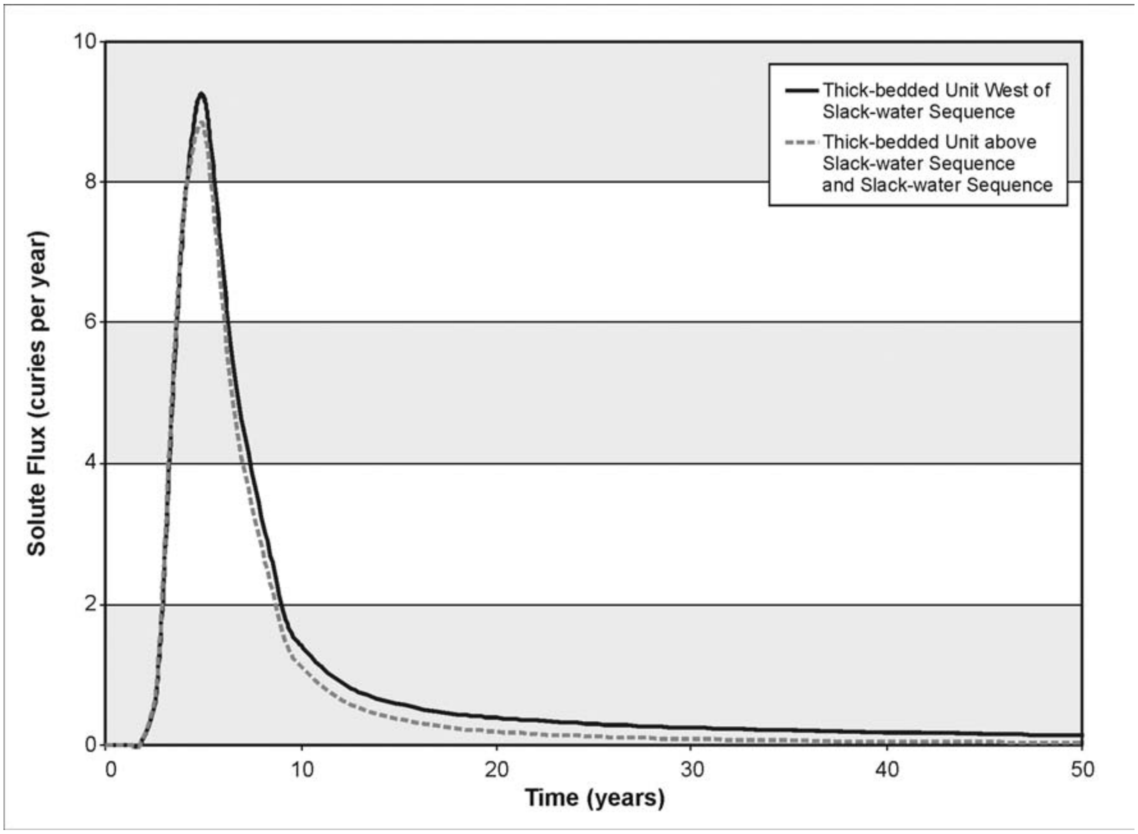


**Figure E–40 Rates of Arrival of Technetium-99 at the Model Boundary for a Source at the Waste Tank Farm Tanks**

The direction of flow through the Waste Tank Farm Tanks is indicated by the flow balance for the excavation is summarized in **Table E–15**. The results indicate that the primary direction of flow is into the excavation from the southwest, around the tanks and out of the excavation to the northeast. Flow balances for portions of the tank located in the center of the excavation are summarized in **Table E–16**. As in the case of the excavation, the primary direction of flow is from the southwest to the northeast through each section of the tank volume.

**Table E–15 Aqueous Flow Balance for the High Level Waste Tank Excavation, Historical Conditions**

| *Direction of Flow* | *Flow Area (square meters)* | *Aqueous Volumetric Flow (cubic meters per year)* |
|---|---|---|
| Into Excavation | | |
| Top, south | 1,600 | 2,655.81 |
| Top, west | 400 | 255.20 |
| Top, center | 600 | 64.53 |
| Out of Excavation | | |
| Top, north | 1,600 | 2,340.16 |
| Top, east | 400 | 404.06 |
| Bottom | 4,800 | 200.85 |
| Side, south | 560 | 7.70 |
| Side, north | 560 | 10.66 |
| Side, west | 420 | 6.98 |
| Side, east | 420 | 5.10 |

Note: To convert square meters to square feet, multiply by 10.764; cubic meters per year to cubic feet per year, multiply by 35.314.

**Table E–16 Aqueous Flow Balance for the Sections of the Waste Tank Farm Tanks, Historical Conditions**

| Section | Aqueous Volumetric Flow (cubic meters per year) — Direction of Flow: In | Aqueous Volumetric Flow (cubic meters per year) — Direction of Flow: Out | Flow Area (square meters) |
|---|---|---|---|
| Gravel Base | | | |
| Top | 37.42 | - | 800 |
| Bottom | - | 31.54 | 800 |
| South Side | 144.22 | - | 40 |
| North Side | - | 137.71 | 40 |
| West Side | 40.81 | - | 20 |
| East Side | - | 53.20 | 20 |
| Grid | | | |
| Top | 43.19 | - | 800 |
| Bottom | - | 37.42 | 800 |
| South Side | 147.85 | - | 40 |
| North Side | - | 140.67 | 40 |
| West Side | 41.39 | - | 20 |
| East Side | - | 54.34 | 20 |
| Ring | | | |
| Top | 64.53 | - | 800 |
| Bottom | - | 58.57 | 800 |
| South Side | 421.49 | - | 800 |
| North Side | - | 382.98 | 800 |
| West Side | 102.85 | - | 400 |
| East Side | - | 147.29 | 400 |

Note: To convert square meters to square feet, multiply by 10.764; cubic meters per year to cubic feet per year, multiply by 35.314.

The results of three-dimensional transport modeling of release of strontium-90 from the vicinity of the Main Plant Process Building can be used to investigate the capability of a one-dimensional transport model. The one-dimensional model is a finite difference solution to the transport equation described in Section G.3.3.1 of Appendix G. In this case, the values of input parameters and results from the 3-D near-field model are used to select conditions for specification of the one-dimensional model. In particular for the three-dimensional model, the width of 40 meters determined from mass balance considerations and mixing across the approximate 6-meter thickness of the thick-bedded unit and slack-water sequence (Table E–11) are selected as the cross-sectional dimension of the one-dimensional flow system. An average linear velocity of approximately 90 meters per year is selected as consistent with the near-field three-dimensional model (Table E–13). Initial inventory of strontium-90 of 200 curies, dispersivity of 5 meters and strontium-90 distribution coefficient of 5 milliliters per gram were also used on the one-dimensional simulation. The one-dimensional model prediction of spatial distribution of concentration of strontium-90 27 years after release is compared with three-dimensional model predictions and measured concentrations in **Figure E–41**. The one-dimensional model result matches the location and magnitude of the peak concentration but does not match the leading edge of the plume where the effect of increase of groundwater velocity in the direction of flow (Table E–12) influences the shape of the concentration profile.

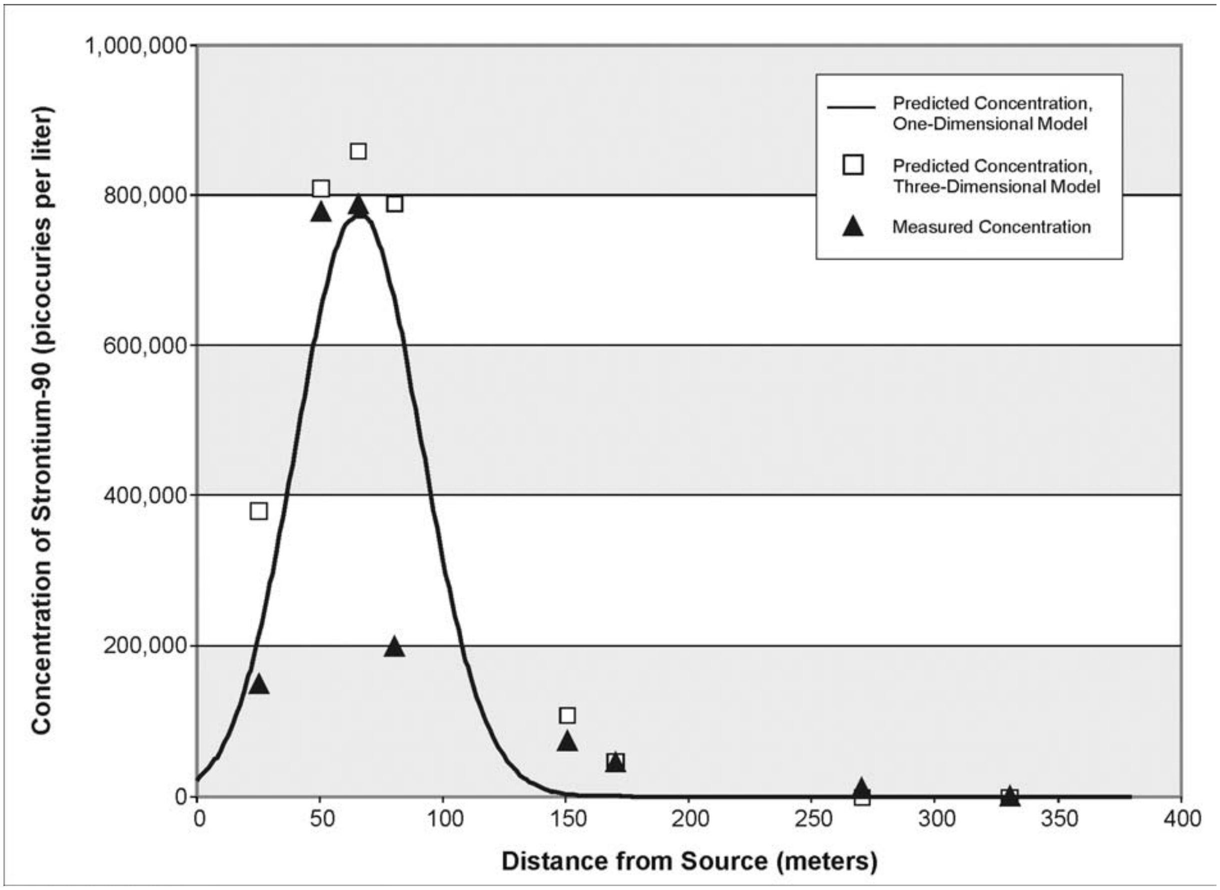


**Figure E–41 One-dimensional Groundwater Transport Model Prediction of Concentration of Strontium-90 in the North Plateau Plume 27 Years After Release**

### E.4.1.2 Engineered Features (Sitewide Close-In-Place Alternative)

The near-field model developed to assess flow conditions with engineered features in place used the same model volume as that for historical conditions but a range of size of grid blocks in the southwest-to-northeast direction to represent a 1-meter thick slurry wall placed 30 meters upgradient of the Main Plant Process Building. The boundary conditions were the same as the historical conditions model with the exception that recharge was reduced upgradient of the slurry wall to reflect influence of the slurry wall and over the Main Plant Process Building, Waste Tank Farm and the lagoons of the Low-Level Waste Treatment Facility to represent placement of caps.

The potential effectiveness of caps was investigated using a simplified model decoupled from the balance of the near-field flow model. The cap model is two-dimensional rectangular block representing a transect of one-half of the cap as shown in **Figure E–42**. The cap comprises four layers: an upper soil layer, a drainage layer, a clay layer and a backfill layer. The layers were sloped at an angle of 2 degrees from the horizontal position. The van Genuchten relationship (Pantex 2004) was used to represent unsaturated flow behavior with the design values assumed for simulation purposes summarized in **Table E–17**. Boundary conditions are no flow for the centerline on the right, no flow for layers other the drainage layer on the right and atmospheric pressure for the drainage layer on the right and the bottom of the study volume. Recharge was varied at the top to investigate the response to differing infiltration conditions. Two cases of degraded performance were also evaluated. In the first case hydraulic conductivity of the drainage layer was decreased by an order of magnitude to reflect clogging and the hydraulic conductivity of the clay layer was increased to reflect desiccation or settling. In the second case, the hydraulic conductivity of the drainage layer was decreased by an additional factor of ten to reflect additional clogging. Results, expressed as portion of the flux of recharge for design conditions are summarized in **Table E–18**. The results indicate that even under degraded conditions, the cap diverts a high percentage of the initial infiltration but that the recharge exiting the bottom of the cap could be as high as 2 centimeters per year for unfavorable conditions. For degraded conditions, the area of the cap represented in the model was less than the area covered by the tumulus producing, an average rate of infiltration through the tumulus of six centimeters per year.

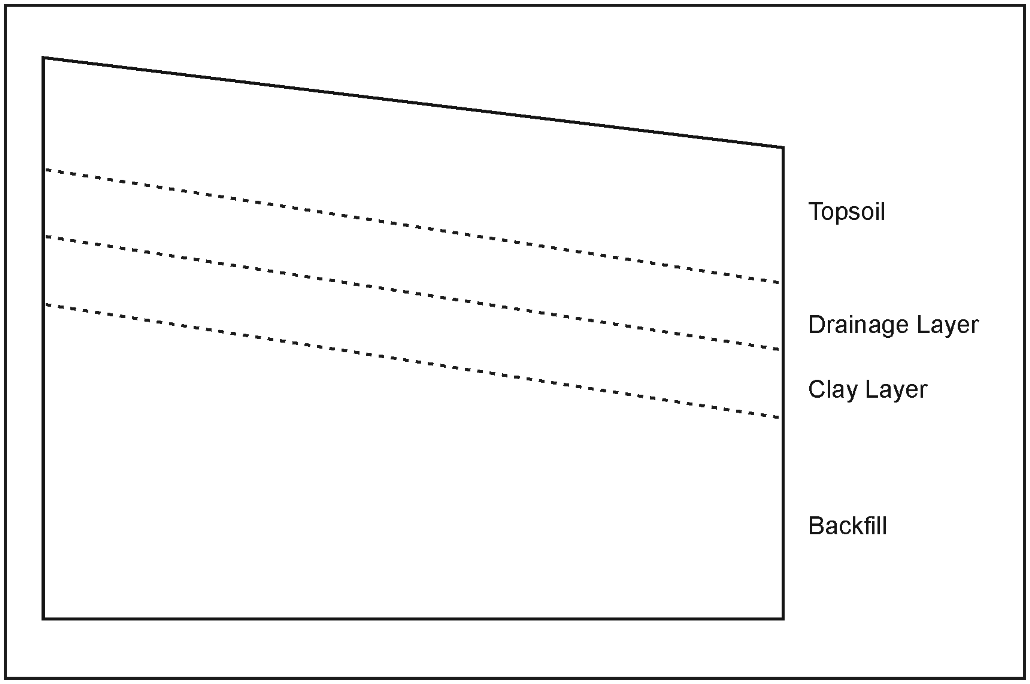


**Figure E–42 Schematic of an Engineered Cap**

**Table E–17 Values of Hydraulic Parameters for an Engineered Cap**

| *Material Type* | *Saturated Moisture Content* | *Residual Saturation* | *α (1/cm)* | *n* | *Saturated Hydraulic Conductivity (centimeters per second)* |
|---|---|---|---|---|---|
| Topsoil | 0.35 | 0.15 | 0.0787 | 1.9 | $1.0 \times 10^{-3}$ |
| Drainage Layer | 0.35 | 0.10 | 0.1214 | 2.5 | 3.0 |
| Clay Layer | 0.324 | 0.20 | 0.0328 | 1.3 | $5.0 \times 10^{-9}$ |
| Backfill | 0.35 | 0.15 | 0.0623 | 1.6 | $1.0 \times 10^{-5}$ |

**Table E–18 Distribution of Flows for an Engineered Cap for Design and Degraded Conditions**

| *Recharge at Top of Cap (centimeters per year)* | *Flux Out of Drainage Layer (centimeters per year)* | *Flux Out of Bottom (centimeters per year)* |
|---|---|---|
| Design Case | | |
| 20 | 19.98 | 0.02 |
| 100 | 99.96 | 0.04 |
| First Degraded Case | | |
| 20 | 19.90 | 0.30 |
| 100 | 99.39 | 0.61 |
| Second Degraded Case | | |
| 20 | 19.00 | 1.00 |
| 100 | 98.00 | 2.0 |

For the Close-In-Place near-field model, the long-term period of time, following loss of institutional control and degradation of engineered facilities, was simulated. For these conditions, hydraulic conductivity of the slurry wall was taken as $1 \times 10^{-6}$ centimeters per second and the recharge through the cap was 6 centimeters per year. Design hydraulic conductivity of the slurry wall is less than $1 \times 10^{-7}$ centimeters per second. The water table map calculated for these conditions is presented in **Figure E–43**. The results indicate that the slurry wall located at a distance of 190 meters and extending into the center of the model area from the west diverts flow to the east, changing water table conditions relative to historical conditions. The slurry wall decreases thickness of the unsaturated zone upgradient of the wall and in combination with the reduced infiltration due to the cap increases thickness of the unsaturated zone immediately down-gradient of the slurry wall. Average linear velocities for flow paths originating at the Main Plant Process Building, Waste Tank Farm, and Low-Level Waste Treatment Facility were 97, 65, and 98 meters per year, respectively.

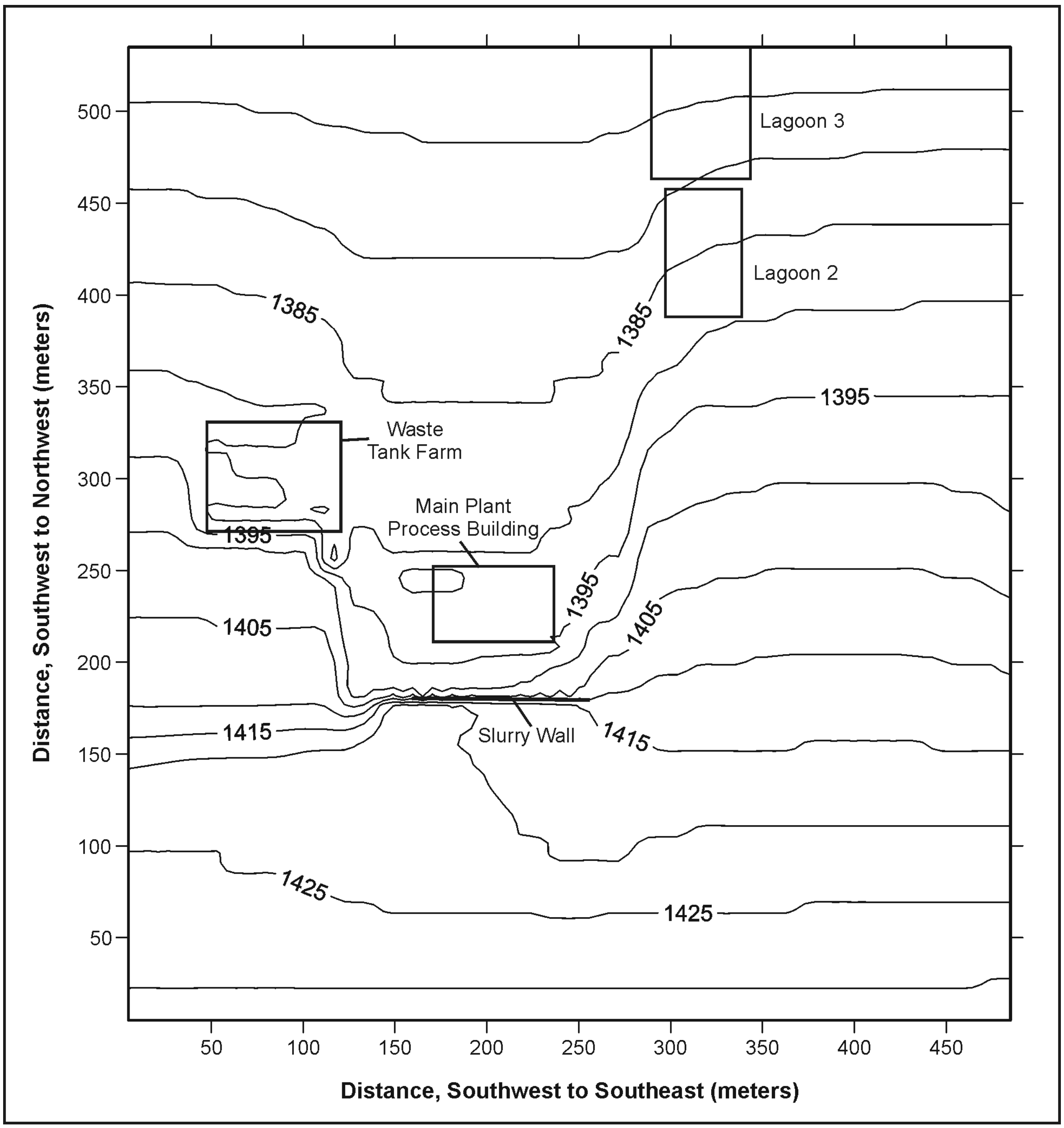


**Figure E–43 Water Table Elevation for Close-In-Place Conditions**

For the Sitewide Close-In-Place Alternative, the tanks of the Waste Tank Farm are filled with controlled low strength materials, the sediments of Lagoons 1, 2, and 3 are grouted and a slurry wall is installed around Lagoon 1. To represent these features the hydraulic conductivities of the tanks and sediments of Lagoons 2 and 3 are assigned values of hydraulic conductivity of $1 \times 10^{-5}$ centimeters per second while the combined affects of barriers at Lagoon 1 is represented by assignment of a value of $1 \times 10^{-6}$ centimeters per second to the material at Lagoon 1.

The direction of flow through sources at the Main Plant Process Building was investigated using aqueous fluxes produced by the near-field flow model. For sources at the Main Plant Process Building beginning at the ground surface and extending downward into the thick-bedded unit such as the General Purpose Cell, the primary direction of flow is downward into the underlying thick-bedded unit and slack-water sequence at the specified rate of recharge as indicated by the flow balance presented in **Table E–19**.

**Table E–19 Aqueous Flow Balance for the General Purpose Cell, Close-In-Place Conditions**

| *Direction of Flow* | *Aqueous Flow (cubic meters per year)* |
|---|---|
| In | |
| Top | 5.93 |
| South | 8.54 |
| East | 0.02 |
| Out | |
| Bottom | 14.25 |
| North | 0.24 |
| West | 0.01 |

Note: To convert cubic meters per year to cubic feet per year, multiply by 35.314.

The direction of flow through the Waste Tank Farm Tanks is indicated by the flow balances for the excavation summarized in **Table E–20**. The results indicate that the primary direction of flow is into the excavation from the southwest, around the tanks and out of the excavation to the northeast and that the combination of the slurry wall and cap reduces flow through the excavation. Flow balances for portions of the tank located in the center of the excavation are summarized in **Table E–21**. As in the case of the excavation, the primary direction of flow is from the southwest to the northeast through each section of the tank volume.

**Table E–20 Aqueous Flow Balance for the High Level Waste Tank Excavation, Close-In-Place Conditions**

| *Direction of Flow* | *Flow Area (square meters)* | *Aqueous Volumetric Flow (cubic meters per year)* |
|---|---|---|
| Into Excavation | | |
| Top | 2,800 | 968.3 |
| Out of Excavation | | |
| Top, | 2,000 | 767.0 |
| Bottom | 4,800 | 177.7 |
| Side, south | 560 | 5.11 |
| Side, north | 560 | 8.74 |
| Side, west | 420 | 5.07 |
| Side, east | 420 | 4.56 |

Note: To convert square meters to square feet, multiply by 10.764; cubic meters per year to cubic feet per year, multiply by 35.314.

**Table E–21 Aqueous Flow Balance for the Sections of the Waste Tank Farm Tanks, Close-In-Place Conditions**

| *Section* | *Aqueous Volumetric Flow (cubic meters per year)* | | |
|---|---|---|---|
| | *Direction of Flow* | | *Flow Area (square meters)* |
| | **In** | **Out** | |
| Gravel Base | | | |
| Top | 23.71 | – | 800 |
| Bottom | – | 27.86 | 800 |
| South Side | 2.23 | – | 40 |
| North Side | 0.78 | – | 40 |
| West Side | 1.01 | – | 20 |
| East Side | 0.12 | – | 20 |
| Grid | | | |
| Top | 20.23 | – | 800 |
| Bottom | – | 23.71 | 800 |
| South Side | 2.02 | – | 40 |
| North Side | 0.55 | – | 40 |
| West Side | 0.91 | – | 20 |
| East Side | – | – | 20 |
| Ring | | | |
| Top | 9.51 | – | 800 |
| Bottom | – | 12.25 | 800 |
| South Side | 3.11 | – | 800 |
| North Side | – | 0.32 | 800 |
| West Side | 1.40 | – | 400 |
| East Side | – | 0.95 | 400 |

Note: To convert cubic meters per year to cubic feet per year, multiply by 35.314.

For the magnitude and direction of flow of groundwater through the sub-surface sediments of the lagoon of the Low-Level Waste Treatment Facility are presented in **Table E–22**.

**Table E–22 Magnitude and Direction of Groundwater Flow through Sub-surface Sediments of the Low-Level Waste Treatment Facility [a]**

| *Direction* | *Volumatic Flow Rate (cubic meters per year)* | | | | |
|---|---|---|---|---|---|
| | *Lagoon 1* | *Lagoon 2* | *Lagoon 3* | *Lagoon 4* | *Lagoon 5* |
| Top | 7.18 | 81.9 | 85.1 | 21.5 | -53.6 |
| Bottom | -7.96 | -57.5 | -83.3 | 46.7 | 49.6 |
| South | 1.12 | 8.4 | 13.7 | 196.9 | 341.8 |
| North | -0.52 | -9.0 | -14.1 | -291.2 | -353.0 |
| West | -0.31 | -29.3 | -3.1 | -4.9 | 7.1 |
| East | 0.49 | 5.5 | 1.6 | 31.0 | 8.2 |

[a] Positive value is for flow in the indicated direction, negative value is for flow opposite to the indicated direction.
Note: To convert cubic meters per year to cubic feet per year, multiply by 35.314.

### E.4.1.3 Phased Decisionmaking Alternative

For the Phased Decisionmaking Alternative, the Main Plant Process Building, the source area of the North Plateau Plume and the lagoons of the Low-Level Waste Treatment Facility would have been removed. A slurry wall would be installed to separate the area of the Main Plant Process Building from the Waste Tank Farm and to separate the area of the lagoons from the portion of the plume not recovered by removal of the source are of the plume. The near-field groundwater flow model developed to assess flow conditions for this alternative uses the same model volume as that defined for historical conditions with the exception that the model area has less extent to the east of the lagoons. The cross-sectional structure of the aquifer is that represented in Figures E–33 through E–36 with the same vertical discretization as the historical conditions case. A total of approximately 120,000 grid blocks were used: 53 in the west-to-east, 61 in the south-to-north and 38 in the vertical directions, respectively. The distribution of hydraulic head predicted for the Phased Decisionmaking Alternative is presented in **Figure E–44**. The results indicate increase of elevation of the water table in the areas occupied by the Main Plant Process Building and lagoons prior to their removal. Flow balances predict flow from the prior area of the Main Plant Process Building through the slurry wall to the west, that is, towards the Waste Tank Farm and from the area of the lagoons both to the east towards Erdmann Brook and to the west through the slurry wall towards the northern extension of the North Plateau Plume.

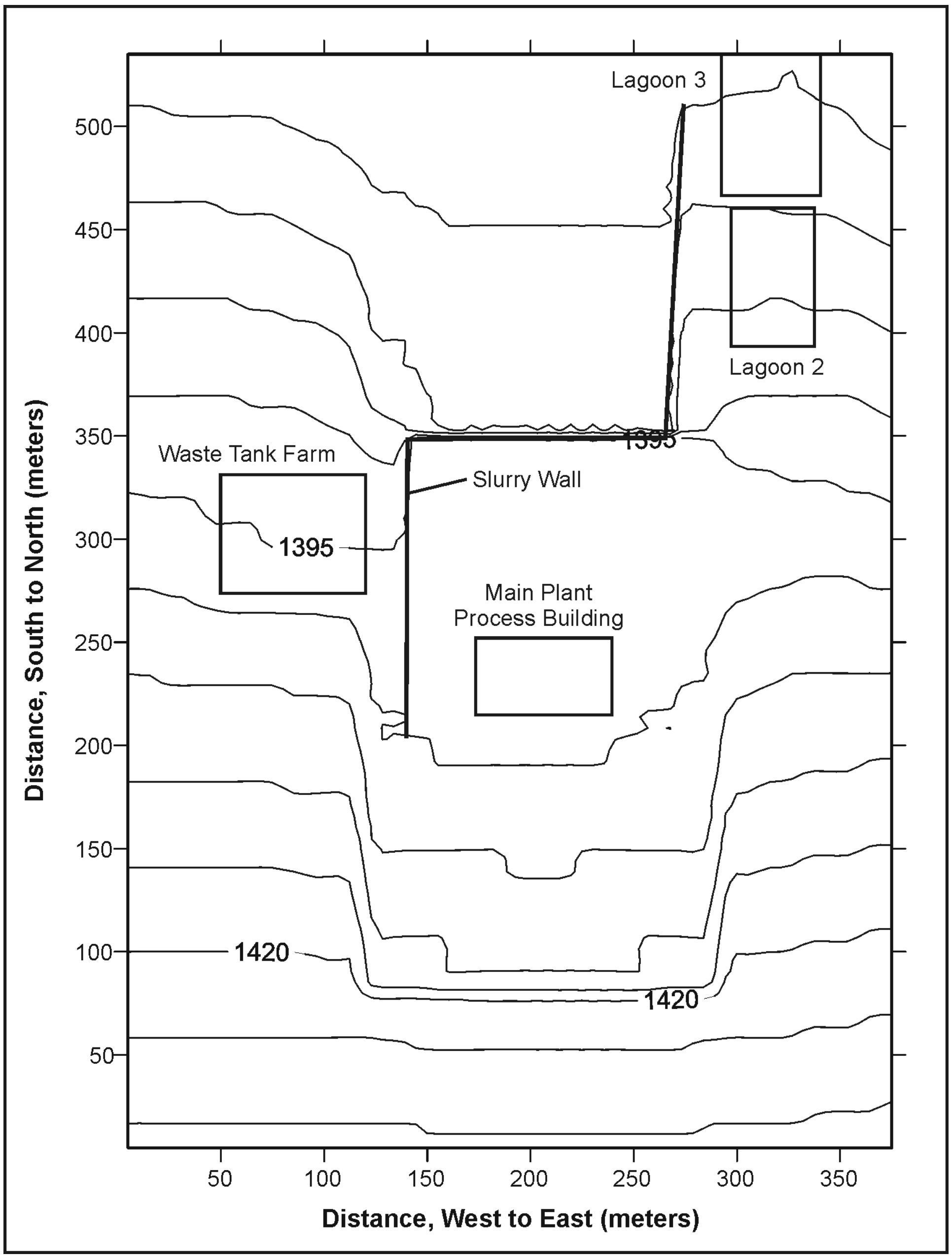


**Figure E–44 Elevation of the Water Table on the North Plateau Phased Decisionmaking Alternative, Near-field Flow Model**

### E.4.2 South Plateau

The model developed for the south plateau has the shape of a rectangular block oriented from the southwest to the northeast that extends from the ground surface to the top of the Kent recessional sequence. The exterior horizontal boundaries of the model are depicted in Figure E–31. The model boundaries on the north, west and east sides are along reaches of Franks Creek and Erdman Brook and near contact with bedrock on the south boundary. Geohydrologic units represented in the model are the portions of the Lavery till differentiated into the near-surface weathered Lavery till, the underlying unweathered Lavery till and portions of till disturbed by holes and trenches excavated for disposal of waste. The hydraulic conductivities of the weathered Lavery till, unweathered Lavery till and disturbed portions of the till were $4.65 \times 10^{-5}$, $6.0 \times 10^{-8}$, and $4.65 \times 10^{-5}$ centimeters per second, respectively. The weathered Lavery till has thickness of approximately 3 meters across the South Plateau while the unweathered Lavery till is approximately 27 meters thick under the South Plateau. For the horizontal directions, grid blocks ranged from 1 to 20 meters in size with a total of 1,978 grid blocks for the historical conditions model and 2,346 grid blocks for the engineered features model. For the vertical direction, the upper 6 meters were represented using 12, 0.25-meter-thick layers, while the lower 27 meters were represented using 27, 1.0-meter-thick layers. Totals of approximately 77,000 and 91,000 grid blocks were used for the historical conditions and engineered features models. Boundary conditions applied for the model are uniform recharge of 2.3 centimeters per year at the ground surface, atmospheric pressure conditions at the bottom of the unweathered Lavery till to simulate a water table in the underlying Kent recessional sequence, atmospheric pressure in the weathered Lavery till on the west, east and north to simulate seepage to the creeks, no flow from the south and no flow into the unweathered Lavery till on all sides. These general elements of the model were developed further into two variants, the first developed for historical conditions as appropriate for the No Action and the Phased Decisionmaking Alternatives and the second incorporated engineered features as appropriate for the Sitewide Close-In-Place Alternative.

#### E.4.2.1 Historical Conditions and Phased Decisionmaking Alternative

Due to the low hydraulic conductivity of the till, the water table is generally high on the South Plateau. In addition, only four non-trending target wells are located on the South Plateau. For these reasons, the calibration target for the South Plateau near-field flow model was location of the water table near the ground surface across the model area. A water table map for recharge of 2.3 centimeters per year produced these conditions as represented in **Figure E–45** and a comparison of measured and predicted leads is presented in **Table E–23**. Approximately, 70 percent of the incoming recharge exited the model volume at the bottom while approximately 14, 7 and 7 percent of the recharge exited through seeps on the north, west and east boundaries of the model area. Estimates of Darcy velocity for the waste disposal areas are presented in **Table E–24**. Because of greater cross-sectional area, the predominant direction of horizontal flow is to the north for sources at the SDA and to the north and west for sources at the NDA.

#### E.4.2.2 Engineered Features (Close-In-Place Conditions)

Engineered features proposed for South Plateau facilities include installation of a slurry wall upgradient of the disposal areas and placement of caps over these areas. Of most interest is performance over the long-term when loss of institutional control and of maintenance of the engineered facilities may occur. For the purpose of analysis, a value of hydraulic conductivity for a degraded slurry wall was taken to be $1 \times 10^{-6}$ centimeters per second. As indicated by the analysis of cap summarized in Table E–18, long-term performance may provide no reduction of recharge below background conditions on the South Plateau. A prediction of water table elevation for these values of engineered conditions is presented in **Figure E–46**. Placement of the slurry wall produces an increase in elevation of the water table upgradient of the slurry wall but only minor change inflow relative to background conditions. Approximately 70 percent of the recharge water exits through the bottom of the model volume with the balance exiting through the weathered Lavery till to the creeks. Estimates of Darcy velocity for the waste disposal areas are presented in **Table E–25**. Because of greater cross-sectional area, the predominant direction of horizontal flow is to the north for sources at the SDA and to the north and west for sources at the NDA.

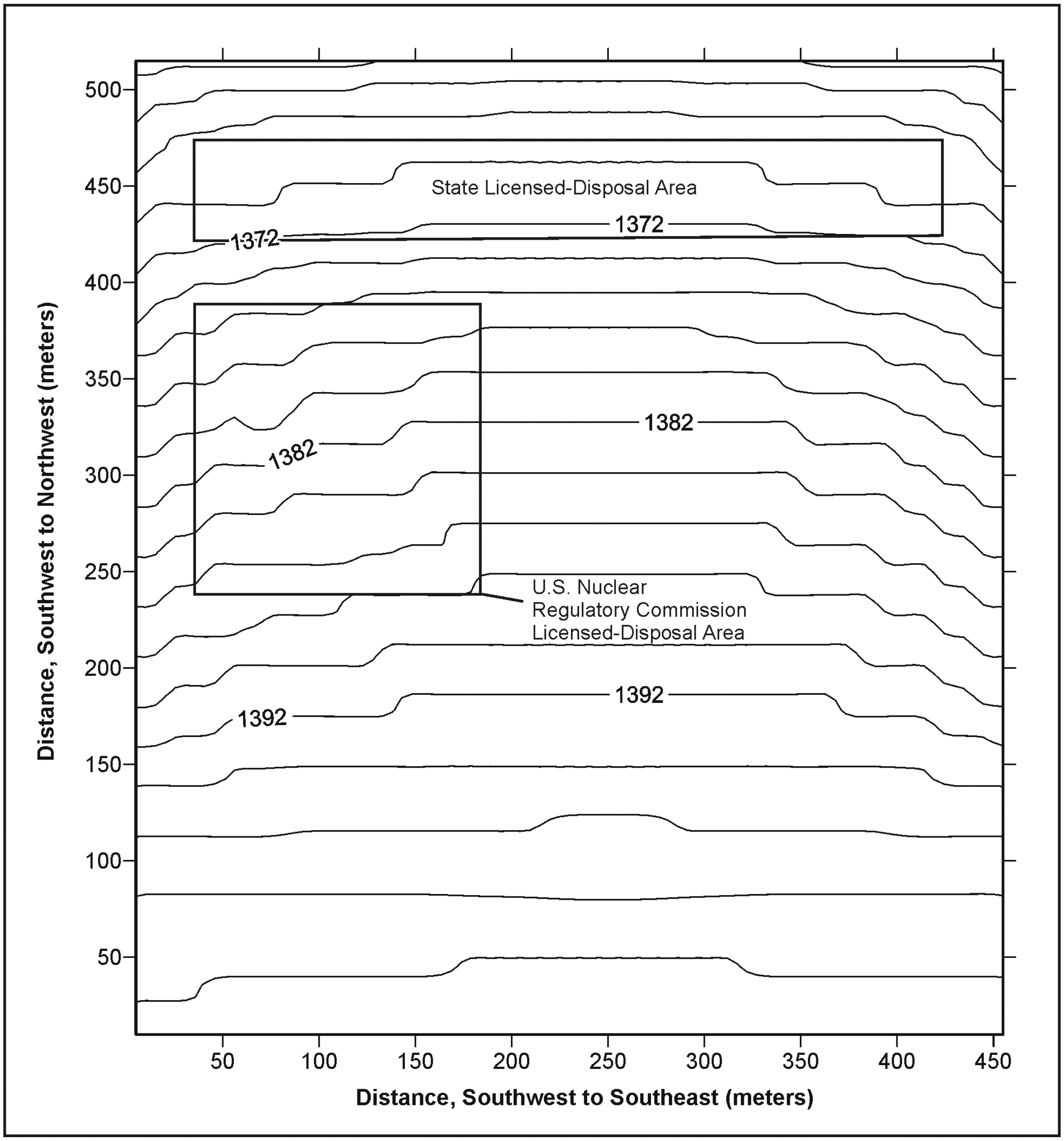


**Figure E–45 Elevation of the Water Table on the South Plateau Historical Conditions, Near-field Flow Model**

**Table E–23 Comparison of Measured and Predicted Heads for the South Plateau Near-field Flow Model**

| *Well* | *Measured Head (feet)* | *Predicted Head (feet)* |
|---|---|---|
| 97 | 1378.2 | 1,385.8 |
| 1007 | 1,379.7 | 1,385.2 |
| 1008c | 1,399.0 | 1,400.6 |
| 96-I-01 | 1,738.0 | 1,379.0 |

**Table E–24 Estimates of Darcy Velocity for Waste Disposal Areas on the South Plateau for Historical Conditions**

| *Disposal Area* | *Darcy Velocity* [a] *(meters per year)* | | | | |
|---|---|---|---|---|---|
| | *Flow Direction* | | | | |
| | *Bottom* | *South* | *North* | *West* | *East* |
| NFS Process | 0.025 | -0.31 | 0.28 | 0.10 | -0.094 |
| NFS hulls | 0.057 | -0.43 | 0.12 | 0.035 | -0.025 |
| WVDP | 0.031 | -0.37 | 0.25 | 0.032 | -0.013 |
| SDA | 0.023 | -0.28 | 0.26 | 0.037 | 0.041 |

[a] Positive magnitude indicates flow in the specified direction.
Note: To convert meters to feet, multiply by 3.2808.

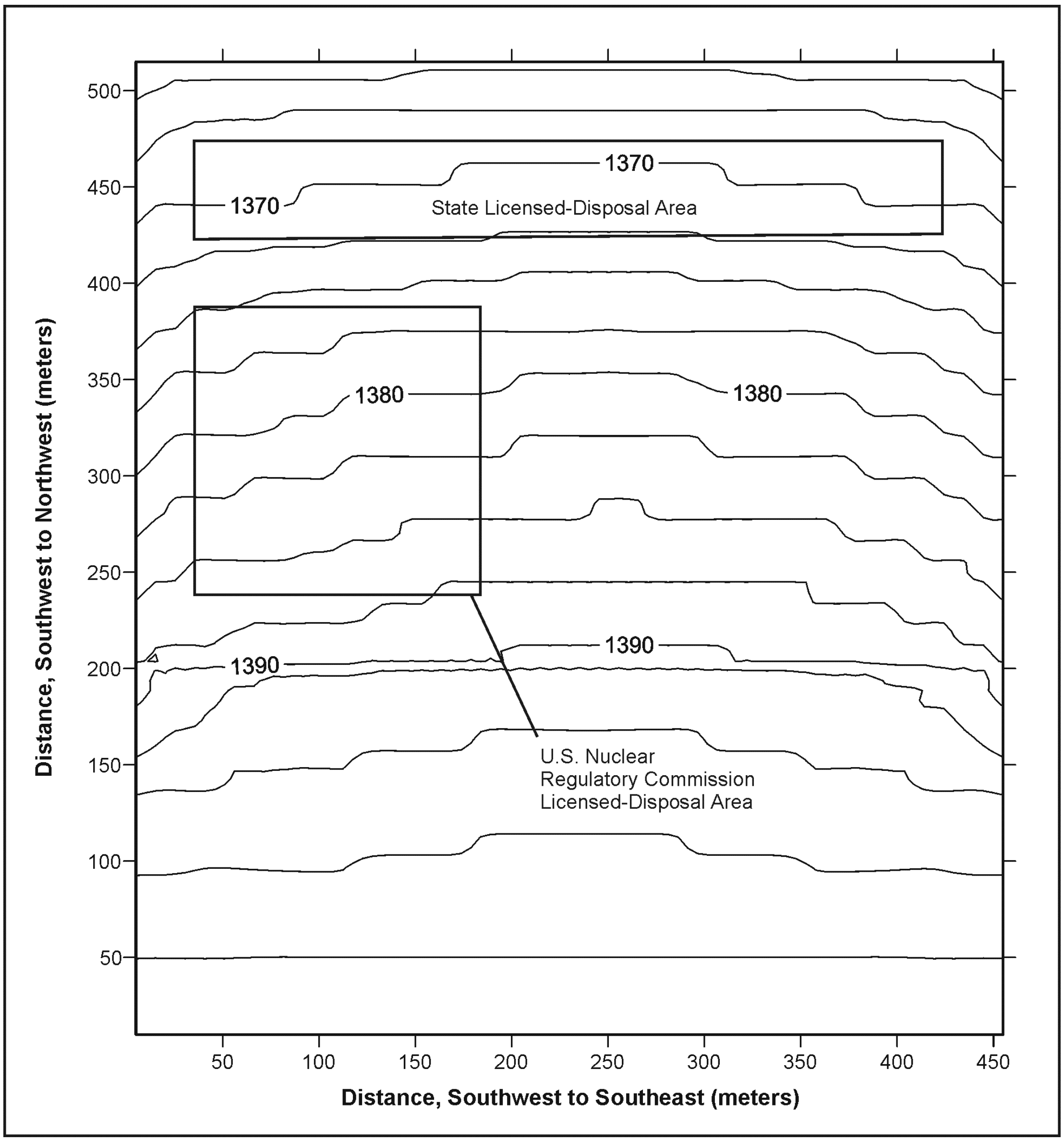


**Figure E–46 Elevation of the Water Table for Long-term Close-In-Place Conditions, Near-field Flow Model**

**Table E–25 Estimates of Darcy Velocity for Waste Disposal Areas on the South Plateau for Close-In-Place Conditions**

| Disposal Area | *Darcy Velocity [a] (meters per year)* | | | | |
|---|---|---|---|---|---|
| | *Flow Direction* | | | | |
| | ***Bottom*** | ***South*** | ***North*** | ***West*** | ***East*** |
| NFS Process | 0.025 | -0.26 | 0.23 | 0.06 | -0.09 |
| NFS hulls | 0.057 | -0.04 | 0.10 | -0.08 | -0.23 |
| WVDP | 0.031 | -0.32 | 0.22 | 0.02 | -0.13 |
| SDA | 0.023 | -0.27 | 0.25 | 0.03 | 0.04 |

[a] Positive magnitude indicates flow in the specified direction.
Note: To convert meters to feet, multiply by 3.2808.

## E.5 References

Bergeron, M. P. and W. M. Kappel, and R. M. Yager, 1987, *Geohydrologic Conditions at the Nuclear-Fuels Reprocessing Plant and Waste-Management Facilities at the Western New York Nuclear Service Center, Cattaraugus County, New York*, U.S. Geological Survey Water-Resources Investigations Report 85-4145, U.S. Geological Survey, Ithaca, New York.

Bergeron, M. P. and E. F. Bugliosi, 1988, *Ground-Water Flow Near Two Radioactive-Waste-Disposal Areas at the Western New York Nuclear Service Center, Cattaraugus County, New York—Results of Flow Simulation*, U.S. Geological Survey Water-Resources Investigations Report 86-4351, U.S. Geological Survey, Albany, New York.

Beven, K., 2006, "A manifesto for the equifinality thesis," *Journal of Hydrology* 320, pp. 18-36.

Cohen, F., 2006, Senior Geologist, URS Corporation, Personal communication (email) to J. Ross, University of Vermont, Burlington, Vermont, October 11.

CWVNW (Coalition on West Valley Nuclear Wastes), 1993, *Confirmation of Anomalous Westward Dip between Springville and West Valley, New York*, East Concord, New York, November 14.

Dames and Moore (Dames and Moore, Inc.), 1995, *Investigation of Strontium Behavior in the Surficial Sand and Gravel - Groundwater System*, 10 805-953-8251, Orchard Park, New York, June 9.

Dana, Jr., R. H., R. H. Fakundiny, R. G. Lafleur, S. A. Mollello, and P. R. Whitney, 1979a, *Geologic Study of the Burial Medium at a Low-Level Radioactive Waste Burial Site at West Valley, New York*, NYSGS/79-2411, New York State Geological Survey/State Museum, Albany, NY.

Dana, Jr., R. H., S. A. Mollello, R. H. Fickies, and R. H. Fakundiny, 1979b, *General Investigation of Radionuclide Retention in Migration Pathways at the West Valley New York Low-Level Burial Site, Annual Report, September 1, 1997 – September 30, 1998,* New York State Geological Survey/State Museum, Albany, p. 99, NUREG/CR-0794, November.

Doherty, J, 2004, *PEST, Model-Independent Parameter Estimation, User Manual*, 5$^{th}$ ed., July.

Domenico, P. A., and F. A. Schwartz, 1990, *Physical and Chemical Hydrogeology*, John Wiley & Sons, New York, pp. 824.

Engelder, T., and P. Geiser, 1979, *The relationship between pencil cleavage and lateral shortening within the Devonian section of the Appalachian Plateau*, New York, Geology, Vol. 7, pg. 460-464, September.

Englund, E., and A. Sparks, 1991, *GEO - EAS 1.2.1, Geostatistical Environmental Assessment Software, User's Guide*, U.S. Environmental Protection Agency Report, EPA 600/4-88/033, March.

EPA (U.S. Environmental Protection Agency), 1991, *The RETC Code for Quantifying the Hydraulic Functions of Unsaturated Soils*, EPA/600/2-91/065, December.

Kappel, W. M., and W. E. Harding, 1987, *Surface-Water Hydrology of the Western New York Service Center, Cattaraugus County, New York*, U.S. Geological Survey Water-Resources Investigations Report 85-4309, Ithaca, New York.

Kool, J. B., and Y. S. Wu, 1991, *Ground-Water Flow and Transport Modeling of the NRC-Licensed Waste Disposal Facility, West Valley, New York*, NUREG/CR-5794, prepared by HydroGeoLogic, Inc. for the Nuclear Regulatory Commission, October.

La Fleur, R. G., 1979, *Glacial Geology and Stratigraphy of Western New York Nuclear Service Center and Vicinity, Cattaraugus and Erie Counties, New York*, USGS Open File Report 79-989, Albany, New York.

LANL (Los Alamos National Laboratory), 2003, Software *Users Manual (UM) for the FEHM Application, Version 2.*21, Rev. No. 00, Document ID: 10086-UM-2.21-00, October.

NYSGS (New York State Geological Survey), 1979, *Research at a Low-level Radioactive Waste Burial Site at West Valley, New York - An Introduction and Summary*, NYSGS Open File Report 79-2413, New York State Geological Survey, Albany, New York.

Pantex (BWXT Pantex, L.L.C.), 2004, *Subsurface Modeling Report for the U.S. Department of Energy/National Nuclear Security Administration Pantex Plant, Amarillo, Texas*, Amarillo, Texas, September.

PNNL (Pacific Northwest National Laboratory), 2000, *STOMP, Subsurface Transport Over Multiple Phases, Version 2.0 Theory Guide*, PNNL-12030, Richland, Washington, March.

Prudic, D. E., 1986, *Ground-Water Hydrology and Subsurface Migration of Radionuclides at a Commercial Radioactive Waste Burial Site, West Valley, Cattaraugus County, New York*, U.S. Geological Survey Professional Paper 1325.

Ritzi, R. W., Z. Dai, D. F. Dominic, and Y.N. Rubin, 2003, "Review of permeability in buried-valley aquifers: centimeter to kilometer scales," in *Calibration and Reliability in Groundwater Modelling: A Few Steps Closer to Reality,* K. Kovar, *ed*., IAHS Publication no. 277, International Association of Hydrologic Sciences Press.

Sandia (Sandia National Laboratories), 2008a, *Evaluation of the West Valley Demonstration Project Groundwater Flow and Transport Model*, Report prepared for the U.S. Department of Energy, West Valley, New York, August.

Sandia (Sandia National Laboratories), 2008b, *Phase II: Calibration of the SAIC West Valley Demonstration Project FEHM Flow Model*, Report prepared for the U.S. Department of Energy, West Valley, New York, August.

URS (URS Corporation), 2002, Report, *An Update of the Structural Geology in the Vicinity of the Western New York Nuclear Service Center, West Valley, New York*, West Valley, New York, May.

USGS (U.S. Geological Survey), 2005, *Computer Program for the Kendall Family of Trend Tests*, U.S. Geological Survey Scientific Investigations Report, 2005-5275.

Weber, D. and E. Englund, 1992, "Evaluation and Comparison of Spatial Interpolators", Mathematical Geology 24:4, pp. 381-391. Also available as available as a research paper at http://www.epa.gov/esd/cmb/research.htm.

WVES (West Valley Environmental Services, LLC), 2007, *Annual Summary for the North Plateau Strontium-90 Groundwater Plume, October 1, 2006 – September 30, 2007*, December 31.

WVNS (West Valley Nuclear Services Company), 1993a, *Environmental Information Document, Vol. I, Geology*, WVDP-EIS-004, Rev. 0, West Valley, New York, March.

WVNS (West Valley Nuclear Services Company), 1993b, *Environmental Information Document, Vol. III, Hydrology, Part 4 of 5, Groundwater Hydrology and Geochemistry*, WVDP-EIS-009, Rev. 0, West Valley, New York, February.

WVNS (West Valley Nuclear Services Company), 1993c, *Environmental Information Document, Vol. III, Hydrology: Part 5 of 5, Vadose Zone Hydrology*, WVDP-EIS-009, Rev. 0, West Valley, New York, February.

WVNS (West Valley Nuclear Services Company), 1994, *Environmental Information Document, Vol. IV, Soils Characterization, Appendices*, WVDP-EIS-008, Rev. 0, West Valley, New York, September 15.

WVNS (West Valley Nuclear Services, Inc.), 1995, *Subsurface Probing Investigation on the North Plateau at the West Valley Demonstration Project*, WVDP-220, West Valley, New York, May 1.

WVNS (West Valley Nuclear Services, Inc.), 1999, *1998 GeoProbe Investigation in the Core Area of the North Plateau Groundwater Plume*, WVDP-346, West Valley, New York, June 11.

WVNS (West Valley Nuclear Services Company), 2007, *Safety Analysis Report for Low-Level Waste Processing and Support Activities*, WVNS-SAR-001, Rev. 11, West Valley, New York, June 28.

WVNS and Dames and Moore (West Valley Nuclear Services Company and Dames and Moore), 1997, *Resource Conservation and Recovery Act Facility Investigation Report Volume 1, Introduction and General Site Overview*, West Valley Demonstration Project West Valley, New York, WVDP-RFI-017, West Valley Nuclear Services Company, Inc., West Valley, New York, July 14.

WVNS and URS (West Valley Nuclear Services Company, Inc. and URS Group Inc.), 2005, *West Valley Demonstration Project, Annual Site Environmental Report, Calendar Year 2004*, West Valley, New York, August.

WVNS and URS (West Valley Nuclear Services Company, Inc. and URS Group Inc.), 2006, *West Valley Demonstration Project, Annual Site Environmental Report, Calendar Year 2005*, West Valley, New York, September.

WVNS and URS (West Valley Nuclear Services Company, Inc. and URS Group, Inc.), 2007, *West Valley Demonstration Project, Annual Site Environmental Report, Calendar Year 2006*, West Valley, New York, September.

Yager, R. M., 1987, *Simulation of Groundwater Flow near the Nuclear-Fuel Reprocessing Facility at the Western New York Nuclear Service Center, Cattaraugus County, New York*, U.S. Geological Survey, Water-Resources Investigations Report 85-4308, U.S. Nuclear Regulatory Commission, Ithaca, New York.

Yager, R., 1993, U.S. Geological Survey, Personal communication (letter) to P. Bembia (NYSERDA), September 2, 1993.

Zadins, Z. Z., 1997, A Hydrogeologic Evaluation of "Geologic and Hydrologic Implication of the Buried Bedrock Valley that Extends from the Western New York Nuclear Service Center into Erie County, NY", Dames and Moore, August.